The Institute of Paper Chemistry

Appleton, Wisconsin

Doctor's Dissertation

The Absorption of Chlorine into Aqueous Media in Light of the Penetration Theory

Charles W. Spalding

June, 1961

THE ABSORPTION OF CHLORINE INTO AQUEOUS MEDIA IN LIGHT OF THE PENETRATION THEORY

A thesis submitted by

Charles W. Spalding

B.S. in Ch.E. 1957, University of Wisconsin
M.S. 1959, Lawrence College

in partial fulfillment of the requirements
of The Institute of Paper Chemistry
for the degree of Doctor of Philosophy
from Lawrence College,
Appleton, Wisconsin

June, 1961

TABLE OF CONTENTS

PRESENTATION OF THE THESIS PROBLEM

The development of the penetration theory of gas absorption (1) has made possible the planning of experiments and the analyzing of the results of these experiments in such a way that fundamental information concerning the mechanisms of gas absorption can be obtained.

There is a need to obtain such fundamental information on the absorption of chlorine gas into aqueous media. The mechanism and speed of the chemical reaction between chlorine and water and the influence these factors have on the absorption rate are unclear.

The objectives of this thesis are to investigate the process of chlorine absorption in terms of the penetration theory and to study the kinetics of the chlorine-water reaction through the use of the penetration theory and gas absorption measurements. Particular attention is paid to testing the applicability of the penetration theory, its assumptions and limitations; to developing and improving techniques which aid in the study of gas absorption; and to finding the driving force which best correlates the absorption data when the system is thermodynamically nonideal. Equal attention is given to the determination of the chlorine-water reaction mechanism which best suits the data, to the determination of the speed of the reaction, and to studying the influence of thermodynamic nonideality on the reaction.

BACKGROUND OF THE THESIS PROBLEM

THE CHLORINE-WATER SYSTEM

THERMODYNAMIC CONSIDERATIONS

If gaseous chlorine is brought into contact with liquid water and the system is allowed to come to equilibrium, this equilibrium state may be represented as follows:

$$Cl_2(g) \rightleftharpoons Cl_2(aq) \qquad (1)$$

$$Cl_2(aq) + H_2O \rightleftharpoons HOCl + H^+ + Cl^- \qquad (2)$$

$$HOCl \rightleftharpoons H^+ + OCl^- \qquad (3)$$

Physical Equilibrium

The addition of a small amount of hydrochloric acid to this system shifts the equilibrium of Reactions (2) and (3) to the left to such an extent that only the equilibrium between gaseous chlorine and unhydrolyzed aqueous chlorine becomes important.

Like most sparingly soluble gases at relatively low partial pressures, the equilibrium represented by Reaction (1) has been experimentally shown (2-4) to follow Henry's law; i.e., the partial pressure of a gaseous solute is proportional to its mole fraction in solution.

$$p_i = K_i x_i \qquad (4)$$

The proportionality constant, K_i, is a function of only the solvent, temperature, and total pressure.

Because chlorine-water solutions are very dilute the mole fraction of the chlorine is directly proportional to its concentration, C_i. Thus, Henry's law may be written as

$$p_i = H_i C_i \qquad (5)$$

Analysis of chlorine solubility measurements in pure water and the equilibrium constant for Reaction (2) shows that the unhydrolyzed chlorine molecules still obey Henry's law even though the hydrolyzed species are present (2).

As must be the case, Henry's law is a particular solution of the Gibbs-Duhem equation (5) which shows the relation between simultaneous changes in pressure, chemical potential, and temperature in a system at thermodynamic equilibrium.

The basic criterion of equilibrium of a substance distributed between two phases is that the chemical potential of that substance be the same in both phases.

$$\mu_i^{v} = \mu_i^{s} \qquad (6)$$

In each phase it is convenient to define model systems which closely follow actual behavior at limiting conditions. In the vapor phase the model gives the relationship between chemical potential and partial pressure as

$$\mu_i^{v} = \mu_i^{o,v} + RT \ln p_i, \qquad (7)$$

and in the solution phase the relationship between chemical potential and concentration is

$$\mu_i^{s} = \mu_i^{o,s} + RT \ln C_i . \qquad (8)$$

$\mu_{\underline{i}}^{\underline{o,v}}$ is a function of temperature only, and $\mu_{\underline{i}}^{\underline{o,s}}$ is a function of temperature and pressure. When the systems involved do not behave as the model systems, chemical potentials are expressed in terms of fugacities and activities which replace the partial pressures and concentrations respectively.

$$\mu_i^{v} = \mu_i^{o,v} + RT \ln f_i \qquad (9)$$

$$\mu_i^{s} = \mu_i^{o,s} + RT \ln a_i \qquad (10)$$

Deviation from the model systems can be attributed to intermolecular forces which are so prominent that the molecules do not behave independently of one another.

The numberical values of $\mu_{\underline{i}}^{\underline{o,v}}$, $\mu_{\underline{i}}^{\underline{o,s}}$, $\underline{f_i}$, and $\underline{a_i}$ are governed by the choice of a standard state for each phase. The choice of a standard state is a matter of convenience.

In this case it is convenient to choose a standard state in the vapor phase at the temperature and pressure of the system such that

$$f_i \longrightarrow p_i \quad \text{as} \quad p_i \longrightarrow 0 . \qquad (11)$$

In this state the molecules behave independently of each other and model behavior results. The variables $\underline{P}$, $\underline{V}$, and $\underline{T}$ are then related in accordance with the ideal gas law. At partial pressures of less than one atmosphere and at 25°C., chlorine has been shown (6) to follow the ideal gas law. Thus,

$$f_i \cong p_i \tag{12}$$

for all pressures and temperatures used in this work.

In the solution phase it is desirable to choose a standard state at the temperature and pressure of the system such that

$$a_i \longrightarrow C_i \quad \text{as} \quad C_i \longrightarrow 0 . \tag{13}$$

The ratio $\underline{a_i}/\underline{C_i}$ is defined as the activity coefficient, $\gamma_{\underline{i}}$.

The dependence of $\gamma_{\underline{i}}$ on $\underline{C_i}$ can now be established. From Equations (6), (9), (10), and (12)

$$\mu_i^{o,v} + RT \ln p_i = \mu_i^{o,s} + RT \ln \gamma_i C_i \tag{14}$$

at equilibrium. Therefore,

$$p_i/\gamma_i C_i = \exp [(\mu_i^{o,s} - \mu_i^{o,v})/RT]. \tag{15}$$

The right-hand side of Equation (15) is a constant which is independent of concentration. Thus,

$$p_i/\gamma_i C_i = H_i' . \tag{16}$$

Experimentation has shown that Henry's law is valid, i.e., $\underline{p_i}/\underline{C_i} = \underline{H_i}$ [Equation (5)]. Therefore,

$$H_i = \gamma_i H_i' . \tag{17}$$

Thus, $\gamma_{\underline{i}}$ is also a constant which is independent of $\underline{C_i}$.

The choice of the standard state used here requires that:

$$\gamma_i \longrightarrow 1 \quad \text{as} \quad C_i \longrightarrow 0 \,. \tag{18}$$

Thus, the activity coefficient is equal to unity at all chlorine concentrations because of its independence of C_i.

In this work it is desired to alter the activity coefficient of the unhydrolyzed chlorine. This is accomplished by salting out the chlorine with an inert salt such as sodium chloride or sodium sulfate. Experimentation has shown (3) that Henry's law is valid for chlorine in such salt solutions.

If the salt solution and pure water are both in equilibrium with the same vapor phase, the chemical potential of the unhydrolyzed chlorine must be the same in both solutions. Thus,

$$\mu_{i,o}^{o,s} + RT \ln \gamma_{i,o} C_{i,o} = \mu_{i,s}^{o,s} + RT \ln \gamma_{i,s} C_{i,s} \tag{19}$$

where the subscript, s, denotes chlorine in the salt solution and o denotes chlorine in water. If the standard state for the salt solution is chosen so that

$$\mu_{i,o}^{o,s} = \mu_{i,s}^{o,s} \,, \tag{20}$$

it is seen that

$$\gamma_{i,o} C_{i,o} = \gamma_{i,s} C_{i,s} \tag{21}$$

or

$$\gamma_{i,s} = (C_{i,o}/C_{i,s})\, \gamma_{i,o} \,. \tag{22}$$

Such a standard state requires that

$$\gamma_{Cl_2} \longrightarrow 1 \quad \text{as} \quad C_{Cl_2} \longrightarrow 0 \quad \text{and} \quad C_{salt} \longrightarrow 0 \qquad (23)$$

Since $\gamma_{\underline{i},\underline{o}}$ was chosen to be unity

$$\gamma_{i,s} = C_{i,o}/C_{i,s} \qquad (24)$$

The fact that the activity coefficient is independent of concentration suggests that any deviation of the system from the model is not because of chlorine-chlorine intermolecular forces but because of chlorine-water intermolecular forces. If chlorine-chlorine intermolecular forces were prominent, the activity coefficient would be concentration dependent. The slight solubility of chlorine in water* also suggests that chlorine-chlorine intermolecular forces are not large because on an average the molecules are not very close together.

There exists the possibility of chlorine-water intermolecular forces. If such forces were prominent the activity coefficient would remain unity for all concentrations because of the choice of the standard state, but the system would deviate from model behavior in the standard state. In other words the standard chemical potential, $\mu_{\underline{i}}^{\underline{o},\underline{s}}$, of the model system would not be equal to the standard chemical potential in the actual system.

No attempt has been made to measure the magnitude of chlorine-water intermolecular forces. If such forces actually exist, they would be the

---

* Unhydrolyzed Cl_2-4.2 g./l. at 25°C. and P_{Cl_2} of 1 atm.

result of

--OH-Cl--

hydrogen bonding.

This type of bonding also contributes to the interaction between acetic acid and chloroform. The association constant for this interaction is listed by Pimentel and McClellan (7) as 0.2. This value is two to four orders of magnitude less than association constants representing other types of hydrogen bonding. The --OH-Cl-- bond probably only partially contributes to the acetic acid-chloroform attraction. Therefore, the force of the --OH-Cl-- attraction is comparatively small. This indicates that the chlorine-water intermolecular forces are not predominant enough in pure water to allow the system to deviate from the model.

In the salt solutions, however, the system deviates from the model because the chlorine-salt intermolecular forces are quite prominent. This is evident from the decreased chlorine solubility exhibited in the salt solutions.

The variation of the activity coefficient with the salt concentration has been shown experimentally (8) to be

$$\ln \gamma_i = b_i I_s \qquad (25)$$

for many other salt and gaseous systems where I_s is the ionic strength of the salt solution. Equation (25) does have some theoretical significance as is shown by Debye and McAulay (9). They attempted to calculate the influence the salt ions had on the chemical potential of the dissolved gas

in dilute solutions. Their results gave an equation which predicted the order of magnitude of the activity coefficient of the dissolved gas and had the same form as Equation (25).

In summary, the equilibrium solubility of chlorine in aqueous solutions can be expressed by $p_i = K' \gamma_i C_i$. For pure water γ_i is chosen to be unity, and for solutions containing an inert salt γ_i is independent of C_i but a function of salt concentration at a given temperature.

Chemical Reaction Equilibrium

If the pH of the chlorine-water system lies between one and five, the equilibrium of Reaction (2) is such that appreciable amounts of hypochlorous acid are present, and the equilibrium of Reaction (3) is shifted far to the left so that negligible amounts of hypochlorite ions are present. There have been several attempts to determine the equilibrium constant for Reaction (2). The most recent and best attempt was made by Connick and Chia (10). By measuring the equivalent conductance of chlorine-water solutions at various concentrations, they established the hydrochloric acid concentration in the solutions and through a material balance calculated the concentration of hypochlorous acid and chlorine. Equilibrium constants based on these concentrations were found to vary with concentration. However, when the activity of the hydrochloric acid was considered, the equilibrium constant based on activities remained constant with concentration. This value was $(3.944 \pm 0.020) \times 10^{-4}$ at 25°C.

At pH values greater than five the dissociation of hypochlorous acid begins to take place. At pH 10 hypochlorous acid has completely dissociated,

and all the chlorine is in the form of chloride and hypochlorite ions. The dissociation constant for hypochlorous acid is listed by Latimer (11) as 3.2×10^{-8} at 25°C.

The distribution of chlorine among these various molecular and ionic forms is shown in Table I which is based on the equilibrium constants presented above and the activity coefficient calculations of Kielland (12).

TABLE I

IONIC AND MOLECULAR CONCENTRATIONS FOR A SOLUTION 0.0400 MOLAR IN TOTAL CHLORINE AT 25°C.

pH	(H^+)	(Cl_2)	(Cl^-)	(HOCl)	(OCl^-)
0.0	1.00	.03569	.00431	.00431	
1.0	10^{-1}	.02816	.01184	.01184	
2.0	10^{-2}	.01409	.02591	.02591	
3.0	10^{-3}	.00294	.03706	.03706	
4.0	10^{-4}	.00034	.03966	.03965	--
5.0	10^{-5}	.00003	.03996	.03983	.00014
6.0	10^{-6}	--	.04000	.03864	.00136
7.0	10^{-7}		.04000	.02963	.01037
8.0	10^{-8}		.04000	.00889	.03111
9.0	10^{-9}		.04000	.00111	.03889
10.0	10^{-10}		.04000	.00011	.03989
11.0	10^{-11}		.04000	--	.04000

In the presence of ultraviolet radiation, chlorine-water solutions undergo numerous side reactions which form oxygenated chlorine compounds such as

chlorates and perchlorates. These reactions are not appreciable if prolonged contact with heat and light is avoided.

KINETIC CONSIDERATIONS

Reaction Rate Determinations

Shilov and Solodushenkov (13) attempted to measure the rate of the hydrolysis reaction by rapidly mixing a chlorine solution with water and allowing it to run at high speed past successive pairs of conductivity electrodes. The concentration of hydrogen and chloride ions at various reaction times could then be estimated from the resulting conductivity measurements. They assumed that the actual kinetic mechanism for the hydrolysis reaction could be represented by Reaction (2) and that the water concentration remained constant. The rate of chlorine disappearance was then represented as follows:

$$R_{Cl_2} = k_1 C_{Cl_2} - k_2 C_{H^+} C_{Cl^-} C_{HOCl} \quad (26)$$

k_1 and k_2 are the forward and reverse reaction-rate constants, respectively. An apparent first-order reaction-rate constant of approximately 105 $min.^{-1}$ at 1°C. was calculated for the forward reaction.

Morris (14) noted that the rate constant calculated by Shilov and Solodushenkov decreased slightly as the reaction proceeded. He suggested that this decrease could be explained if it is assumed that the hydroxyl ion partakes in the rate-determining step, because the hydroxyl ion concentration decreased as the reaction proceeds. He recalculated the data of Shilov and Solodushenkov on the basis of the mechanism

$$Cl_2 + OH^- \rightleftharpoons HOCl + Cl^- \qquad (27)$$

and obtained a second-order forward reaction-rate constant of 5×10^{14} l./(mole)(sec.) which was relatively constant with time.

Shilov and Solodushenkov (15) then made more accurate measurements and, by again assuming Reaction (2) to represent the mechanism, obtained consistent results.

Liftshitz and Perlmutter-Haymen (16) reinvestigated the kinetics of the hydrolysis reaction in an attempt to firmly establish the proper mechanism and to determine the reaction rate. They rapidly mixed a chlorine-water solution and water and measured the temperature rise of the reaction mixture as it flowed through a tube. The concentration of products at different reaction times was then calculated by assuming that the concentration changes were proportional to the temperature changes. This assumption is valid if the heat capacity of the reaction mixture and the heat of reaction remain constant as the reaction proceeds. This is probably the case because of the extremely small concentration and temperature changes involved. Their results gave an apparent first-order reaction-rate constant of 5.60 ± 0.45 sec.$^{-1}$ at 9.5°C. by assuming Reaction (2) to be the proper mechanism and gave inconsistent results when the hydroxyl ion was assumed to be the reactant.

Hydrolysis Reaction Mechanism

Eigen (17) states that bimolecular reactions in aqueous solution involving hydrogen or hydroxyl ions usually have rate constants in the order of 10^{10} to 10^{11} l./(mole)(sec.). The calculations of Onsager (18), Debye

(19), and others (20, 21) show that ions in solution must combine on every collision to exhibit a reaction rate constant of this order. Thus, Morris's constant of 5×10^{14} l./(mole)(sec.) is several orders of magnitude higher than the theoretical upper limit.

Liftshitz and Perlmutter-Haymen (16) state that at the low pH's exhibited by chlorine-water solutions the hydroxyl ion cannot be regenerated at a sufficient rate to satisfy the chlorine demand. The data of Eigen and deMaeyer (22) show that the rate of formation of hydroxyl ions in water is 1.4×10^{-3} l./(mole)(sec.) at 25°C. which is much slower than the rate of hydrolysis of chlorine at this temperature.

At high hydroxyl ion concentrations where the dissociation of water is unimportant, the reaction is between the hydroxyl ions and chlorine as is evident by the absorption experiments of Pozin (23) which will be discussed later. This cannot be classified as a hydrolysis reaction, but it does indicate that Reaction (27) is probably taking place even at low pH's. Its influence on the over-all reaction rate is not shown until relatively high pH's are reached. At what point this influence becomes controlling is not known.

In summary, there is much theoretical and experimental evidence showing that the kinetic mechanism suggested by Morris does not represent the rate-controlling hydrolysis reaction of chlorine in pure water. However, there is evidence showing that at high hydroxyl ion concentrations the rate-controlling reaction is between chlorine and the hydroxyl ion. In other words there exists the possibility that both Reaction (2) and Reaction (27) are taking place in water and that depending upon the pH, one, the other, or both are rate controlling.

THE PENETRATION THEORY OF GAS ABSORPTION

THE MATHEMATICAL MODEL

Physical Absorption

The mathematical model comprising the penetration theory consists of a semi-infinite liquid phase which is suddenly brought into contact with a gas phase containing a soluble gas. The interface of the liquid phase is assumed to be immediately at the equilibrium concentration of soluble gas. The gaseous solute then begins to diffuse or "penetrate" into the liquid phase. Because of the equilibrium condition at the interface every molecule which diffuses from the interface is immediately replaced by a molecule from the gas phase. The rate of gas absorption then is equal to the rate of diffusion of the gaseous solute molecules away from the interface.

If Fick's first law of diffusion holds for the system involved, the rate of diffusion per unit area past a given plane in the liquid is equal to the diffusivity times the negative concentration gradient at that plane. If no chemical reaction takes place between the solute and solvent, the rate of accumulation of solute within a differential segment in the liquid phase is equal to the rate of diffusion into the segment minus the rate of diffusion from the segment. This is illustrated in Fig. 1.

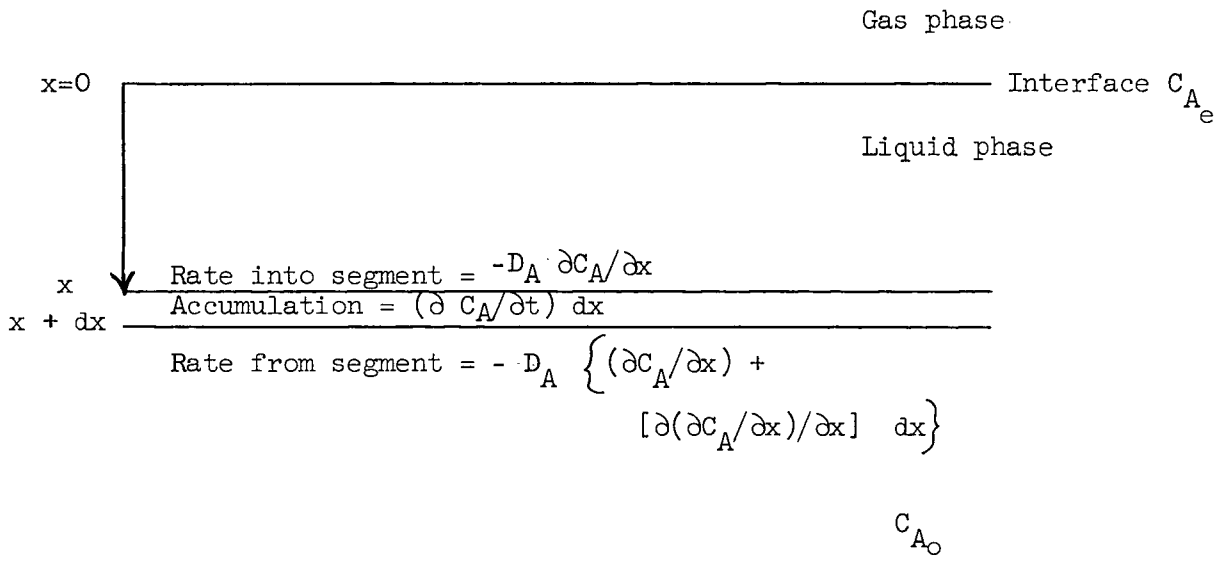

Figure 1. Unsteady State Diffusion in Liquid

Writing this material balance gives

$$(\partial C_A/\partial t)dx = -D_A(\partial C_A/\partial x) + D_A \left\{\partial C_A/\partial x + [\partial(\partial C_A/\partial x)/\partial x]\, dx\right\}, \qquad (28)$$

or

$$\partial C_A/\partial t = D_A\, \partial^2 C_A/\partial x^2, \qquad (29)$$

where $\underline{D_A}$ is the diffusion coefficient of the solute $\underline{A}$ in the absorbent. It is assumed that $\underline{D_A}$ ~~is assumed that $\underline{D_A}$~~ is independent of concentration.

The rate of absorption or the rate of diffusion from the interface is found by solving Equation (29) for $\partial \underline{C_A}/\partial \underline{x}$ as a function of $\underline{x}$ and $\underline{t}$ and letting $\underline{x} = 0$.

$$N_A = -D_A(\partial C_A/\partial x)_{x=0}\ . \qquad (30)$$

The boundary conditions required to find such a solution are obtained by assuming that at zero time there exists no concentration gradients

within the liquid and by assuming continuous equilibrium at the interface. These conditions are

$$C_{A(x,o)} = C_{A,o} \tag{31}$$

and

$$C_{A(o,t)} = C_{A,e} \cdot \tag{32}$$

Another condition which is a consequence of Equation (29) is

$$C_{A(\infty,t)} = C_{A,o} \cdot \tag{33}$$

The mathematical details of the solution of Equation (29) with these boundary conditions is given in Appendix I. The instantaneous rate of absorption after a time, $\underline{t}$, is found to be

$$N_A = (C_{A,e}-C_{A,o}) \sqrt{D_A/\pi t} , \tag{34}$$

After integrating over the total time of exposure, $\underline{t_e}$, the average rate of absorption for this period is

$$\overline{N}_A = 2(C_{A,e}-C_{A,o}) \sqrt{D_A/\pi t_e} . \tag{35}$$

The liquid side mass transfer coefficient, $\underline{k_L}$, which is defined as the average rate of absorption divided by the driving force is then given by

$$k_L = 2\sqrt{D_A/\pi t_e} . \tag{36}$$

Equation (29) and its particular solutions have long been utilized in heat transfer and diffusion studies. It was not until 1935 that Higbie (1) suggested that this mathematical model could be used to describe gas

absorption, provided that the conditions of the system coincide with the assumptions involved in deriving and solving the equations.

At this time it might be wise to list the assumptions involved in the penetration theory.

1. There is no relative motion within the fluid.
2. There exist no concentration gradients within the liquid at the beginning of the exposure period.
3. The depth of penetration of solute molecules must never reach a boundary plane in the liquid.
4. The interfacial liquid concentration remains in equilibrium with the gas phase at all times.
5. Fick's laws of diffusion are valid for the system involved.

Absorption with Chemical Reaction

When the gaseous solute undergoes a chemical reaction in the liquid phase, the concentration of solute molecules is less at any given plane (except at the interface) than if there were no chemical reaction. This causes the concentration gradient of the solute to increase, which in turn increases the rate of diffusion from the interface or, in other words, increases the rate of absorption. The alteration of the concentration profiles by chemical reaction is illustrated in Fig. 2.

When a chemical reaction takes place the rate of accumulation of solute in a differential segment of the liquid becomes equal to the rate of diffusion into the segment minus the rate of diffusion out of the segment minus the rate of depletion of the solute due to chemical reaction, R_i. The differential equation describing this situation is

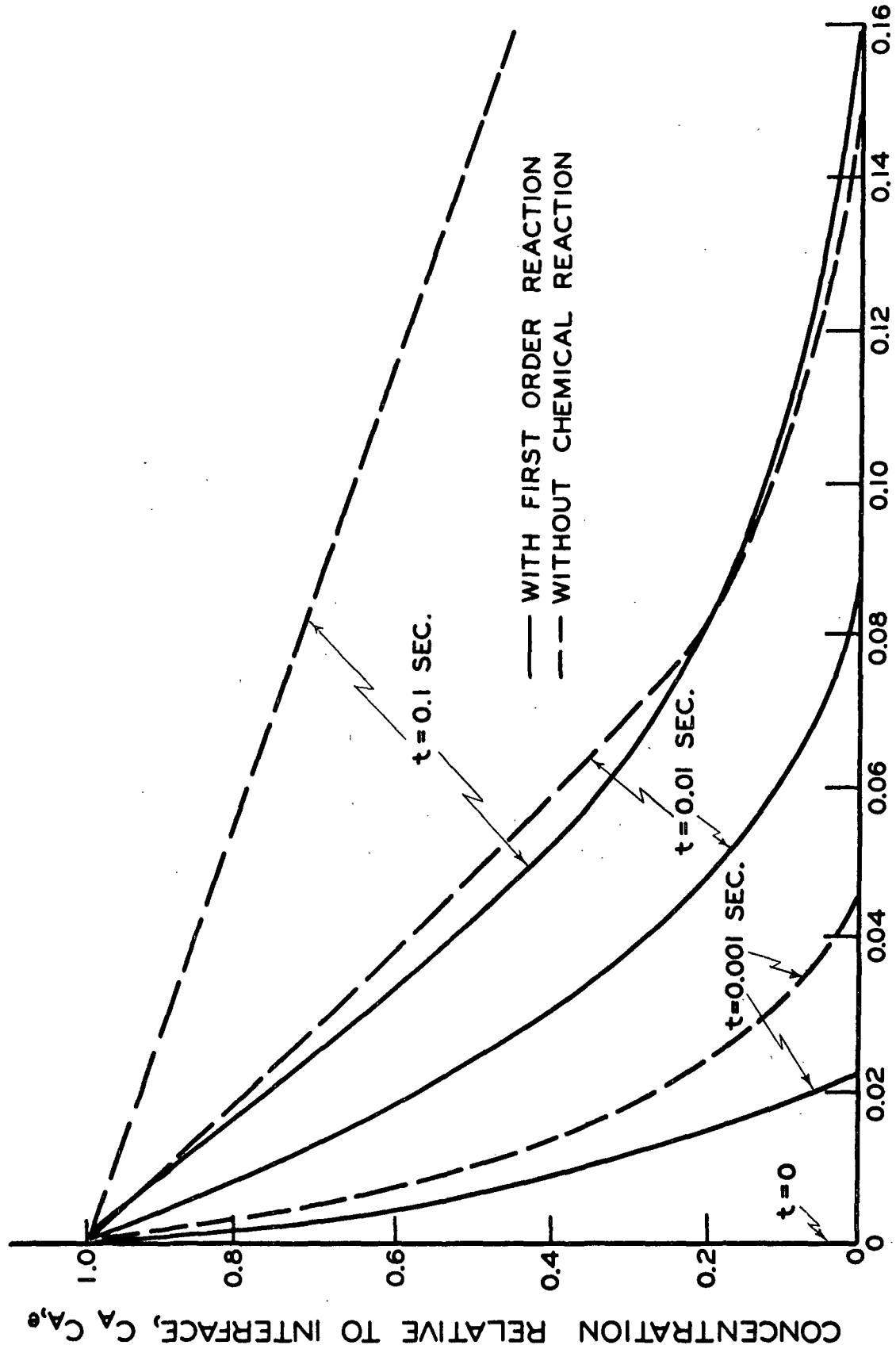

Figure 2. Typical Concentration Profiles for Absorption as Calculated by Pigford (81)

$$\partial C_i/\partial t = D_i \partial^2 C_i/\partial x^2 - R_i \quad . \qquad (37)$$

It becomes necessary to write such an equation for each molecular species taking part in the reaction in order to completely describe the system.

Solutions to Equation (37) for various types of chemical reactions have been found by Danckwerts (24) and others (25-27). The mathematical details for a first-order irreversible reaction and for an infinitely fast chemical reaction are presented in Appendix I.

Solutions to Equation (37) may be presented in the general form

$$\bar{N}_A = 2(C_{A,e}-C_{A,o})\sqrt{D_A/\pi t_e} \cdot \Phi . \qquad (38)$$

The function, Φ, is a function of some or all of the following: exposure time, initial product and reactant concentrations, product and reactant diffusivities, reaction rate constants, and the equilibrium constant. It is convenient to express the solutions in the form of Equation (38) because the factor, Φ, then becomes equal to the average rate of absorption with chemical reaction divided by the average rate of absorption without chemical reaction. This ratio is always greater than unity for absorption with chemical reaction.

THE PENETRATION THEORY AS APPLIED TO CHLORINE ABSORPTION

Previous Work

Vivian and Whitney (28) investigated the absorption of chlorine into water in a tower packed with 1-inch Raschig rings at various liquid flow rates and found that the absorption rate was greater than that predicted

from previously taken oxygen data. Craig (29) then absorbed chlorine into 0.15N hydrochloric acid on the same tower and over the same flow rate range. Liquid mass transfer coefficients based upon an unhydrolyzed chlorine driving force were then calculated for each run. The best line through each set of data is shown in Fig. 3.

The ratio of a value on line AA to a value on line BB at a given liquid flow rate then becomes the function, Φ, which represents the influence of chemical reaction on the rate of absorption. At low liquid flow rates (1000 lb./hr. sq. ft.) where the time of exposure, t_e, is large, the presence of the hydrolysis reaction increases the rate of absorption by a factor of $\Phi = 1.6$. At high liquid flow rates (15,000 lb./hr. sq. ft.) where the time of exposure is not great enough for the reaction to remove an appreciable amount of chlorine, the function Φ approaches unity.

Direct application of the penetration theory to packed tower data is difficult because of the uncertainty in describing the hydrodynamic characteristics of the tower. It is required to assume that as the liquid flows over a piece of packing, laminar flow exists and that after the fluid leaves one piece of packing and comes upon the next, complete mixing occurs. Also the exposure time of the liquid on a packing piece can only be estimated.

The data of Vivian and Whitney and of Craig are analyzed in accordance with the above assumptions in Appendix X. The factor, Φ, is estimated as a function of exposure time. A first-order irreversible reaction between chlorine and water is assumed, and its rate constant calculated. This constant compares favorably with that obtained by Shilov and Solodushenkov (15)

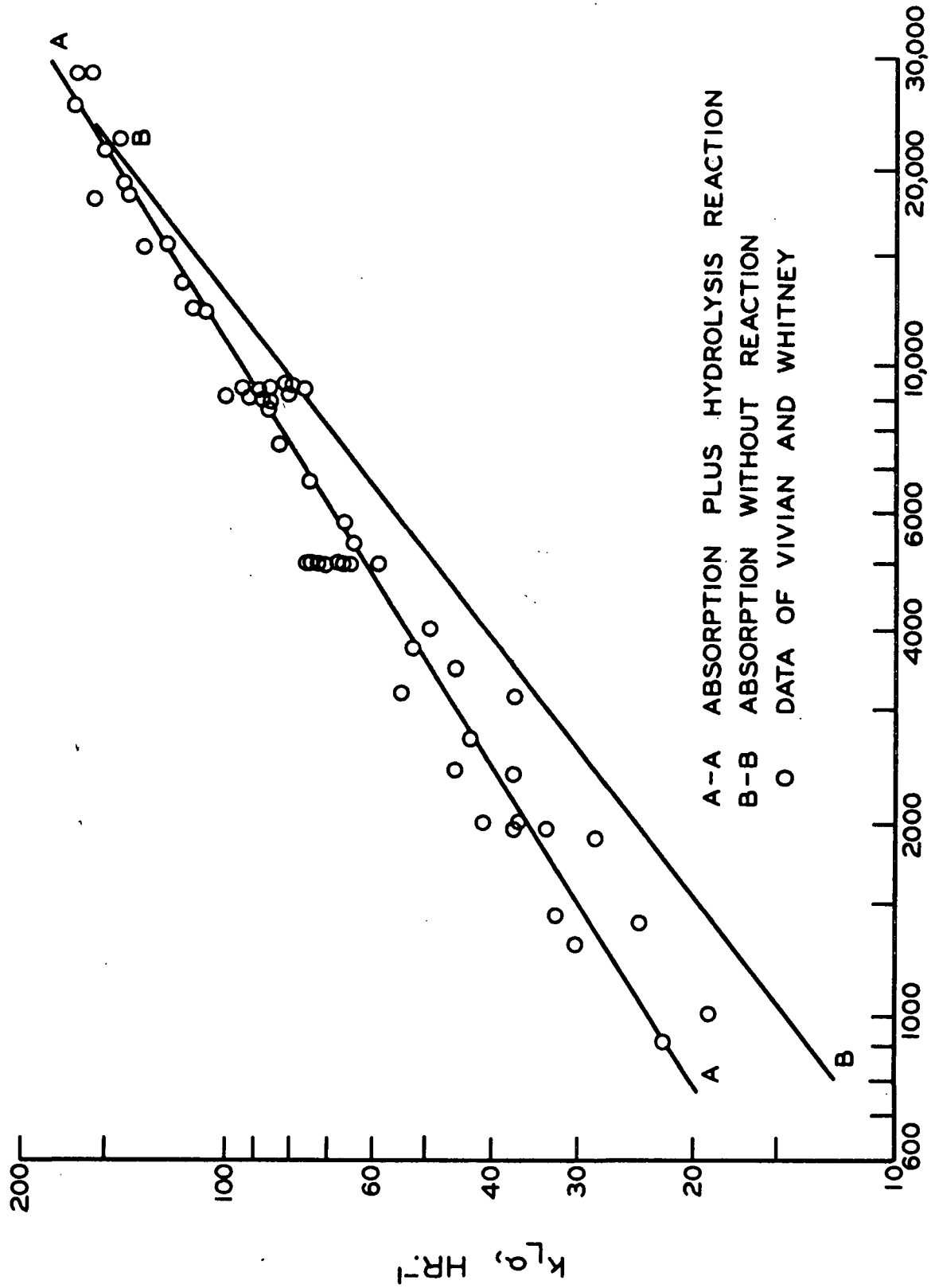

Figure 3. Mass-Transfer Coefficients of Vivian and Whitney (28) and Craig (29) as a Function of Liquid Flow Rate

which indicates the validity of the assumptions made. The topic of packed towers and the penetration theory is discussed further in Appendix X.

Vivian and Whitney (30) were the first to correlate gas absorption with chemical reaction data by using the unreacted solute species as a driving force instead of the total concentration of reactant and products. The penetration theory states that it is the diffusion of the unreacted species away from the interface which determines the rate of absorption. The chemical reaction merely alters this diffusion process. Thus, the driving force of unreacted solute is in conformance with the penetration theory and is indeed the only realistic driving force.

Pozin (23) investigated the absorption of chlorine in sodium hydroxide solutions on a wetted-wall column. He assumed that the reaction was between chlorine and hydroxyl ions and was infinitely rapid. Hydrodynamic effects prevented him from getting exact agreement with the penetration theory for absorption with an infinitely fast reaction (see Appendix I), but he was able to correlate his data in the form of the theoretical equation, particularly with regard to the role of the hydroxyl ion. This indicates that the assumptions concerning the kinetics of the reaction are valid.

Peaceman (31) studied the desorption of chlorine from dilute hydrochloric acid solutions and from water on short wetted-wall columns (1/2 to 2 inches). The desorption of chlorine from hydrochloric acid solutions resulted in rates that were 10 to 30% lower than the rates predicted by the penetration theory of physical absorption. This difference was attributed

to an incomplete analysis of the hydrodynamics within the wetted-wall columns and not to a fallacy in the penetration theory. Chlorine was then desorbed from water, and the factor, Φ, determined as a function of initial chlorine concentration and a hypothetical exposure time calculated from the physical absorption measurements. Equation (37) was simplified by assuming steady state diffusion ($\partial C_A/\partial t = 0$) and solved for the reaction mechanism suggested by Shilov and Solodushenkov and also the one suggested by Morris. The reaction-rate constants calculated by each of these investigators were used. The experimental points did not correlate with either of the proposed mechanisms. Both reaction mechanisms predicted a decrease in Φ with concentration, whereas the experiments seemed to show an increase at total chlorine concentration greater than 0.04 moles/l. Peaceman offered no explanation for this behavior. The oversimplification of the hydrodynamics in the wetted-wall column and the large scatter in Peaceman's data are believed to be factors contributing to the poor agreement with theory.

Kinetic Information from Gas Absorption Measurements

Analysis of the previous work on chlorine absorption in terms of the penetration theory has yielded some kinetic information about the chlorine hydrolysis reaction. Such absorption experiments are usually easier to carry out than direct kinetic measurements and therefore are a valuable tool in studying the kinetics of reactions between soluble gases and liquids.

It is suggested that exact controlled determinations of the function, Φ, for the absorption of chlorine into water should yield kinetic information which would clarify the unknown aspects of the chlorine hydrolysis reaction, i.e., the mechanism and speed of the reaction in various pH ranges.

THE DRIVING FORCE-RESISTANCE CONCEPT

It has been found convenient to analyze the rate of transport processes in terms of the driving force-resistance concept. The rate of the process is expressed as a driving force divided by a resistance. The only requirement governing the choice of the driving force and resistance is that when the process has progressed to equilibrium, the rate expression satisfies all thermodynamic axioms. Ideally, it would be desirable to choose a driving force which satisfies the thermodynamic requirements and is independent of the resistance. The rate would then be directly proportional to the driving force. Such is the case with electrical circuits obeying Ohm's law.

DIFFUSION

In gas absorption work when the rate of absorption is expressed in terms of a liquid phase driving force, concentration units are usually used. For systems exhibiting model behavior this practice is satisfactory because these systems usually follow Fick's first law of diffusion,

$$J = -D_A \nabla C_A \tag{39}$$

which is an experimental law. $\underline{J}$ is the rate of diffusion per unit area. Some model systems, however, have diffusion coefficients which are not independent of the concentrations. In these cases an average value of the diffusivity over the concentration range used is employed in Equation (39). Such an average value may be defined as follows:

$$\bar{D}_A = [1/(C_2-C_1)] \int_{C_1}^{C_2} D_A \, dC \tag{40}$$

When the system does not exhibit model behavior some workers choose to express absorption rates with a concentration driving force (32), while others use an activity or thermodynamic driving force (34). From a practical standpoint it is an arbitrary choice which driving force is employed because both satisfy the thermodynamic requirement at equilibrium and because of the concept of average transfer coefficients. The choice is usually governed by the availability of data and by convenience.

From a fundamental viewpoint, however, the thermodynamic driving forces of activity or chemical potential are closer than concentration to the actual causes of mass transfer. When a molecule diffuses from one point to another, it undergoes a random walk process the net result of which is a transfer of the molecule in a particular direction. The cause of this random process is that the molecule is influenced by the electrostatic and magnetic force fields of its neighbors. The thermodynamic properties of activity and chemical potential are more closely related to these intermolecular forces than is concentration. In many instances mass may be transferred from regions of low concentration to regions of high concentration, as in the case of absorption of a gas into a liquid across an interface. However, mass transfer always occurs in the direction of lower chemical potential.

The second law of thermodynamics states that every system undergoing an irreversible process is accompanied by an increase in entropy if the process is unaffected by external forces. It can be shown (36) that the rate of increase of entropy is related to the rate of the process as follows

$$ds/dt = \sum_k J_k X_k > 0 \qquad (41)$$

where J_k is the process rate and X_k is a generalized force or affinity. With this as a starting point many theories have been developed (37-39) through the use of molecular mechanics which attempt to describe such rate processes as heat conduction and Brownian motion or diffusion.

These theories are far from complete because of the molecular assumptions that must be made. In certain limiting cases, however, the theories do lead to the common experimental laws such as Fick's first law with a thermodynamic driving force.

Despite these considerations, concentration is continually used as the driving force for absorption into nonideal systems. The resistance then becomes a strong function of the intermolecular forces. It is felt that if a thermodynamic driving force is used in conjunction with the driving force-resistance concept, the resistance will then become less a function of the intermolecular forces and thus, should correlate more simply with the properties of the system.

CHEMICAL REACTION

For a chemical reaction to take place the reacting molecules must come close enough to one another to form some sort of combination. The factors governing the rate at which the molecules reach this degree of closeness are all related to the intermolecular forces. Thus, any expression of the reaction rate in terms of a driving force and a resistance should be made with a driving force that is a strong function of these

forces. For this reason it would be expected that a thermodynamic driving force would yield more consistent results than a concentration driving force.

In most reaction-rate studies the reaction-rate constant is defined in terms of a concentration driving force. This practice is very satisfactory for systems that do not deviate markedly from ideal behavior. For nonideal systems, however, the reaction rate constants become a function of the deviation from ideality. In ionic solutions, for example, the reaction rate constant is a function of the ionic strength of the solution. The use of an activity driving force in these cases does not yield independent reaction-rate constants but does greatly simplify the dependence of the constant on the ionic strength. This is illustrated by considering the transition-state theory of reaction rates.

It is assumed in this theory that during a chemical reaction an activated complex is formed which is in equilibrium with the reactants and that the rate of the reaction is proportional to the concentration of this activated complex. Considering the reaction

$$A + B \rightleftharpoons M^{\ddagger} \longrightarrow \text{Products} \qquad (42)$$

where $\underline{A}$ and $\underline{B}$ are the reactants and $\underline{M}^{\ddagger}$ is the activated complex. The rate of the reaction is equal to

$$\epsilon\, C_{M^{\ddagger}} \qquad (43)$$

where ϵ is the proportionality constant which is a function of temperature. The equilibrium of Reaction (42) can be expressed by an equilibrium constant, $\underline{K}_{\underline{S}}^{\ddagger}$.

$$K_S^{\ddagger} = a_{M^{\ddagger}}/a_A a_B = (C_{M^{\ddagger}}/C_A C_B)(\gamma_{M^{\ddagger}}/\gamma_A \gamma_B) \tag{44}$$

Thus,

$$\text{rate of reaction} = \epsilon K_S^{\ddagger} C_A C_B \gamma_A \gamma_B / \gamma_{M^{\ddagger}} \tag{45}$$

Thus, in terms of a concentration driving force the rate constant is

$$\epsilon K_S^{\ddagger} \gamma_A \gamma_B / \gamma_{M^{\ddagger}} , \tag{46}$$

while in terms of an activity driving force the rate constant is

$$\epsilon K_S^{\ddagger} / \gamma_{M^{\ddagger}} . \tag{47}$$

It is seen that an activity driving force results in a rate constant which is less of a function of the solution nonideality than is the rate constant defined in terms of a concentration driving force. This has been shown experimentally for some systems (40).

Reaction rates are sometimes analyzed in terms of the collision theory. In this theory the rate of the reaction is said to be equal to the number of collisions between the reacting molecules per unit of time times the probability that a collision results in chemical combination. The rate of collision is assumed to be proportional to the concentration of each reacting species for systems that are thermodynamically ideal. The theory is seldom applied to thermodynamically nonideal systems and thus does not indicate the most suitable driving force.

THE CHOICE OF THE ABSORPTION APPARATUS

VARIOUS APPARATUS TYPES

It is necessary to choose an absorption apparatus in which the hydrodynamic characteristics are simple enough to be readily analyzed and closely correspond with the assumptions and limitations of the penetration theory. Several different types of apparatus have been tried with varying degrees of success. Many of these are listed in Table II with the appropriate references.

Disk, sphere, gas bubble, and falling drop columns are not suitable for the present study because of the difficulty in analyzing the hydrodynamics of the liquid movement. The single gas bubble is not applicable because the exposure periods required for measurement are so long that the chlorine-hydrolysis reaction would reach equilibrium at the liquid interface and thus hamper the study of the kinetics of the reaction.

Wetted-wall columns have been used with some success but have the shortcomings of surface rippling and end effects. Long columns create a rippling effect on the water surface which alters the interfacial area available for absorption and distorts the concentration gradients set up within the liquid. Short wetted-wall columns eliminate this rippling effect but create end effects which are difficult to correct for.

Danckwerts' (51) rotating drum apparatus has been shown to present a good liquid surface to the gas for absorption except at the entrance and exit points where a slight rippling occurs. This apparatus might have been suitable for this study except for the difficulty and expense involved in

TABLE II

SUMMARY OF GAS ABSORPTION APPARATUS

Apparatus	Description	Reference
Wetted-wall column	The liquid enters the column over a weir and flows down the inside of a cylindrical tube in a thin film. The gas flows counter- or co-current to the liquid through the tube.	(31,41-45)
Disk column	The liquid enters the column and flows over a series of disks arranged edge to edge and at right angles to each other. The gas flows through a chamber surrounding the disks.	(46)
Sphere column	The liquid flows over a column of spheres resting one atop of another. The gas flows through a chamber surrounding the spheres.	(47)
Single gas bubbles	A single bubble of the gas is generated at a point and either its rate of decay is measured or the amount of gas required to keep it at a constant size is determined.	
Gas bubble column	A column is filled with the liquid and the gas is allowed to bubble up through it.	(48,49)
Falling-drop column	A column is filled with the gas and the liquid falls through it in drops.	(50)
Rotating drum	A cylindrical drum is rotated through the liquid picking up a thin film which is then exposed to the gas for a measurable time period.	(51)
Liquid jets	The liquid is issued from a nozzle into an atmosphere of the gas. The cylindrical column of flowing liquid is then suddenly terminated, ending the exposure period.	(52-54)

constructing it in such a manner that it would not be attacked by wet chlorine gas or chlorine-water. Also the range of exposure times that may be used is limited.

LAMINAR LIQUID JETS

It was decided that the laminar liquid jet best fulfilled the requirements of the thesis. The jet can be made to present the liquid to the gas with a minimum of disturbance and to suddenly terminate the exposure period without entraining any gas and without appreciable end effects. The interfacial area and exposure time are readily estimated and varied. A range of exposure times are available, and the construction of the apparatus is relatively simple.

When the liquid leaves the jet nozzle, it forms a smooth flowing cylinder into which the gas is absorbed. The time which the liquid is exposed to the gas can be regulated by the flow rate and length of the jet.

There are two other factors which influence the exposure time, however. First, as the liquid leaves the nozzle it is accelerated by gravity. This effect can be accounted for by calculating the jet velocity as the jet moves downward. Second, the velocity at the jet surface is zero at the nozzle exit because of the drag against the walls of the nozzle. This surface velocity quickly approaches the main velocity of the jet and a flat velocity profile results. The effect of this velocity lag on the exposure time can be estimated from the boundary-layer theory.

Appendix III gives a complete discussion of absorption in a laminar liquid jet.

APPARATUS AND PROCEDURES

THE SECONDARY EXPERIMENTS

PHYSICAL PROPERTIES OF ABSORBENTS

The densities of the salt solutions were measured in a 25-ml. pycnometer at 25°C. The viscosities were measured in a modified Oswald viscometer with an efflux time of 61 seconds for distilled water at 25°C. These values were needed to analyze the hydrodynamics of the jet and to calculate the absorption rates.

SOLUBILITY MEASUREMENTS

The equilibrium solubility of molecular chlorine in the absorbents was needed to analyze the absorption rates in terms of the penetration theory.

At first an attempt was made to measure the solubility of chlorine in the various absorbents by bubbling nitrogen-chlorine mixtures through the solution for a long period of time and then sampling and analyzing the gas and the solution. It was found that a supersaturation of the chlorine occurred which made it difficult for the system to reach equilibrium. It was felt that the supersaturation occurred because of the dynamic approach to equilibrium, i.e., the continued bubbling of gas.

The absorbent and chlorine gas were then placed in a two-necked spherical bulb. For most of the runs the pressure of the gas was made to be slightly above atmospheric. Equilibrium was allowed to take place statically, i.e., the gas was not bubbled through the absorbent. The

bulb was shaken slightly in a constant temperature bath to create new liquid surface and speed the approach to equilibrium. After a suitable time period, the pressure in the bulb was relieved by opening it to the atmosphere for a fraction of a second. Equilibrium was obtained again, causing chlorine to desorb from the solution and build up a pressure within the bulb. This process was repeated several times until finally the solution was in equilibrium with saturated chlorine at a pressure which was the same as the atmosphere.

For the runs made at reduced pressure the chlorine pressure was reduced with an aspirator and equilibrium allowed to take place. The equilibrium pressure was measured with a manometer.

After equilibrium the solutions were sampled and analyzed. Great care was taken to prevent a change in the solution concentration during the sampling and analyzing procedures.

A detailed discussion of these procedures is given in Appendix IV.

DIFFUSIVITY MEASUREMENTS

The diffusion coefficient of molecular chlorine in the absorbents was required to analyze the absorption rates in terms of the penetration theory.

Attempts were made to measure the diffusivity of the unhydrolyzed chlorine in the absorbents by a sintered glass diaphragm method similar to that used by Peaceman (31). The aqueous chlorine solutions were placed on one side of the diaphragm and the solvent on the other. Diffusion was

allowed to take place through the diaphragm. Consistent results could not be obtained.

The diffusivity of chlorine through 0.15N hydrochloric acid was measured on a Beckman, Spinco Model-H electrophoresis-diffusion apparatus. In this apparatus a free boundary between the chlorine solution and the solvent was formed and diffusion allowed to take place. The progress of the diffusion process was followed by measuring the index of refraction changes as the boundary spread. These changes were photographed as Rayleigh interference fringes. If it is assumed that the index of refraction of the solution is a linear function of the concentration, the diffusion coefficient can be calculated from these fringe patterns and the amount of time that diffusion had been taking place.

Details of these methods are given in Appendix V.

THE ABSORPTION EXPERIMENTS

Absorption experiments were carried out in 0.10N hydrochloric acid to test the applicability of the penetration theory to the system, in concentrated acidic sodium chloride solutions to determine the effect of thermodynamic nonideality on the absorption rates, in acidic and basic solutions to study the chlorine-water reaction kinetics, and in sodium sulfate solutions to determine the effect of solution ionic strength on the rate of chlorine hydrolysis.

ABSORPTION APPARATUS

The absorption apparatus is similar to that used by Scriven (54). A schematic diagram of the apparatus is shown in Fig. 4. A complete

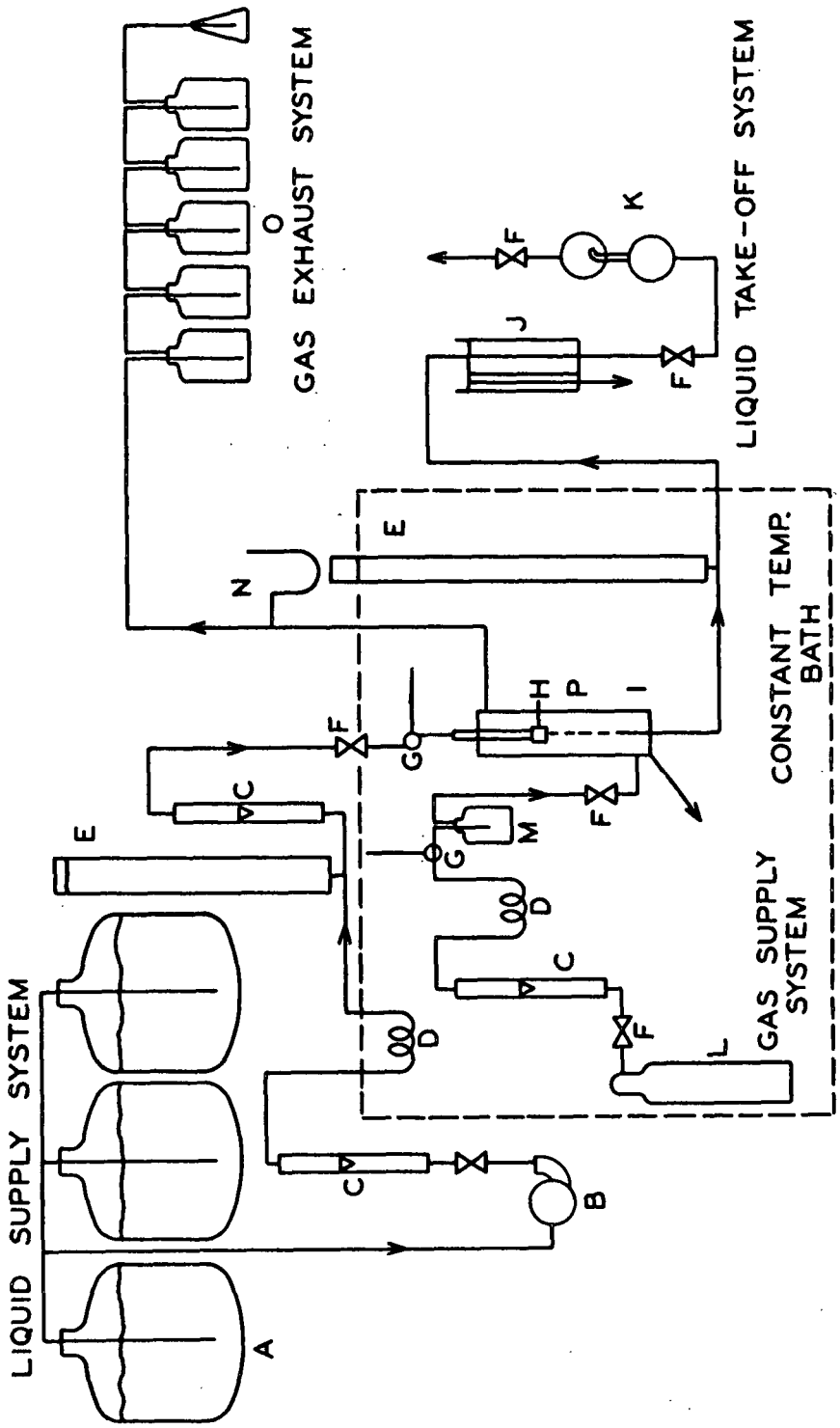

Figure 4. The Absorption Apparatus

detailed description of its components and auxiliaries is given in Appendix II. A general description follows.

Liquid Supply System

During an absorption run the absorbent was pumped from the storage bottles, through a rotameter and a coil, past a surge tube, through another rotameter and into the jet nozzle. The surge tube was placed as close to the jet nozzle as possible so that any variations in flow rate which occurred before the nozzle would be dampened. Rotameters and valves were placed before and after the surge tube to facilitate adjustment of the flow so that the level in the surge tube remained constant. No variations or oscillation in the flow delivered to the nozzle could be detected.

The Jet Nozzle and Take-off Tube

The absorbent flowed through a straight portion of tube into the nozzle and issued as a small cylindrical jet. The jet nozzle had a bell-shaped orifice with an exit diameter of 1.65 mm. The appearance of the jet is shown in Fig. 5. The position of the jet was adjusted by an aligning mechanism so that the chlorine-water flowed into a take-off tube. The height of the fluid in the take-off tube was regulated to be level with the top of the take-off tube so that no entrainment of chlorine gas could occur. (See Fig. 8.)

Liquid Take-off System

After leaving the jet chamber the chlorine-water flowed past a surge tube into a leveling device, through a sampling pipet and to the drain.

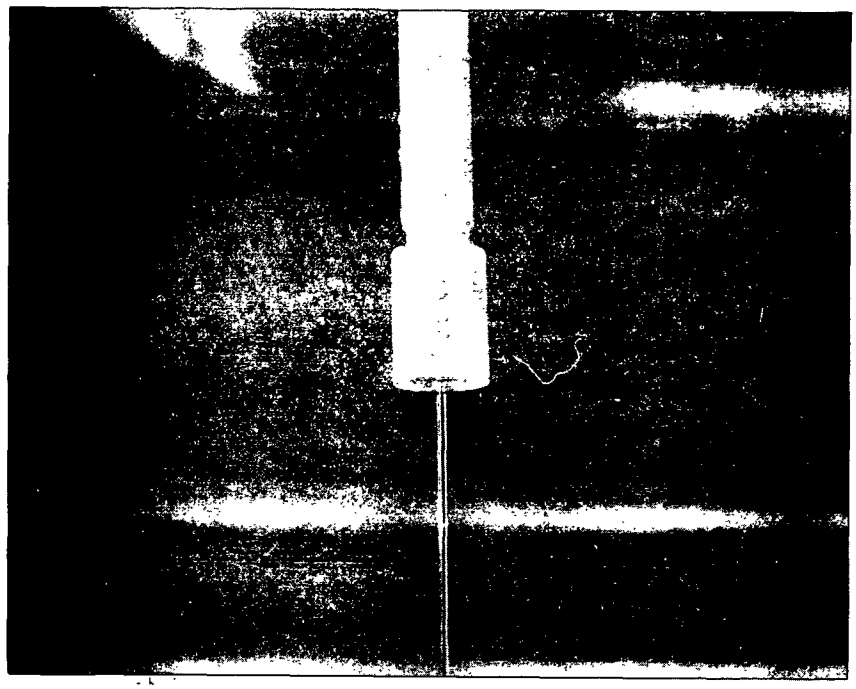

Figure 5. Appearance of Jet
(2/3 actual size)

The surge tube was placed in this line to provide a means of getting rid of small bubbles of gas which collected on the walls of the line during the adjustment period of a run. A fine plastic coated wire was run down the tube and along the line to knock off the bubbles.

The level of the absorbent in the take-off tube was adjusted by means of a leveling device. The height of the liquid in the leveling tube above the top of the take-off tube was equal to the jet velocity head plus the pressure head inside the chamber when proper adjustment was reached. There was no danger that desorption of chlorine from the leveling tube would affect the results because the inlet stream of chlorine water was just above the outlet point. Any chlorine-water that did reach

the surface had to go down the down-comer to the drain and could not reach the sampling pipet.

The chlorine water then flowed through the sampling pipet to the drain. The sampling pipet was double-bulbed so that the delivered sample was never exposed to the air or to a weaker solution.

The Gas Supply and Exhaust System

Pure chlorine gas was issued from a cylinder, filtered, metered, brought to temperature, saturated with water vapor, and allowed to flow into the jet chamber around the jet. After leaving the jet chamber, the chlorine was exhausted by bubbling it through 25% sodium hydroxide.

PROCEDURES FOR THE ABSORPTION RUNS

Preparation of Solutions

All of the absorbent solutions were made with degassed, distilled water. The degassing unit is described in Appendix II. The water used had the following analysis after degassing:

% solids	-	0.00
Specific resistance	-	320,000 to 500,000 ohm cm.
Dissolved oxygen	-	0.3 to 0.8 p.p.m.
pH	-	6.95 - 7.00

Acidic and basic absorbents were made by preparing concentrated standard solutions of hydrochloric acid, sulfuric acid, and sodium hydroxide, analyzing them in accordance with methods described in Appendix VI, and diluting an aliquot of them to volume. The concentrated sodium chloride and sodium sulfate solutions were prepared by dissolving the salt in a

portion of the liquid and then diluting to volume. At all times care was taken not to introduce air into the solution. A layer of n-heptane was placed on the prepared solutions to reduce air absorption during storage. The solubility of n-heptane in the absorbents is not great enough to affect the results. The solutions were never stored more than 15 hours before use.

Starting a Run

The pump was started and the surge tube filled with absorbent. Next the absorbent was allowed to flow from the nozzle and flood the jet chamber, the excess being siphoned from the chamber to the drain. Suction was then applied to the nozzle approach tube by a squeeze bulb through a tee. This sucked absorbent back through the nozzle from the chamber and cleared the nozzle and its approach tube of air bubbles. The chamber was then drained while the absorbent continued to flow. When the chamber was drained, the jet was adjusted to hit the center of the take-off tube. The leveling device and sampling pipet were then filled. Next the gas was turned on and the pressure in the jet chamber allowed to build up. During this procedure any overflow from the take-off tube was siphoned to the drain. At this point the level in the take-off tube was adjusted to be about 1 cm. below the top of the tube. See Fig. 6. The jet position was then finely adjusted to hit the exact center of the take-off tube. Considerable entrainment of gas resulted with the level in this position. The level in the take-off tube was then adjusted so that a slight overflow of absorbent occurred. See Fig. 7.

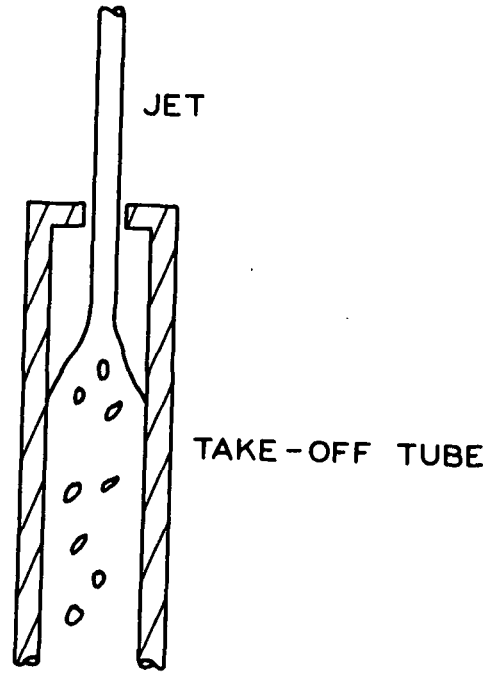

Figure 6. Centering the Jet

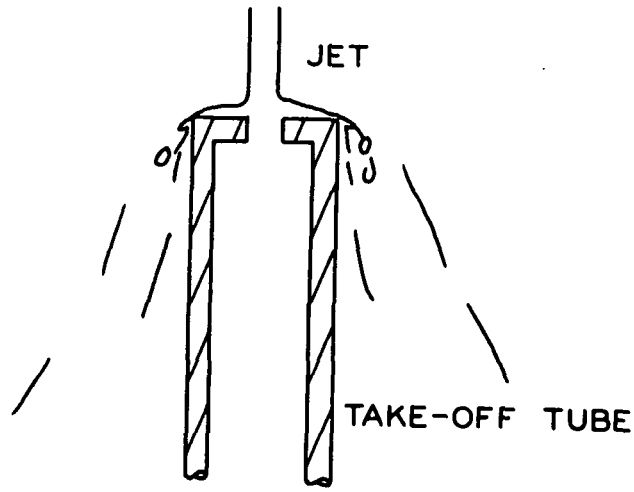

Figure 7. Flooding the Jet

This allowed the entrained bubbles to be removed from the walls of the take-off tube and subsequent tubing without entraining any more gas.

The level in the take-off tube was then adjusted so that it was even with the top of the tube. See Fig. 8.

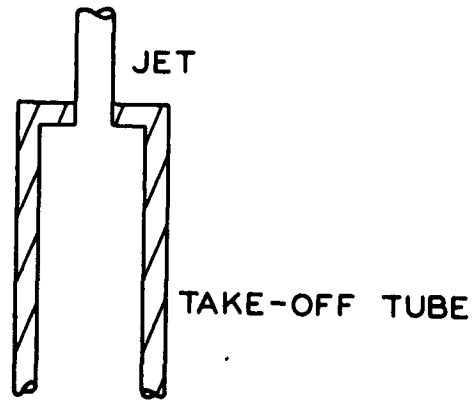

Figure 8. The Stable Jet

The system was stable in this position for as long as the absorbent supply lasted or until a drastic change in atmospheric pressure occurred.

Continuing and Ending a Run

The chlorine water was allowed to flow through the sampling pipet until about ten volumes had passed. During this time the temperature of the water bath, the gas stream, and the inlet and outlet liquid streams were recorded. The gas and liquid rotameter readings were noted. The atmospheric and chamber pressures were measured, and preparations were made for sampling. A sample was taken by removing the sampling pipet and diverting all the chlorine water down the leveling tube down-comer. The sample was introduced beneath the surface of a 10% potassium iodide solution and the pipet was returned to the apparatus to collect a new sample.

While the sampling pipet was being refilled, the chlorine water from both the down-comer and pipet was run into a tared flask for four minutes. The flask was then stoppered and weighed to obtain the flow rate.

Three samples were taken for each run and analyzed as described in Appendix VI.

After the last sample was taken the pump and chlorine cylinder were turned off and the solution allowed to drain from the system. If a new solvent was to be used for the next run the system was flushed with water. Finally the height of the jet nozzle orifice above the top of the take-off tube was measured with a cathetometer.

RESULTS AND DISCUSSION

THE SECONDARY EXPERIMENTS

THE PHYSICAL PROPERTIES OF THE ABSORBENTS

The densities and relative viscosities of all the absorbents used are given in Table III. Those values marked with an asterisk were taken from the International Critical Tables (56). The others were determined experimentally.

TABLE III

DENSITY AND RELATIVE VISCOSITY OF AQUEOUS SOLUTIONS OF SODIUM SULFATE, SODIUM HYDROXIDE, AND SODIUM CHLORIDE--0.1N HYDROCHLORIC ACID, AS A FUNCTION OF CONCENTRATION AT 25°C.

Solute	Concentration, g./l.	Density, g./cc.	Relative Viscosity, μ/μ_{H_2O}
Sodium sulfate	25	1.0183*	1.058
	50	1.0390*	1.124
	100	1.0796*	1.352
	150	1.1213*	1.593
Sodium hydroxide	1	1.0009*	1.003*
	10	1.0091*	1.054*
	50	1.0476*	1.307*
	100	1.0963*	--
Sodium chloride in 0.1N HCl	50	1.0334	1.098
	150	1.0986	1.312
	250	1.1594	1.655
	300	1.1882	1.899

These data are plotted in Fig. 9 and 10. Values from these plots were used in calculating the interfacial area and exposure time as is described in Appendix III.

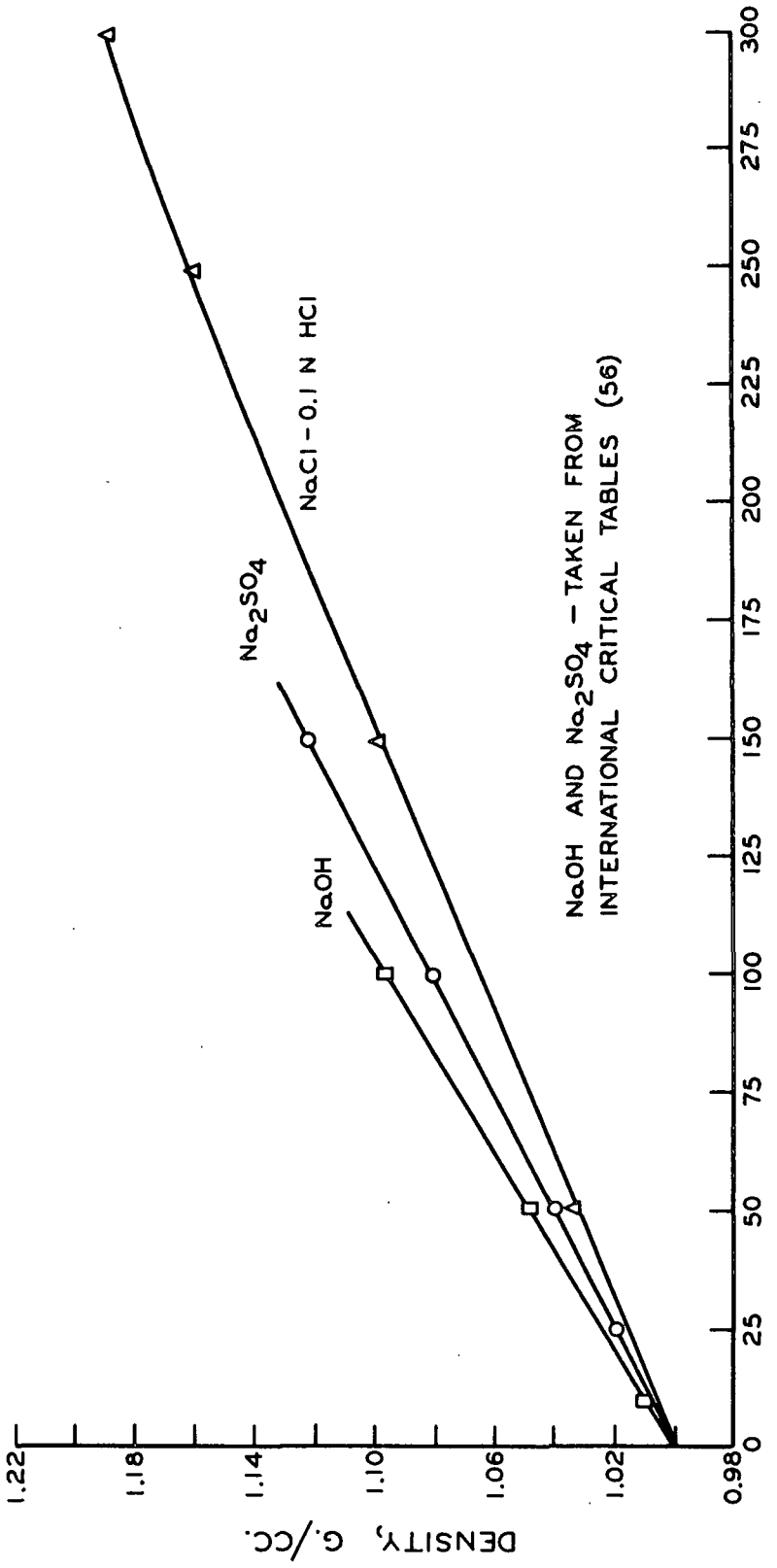

Figure 9. Density of Absorbents at 25°C.

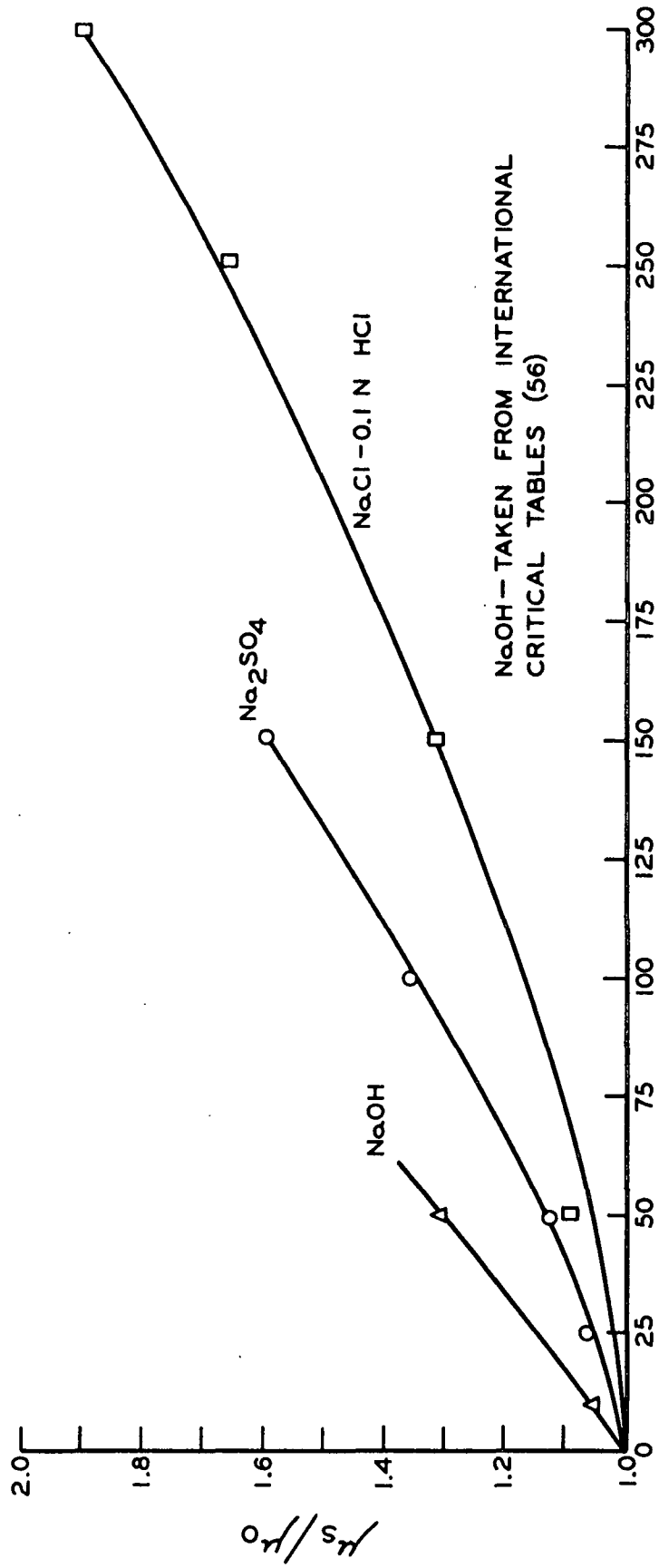

Figure 10. Relative Viscosity of Absorbents at 25°C.

EQUILIBRIUM SOLUBILITY MEASUREMENTS

The results of the equilibrium solubility measurements are given in Table IV.

TABLE IV

THE SOLUBILITY OF CHLORINE IN AQUEOUS HYDROCHLORIC ACID, SODIUM SULFATE, AND SODIUM CHLORIDE SOLUTIONS AT 25°C. AND A CHLORINE PARTIAL PRESSURE OF 760 mm. Hg

Solution	Chlorine Solubility, g./l.
H_2O	6.43 ± .03
0.1N HCl	4.27 ± .03
0.15N HCl	4.22 ± .03
50 g./l. NaCl-0.1N HCl	3.53 ± .02
100 g./l. NaCl-0.1N HCl	3.07 ± .02
150 g./l. NaCl-0.1N HCl	2.68 ± .02
200 g./l. NaCl-0.1N HCl	2.32 ± .02
25 g./l. Na_2SO_4-0.15N HCl	3.78 ± .02
50 g./l. Na_2SO_4-0.15N HCl	3.55 ± .02
100 g./l. Na_2SO_4-0.15N HCl	2.96 ± .02
150 g./l. Na_2SO_4-0.15N HCl	2.46 ± .02

The Applicability of Henry's Law

Other investigators (2, 3) have studied the solubility of chlorine in aqueous solutions and found that the unhydrolyzed chlorine molecules follow Henry's law. To check these findings, runs were made on some of the salt solutions at reduced chlorine pressures. In every case Henry's law was valid. Figure 11 shows the chlorine partial pressure--solubility line for the 0.1N hydrochloric acid solution. The other results are reported in Appendix IV.

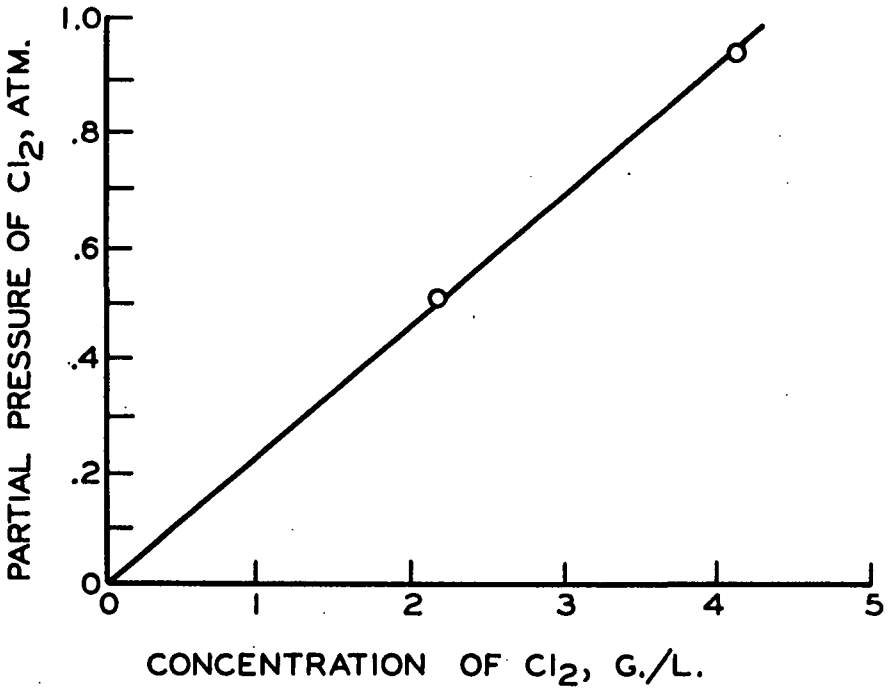

Figure 11. Solubility of Cl_2 in 0.1N Hydrochloric Acid at 25°C.

The Activity of the Molecular Chlorine

It has been stated that the activity of unhydrolyzed chlorine in all the absorbents is the same as in pure water. The equilibrium concentration of unhydrolyzed chlorine in water was calculated from the total chlorine concentration and the equilibrium constant of Connick and Chia (10). This value was found to be 4.22 g./l. at 25°C. and a chlorine partial pressure of 760 mm. Hg. The activity coefficient in water is defined as being unity. Thus, the activity is equal to 4.22 in terms of g./l. concentration units.

The solubility of chlorine in 0.1N hydrochloric acid is very near the calculated concentration of molecular chlorine in water indicating

that the hydrochloric acid concentration is not great enough to cause an appreciable salting out of the chlorine. Thus, the activity coefficient of chlorine in the dilute acid solutions may be taken as unity. This also indicates that the hydrochloric acid resulting from the reaction between chlorine and water does not exhibit an appreciable salting out effect on the chlorine.

Comparison of Results with Other Work

Sherril and Izard (55) determined the solubility of chlorine in sulfuric acid solutions of various concentrations. By extrapolating the data to zero acid concentration in the region where the hydrolysis reaction was suppressed, they estimated the concentration of unhydrolyzed chlorine in pure water to be 4.20 g./l. at 25°C. and a chlorine partial pressure of 760 mm. Hg. This compares very well with the value of 4.22 g./l. which was determined in this work.

Whitney and Vivian (2) obtained a value of 6.47 g./l. for the total solubility of chlorine in pure water at 25°C. and a chlorine partial pressure of 760 mm. Hg. The value of 6.43 g./l. determined in this work agrees well with their value.

Other chlorine solubilities reported by Sherril and Izard (55) and by the International Critical Tables (56) are from 0 to 5% higher than the values determined in this work. This discrepancy cannot be attributed to a failure to reach equilibrium because in the majority of runs made here equilibrium was approached by desorption. Also great care was taken to prevent any chlorine loss during the sampling and analyzing procedures. For these reasons the results obtained here are felt to be very reliable.

With the exception of the two cases mentioned above, no two independent sets of data from various workers were found to agree within 2%.

DIFFUSIVITY MEASUREMENTS

Diffusion Coefficient in Water

The diffusivity of chlorine through 0.15N hydrochloric acid was determined on the Beckman Spinco Model-H electrophoresis-diffusion apparatus. The dilute acid was used as a solvent to suppress the hydrolysis reaction. The nature of this apparatus was such that the runs had to be made at a temperature well below room temperature.

The results were corrected for temperature and viscosity differences by assuming that $D_A\mu/T$ was a constant. This has been shown to be a good assumption provided that the solvent remains chemically unchanged (57, 58).

A run was made at 0.4°C. and the results corrected to 25°C. The value obtained was 1.45×10^{-5} sq. cm./sec. for chlorine in water at 25°C. To test the soundness of the temperature correction a run was made at the highest temperature that the apparatus could obtain. This was 20.4°C. The resulting diffusion coefficient corrected to 25°C. was 1.49×10^{-5} sq. cm./sec.

The results of the sintered glass diaphragm runs indicate that the diffusion coefficient at 25°C. is in the vicinity of 1.50×10^{-5} sq. cm./sec.

Peaceman (31) obtained a value of 1.48×10^{-5} sq. cm./sec. for the diffusion coefficient of molecular chlorine in water at 25°C. on a

sintered glass diaphragm apparatus. The results of his diffusion work are felt to be very reliable.

In view of Peaceman's work and the results obtained here, the value of 1.48×10^{-5} sq. cm./sec. was used throughout the course of this thesis for the diffusion coefficient of molecular chlorine in water at 25°C.

The diffusion experiments carried out here and Peaceman's work both indicate that the diffusion coefficients determined are not dependent upon the chlorine concentration.

Diffusion Coefficients in the Salt Solutions

The attempts to measure the diffusion coefficient of molecular chlorine in the salt solutions by using the Spinco Model-H electrophoresis-diffusion apparatus were unsuccessful. With both sodium chloride and sodium sulfate solutions the number of Rayleigh interference fringes became less and less as diffusion progressed. In other words, the index of refraction difference between solvent and solution was continually changing. This indicates that the number of molecular units in the solvent, the solution, or both was slowly changing. It is hypothesized that this was caused by a complexing between the salt ions and the chlorine molecules.

Whatever the reason for the observed behavior, it should not affect the absorption experiments because the absorption times were around 0.03 second; whereas the fringe number became slightly less over several hours.

THE ABSORPTION EXPERIMENTS

AGREEMENT WITH THE PENETRATION THEORY

Summary of Runs

Twelve absorption runs were made with 0.1N hydrochloric acid as the absorbent over an exposure time range of 0.008 to 0.04 second. The absorption rate and exposure times were calculated as described in Appendix VIII. Three of these runs were made at 0.020 second at different gas flow rates to test for the presence of a gas-phase resistance to absorption. The results of these runs are plotted in Fig. 12. The average rate of absorption over the exposure period per unit of interfacial area is plotted against the inverse of the square root of the exposure time in accordance with Equation (35).

The Effects of Gas Flow Rates

The gas phase in all the absorption runs consisted of pure chlorine gas saturated with water vapor. It was not expected that the diffusion of the chlorine through this small amount of water vapor would be great enough to cause an appreciable partial pressure gradient of chlorine at the liquid interface. If such a gradient existed, it would be altered by the rate of gas flow past the liquid interface. This would in turn alter the rate of absorption because the chlorine partial pressure at the interface would change. The results show that there is no significant difference between the three runs made at gas flow rates ranging from 500 to 5000 cc./min. at 14.7 p.s.i. and 70°F., thus indicating the absence of such a partial pressure gradient.

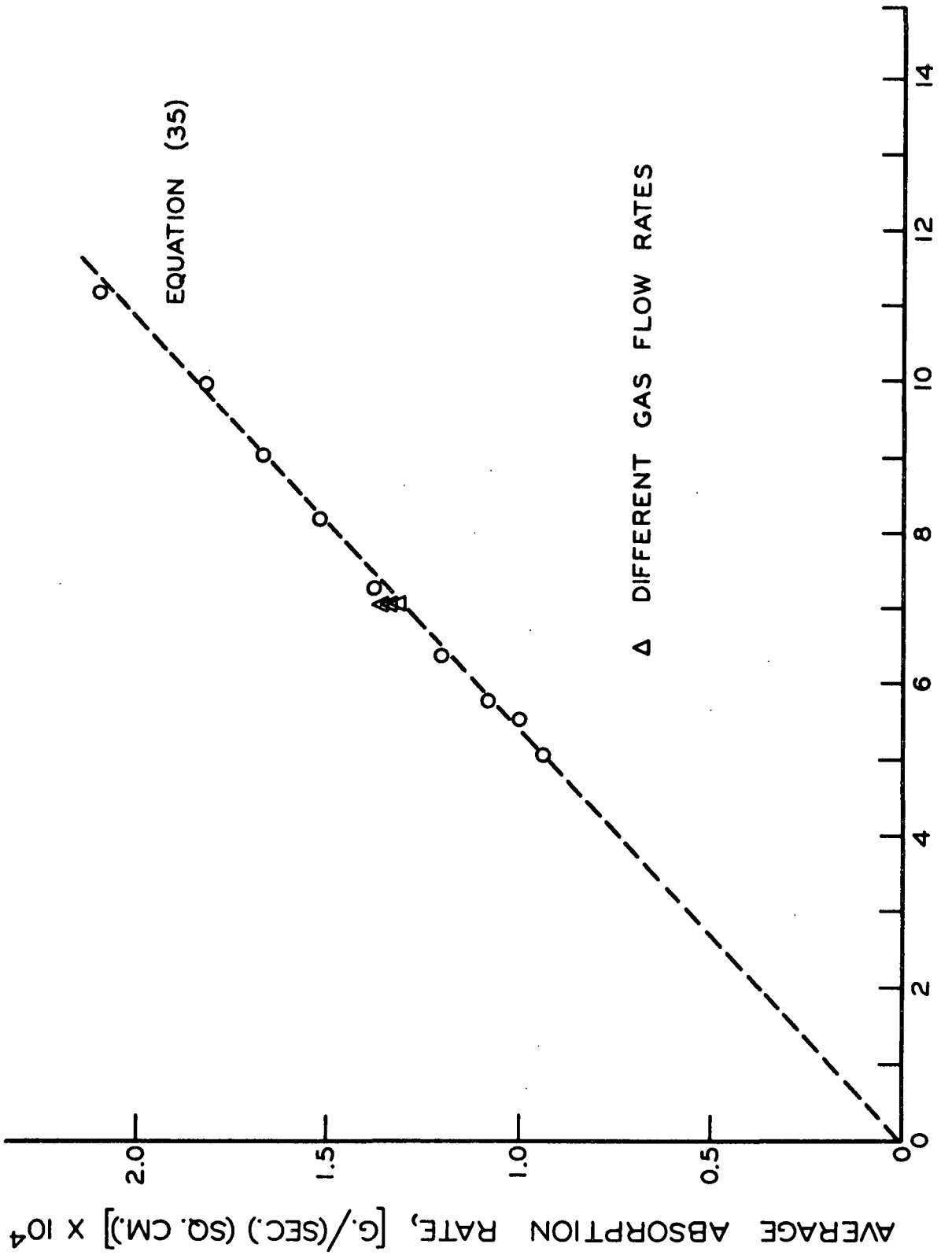

Figure 12. Absorption in 0.1N Hydrochloric Acid

The Extent of the Agreement

The penetration theory predicts that the rate of absorption without chemical reaction is given by Equation (35). Equation (35) is shown on Fig. 12 by the dashed line. The equilibrium solubility, $C_{A,e}$, used in plotting Equation (35) was that determined in the solubility experiments in 0.1N hydrochloric acid, and the diffusivity used was that determined on the diffusion apparatus with a very small correction for the viscosity difference between pure water and 0.1N hydrochloric acid.

The best line through the data points has a slope of $1.87 \pm .04 \times 10^{-5}$ g./(sq. cm.)(sec.)$^{3/2}$. A statistical test of the validity of the 0-0 intercept shows a limit of 95% confidence. Equation (35) predicts a straight line with a slope of $1.85 \pm .05 \times 10^{-5}$ g./(sq. cm.)(sec.)$^{3/2}$ and a 0-0 intercept. The agreement of the absorption data with the penetration theory is considered to be very good.

At equilibrium the chlorine in 0.1N hydrochloric acid is about 3% hydrolyzed. The rate of the hydrolysis reaction in such a solution is so slow that it would not affect the absorption rate at such short exposure times. Even if the reaction were infinitely fast, such a small conversion would not affect the absorption rate enough to be detectable. Thus, the data represent truly physical absorption.

The excellent agreement between the absorption data and the penetration theory indicates the following:

1. The hydrodynamics of the jet conform to the assumptions of the penetration theory and are analyzed correctly.

2. The interface of the liquid reaches equilibrium with the gas phase in what amounts to an infinitely small time.
3. Temperature, end, and other effects that could affect the absorption rate are negligible.
4. Conclusions drawn from analyzing the absorption data in accordance with the penetration theory in the rest of the thesis are unaffected by fallacies in the jet apparatus or the theory.

MOST SUITABLE DRIVING FORCE FOR ABSORPTION

Summary of Runs

From five to seven runs were made in each of four sodium chloride--0.1N hydrochloric acid solutions at exposure times ranging from 0.01 to 0.04 second. The concentration of sodium chloride in the solutions was 50, 100, 150, and 200 grams per liter. The absorption rates were plotted against the inverse of the square root of the exposure time as is done in Fig. 12. The slopes of the best lines through the sets of data were taken and from these the product of the driving force and the square root of the diffusivity (D.S.D. product) were determined. [See Equation (35).] This product is shown as a function of sodium chloride concentration in Fig. 13 and in Table V.

Concentration as a Driving Force

The diffusion coefficient in terms of a concentration driving force was calculated for chlorine in each of the sodium chloride solutions from the D.S.D. product and the equilibrium concentrations determined in the solubility measurements. These coefficients are given in Table VI.

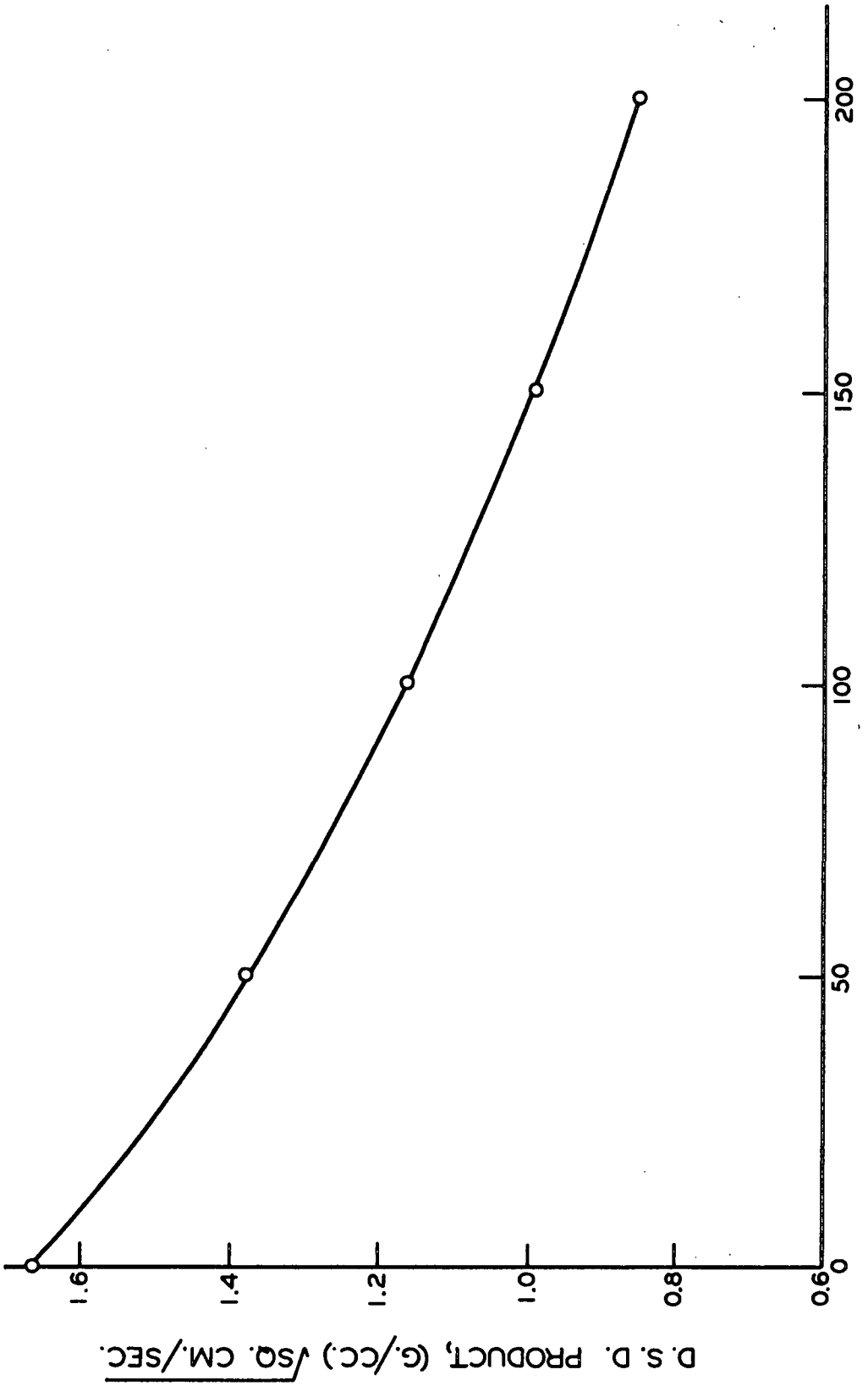

Figure 13. D.S.D. Product vs. Sodium Chloride Concentration

TABLE V

THE PRODUCT OF THE DRIVING FORCE AND THE SQUARE ROOT OF THE DIFFUSIVITY FOR THE ABSORPTION OF CHLORINE INTO SODIUM CHLORIDE--0.1N HCl SOLUTIONS VS. SODIUM CHLORIDE CONCENTRATION

NaCl Concentration, g./l.	D.S.D. Product, $\frac{(g./cc.)}{\sqrt{sq.\ cm./sec.}}$
0	$(1.65 \pm .04) \times 10^{-5}$
50	$(1.38 \pm .04) \times 10^{-5}$
100	$(1.16 \pm .03) \times 10^{-5}$
150	$(0.99 \pm .03) \times 10^{-5}$
200	$(0.85 \pm .03) \times 10^{-5}$

TABLE VI

THE DIFFUSIVITY OF CHLORINE IN SODIUM CHLORIDE-0.1N HCl SOLUTIONS BASED ON A CONCENTRATION DRIVING FORCE AS A FUNCTION OF SODIUM CHLORIDE CONCENTRATION

Salt Concentration, g./l.	Diffusivity, sq. cm./sec.
0	1.48×10^{-5}
50	1.53×10^{-5}
100	1.44×10^{-5}
150	1.37×10^{-5}
200	1.33×10^{-5}

The diffusivities calculated in Table VI represent one of two things. They are either concentration independent diffusivities or they are integral diffusivities over the chlorine concentration ranges encountered. If they are concentration independent values they should be able to be

correlated with the physical and chemical properties of the salt solutions in accordance with the generalized diffusion correlations that have been established for other systems.

The Stokes-Einstein treatment of the diffusion of rigid spheres in solution predicts that the product, $\underline{D}_A\mu/\underline{T}$, should remain constant for a given diffusing species. This relationship has been found to be valid for most systems when only temperature and viscosity changes within one solvent are considered (57). When the solvent changes, it has been found that the number, $\underline{D}_A\mu/\underline{T}$, then becomes a function of the solvent. Many attempts (57-59) have been made to correlate $\underline{D}_A\mu/\underline{T}$ with such solvent properties as molecular weight, latent heat of vaporization, and molar volume. These correlations all show that the addition of a salt to water would change the solvent properties in such a way that the diffusion coefficient should decrease with increased salt concentration. Theoretical considerations (60) point to the same conclusion. The fact that the results here show a maximum in the diffusion coefficient with increased salt concentration would indicate the inadequacy of the assumption of a concentration independent diffusivity. It is felt that the accuracy of the data is good enough to conclude that the maximum is real.

In conclusion, the diffusion coefficients defined on the basis of a concentration driving force are not concentration independent for chlorine-water systems not exhibiting model behavior and represent integrated values over the chlorine concentration ranges encountered.

Activity as a Driving Force

In subsequent experiments it is desired to account for the effect of ionic strength on the absorption rates. It is seen that the diffusion coefficients defined in terms of a concentration driving force are not a simple function of the salt concentration. To see if a more convenient function between diffusion coefficient and salt concentration could be obtained, a diffusion coefficient defined in terms of an activity driving force was substituted into Fick's laws of diffusion and the absorption equations were derived in terms of this activity driving force and diffusion coefficient.

Differential Equation (29) for absorption without chemical reaction written in terms of an activity driving force for diffusion becomes

$$\partial c_A/\partial t = \mathcal{D}_\eta \partial^2 a_A/\partial x^2 , \tag{47}$$

or

$$\partial(a_A/\gamma_A)/\partial t = \mathcal{D}_\eta \partial^2 a_A/\partial x^2 , \tag{48}$$

where $\mathcal{D}_\eta$ is the diffusion coefficient defined in terms of an activity driving force.

$$J = - \mathcal{D}_\eta \nabla a \tag{49}$$

Since γ_A is independent of x, t, and a,

$$\partial a_A/\partial t = \mathcal{D}_\eta \gamma \partial^2 a_A/\partial x^2 . \tag{50}$$

The solution to this equation with its appropriate boundary conditions is the same as the solution for Equation (35). Thus, the average rate of absorption is given by

$$\bar{N}_A = 2\, a_{A,e}\sqrt{\mathfrak{M}\gamma_A/\pi t_e}\,. \qquad (51)$$

The D.S.D. product given in Table V is thus $\underline{a}_{\underline{A},\underline{e}}\sqrt{\underline{\mathfrak{M}}\gamma_{\underline{A}}}$, if activity is assumed to be the driving force. Again, $\underline{\mathfrak{M}}$, can be either an activity independent or integral quantity.

The values of $\underline{\mathfrak{M}}\gamma_{\underline{A}}$ and $\underline{\mathfrak{M}}$ calculated from the D.S.D. product and an activity driving force are shown in Table VII. The standard state chosen for the definition of the activity is that of infinite dilution as was described earlier. This choice was made so that the activity would be numerically equal to the concentration when the system behaved as the model. Any other choice of standard state would merely change the results by a constant factor (the activity coefficient of the solute in the ideal solution).

TABLE VII

THE DIFFUSION COEFFICIENT AS DEFINED BY AN ACTIVITY DRIVING FORCE FOR THE DIFFUSION OF CHLORINE THROUGH SODIUM CHLORIDE--0.1N HCl SOLUTIONS AS A FUNCTION OF SODIUM CHLORIDE CONCENTRATION

NaCl Concentration, g./l.	$\underline{\mathfrak{M}}\gamma_{\underline{A}}$, sq. cm./sec.	$\gamma_{\underline{A}}$	$\underline{\mathfrak{M}}$, sq. cm./sec.
0	1.48×10^{-5}	1.000	1.48×10^{-5}
50	1.07×10^{-5}	1.195	$.896 \times 10^{-5}$
100	$.755 \times 10^{-5}$	1.375	$.549 \times 10^{-5}$
150	$.552 \times 10^{-5}$	1.575	$.350 \times 10^{-5}$
200	$.403 \times 10^{-5}$	1.820	$.222 \times 10^{-5}$

It is seen that $\underline{\mathfrak{M}}$ is an ever decreasing function of salt concentration as would be expected from considering the generalized diffusion correlations (57-59).

The Chang and Wilke correlation (57) states that

$$D_A\mu/T \propto (\chi M)^{1/2} \qquad (52)$$

for a given solute. M is the molecular weight of the solvent and χ is an empirical association parameter which is a function of the polarity of the solvent. It is not possible to evaluate this parameter for the salt solutions, and therefore a direct application of the correlation cannot be used.

The effective polarity of the salt solutions would have to decrease with increasing salt concentration in order for Equation (52) to fit the $\mathcal{M}\gamma_A$ data. This is a reasonable conclusion if the salt ions are pictured as interfering with the water polar bonds and causing an over-all decrease in the polarity of the solvent.

It should be realized that the generalized diffusion correlations cited were derived from systems which were for the most part nonionic and therefore any conclusions drawn from them on ionic systems should be viewed with caution.

It was seen that the product $\mathcal{M}\gamma_A$ is equivalent to the concentration diffusivity, D_A, and for this reason it was decided to correlate this product with the solvent properties. In view of the Stokes-Einstein relationship the product $(\mathcal{M}\eta\gamma_A)$ should be a simple function of the solvent properties. η is the viscosity of the solvent relative to water. It was found that the product $(\mathcal{M}\eta\gamma_A)$ is proportional to $\gamma_A^{-1.5}$; therefore, the product $(\mathcal{M}\eta\gamma_A^{2.5})$ is a constant. (See Table VIII.)

TABLE VIII

THE PRODUCT ($\mathcal{M}\eta\gamma_A^{2.5}$) AS A FUNCTION OF SODIUM CHLORIDE CONCENTRATION

NaCl Concentration, g./l.	$\mathcal{M}\eta\gamma_A^{2.5}$
0	1.48×10^{-5}
50	1.47×10^{-5}
100	1.44×10^{-5}
150	1.44×10^{-5}
200	1.48×10^{-5}

The fact that this correlation exists does not prove that $\mathcal{M}$ is independent of the activity, but it does show that $\mathcal{M}$ is a simple function of the system properties.

Chemical Potential as the Driving Force

Written in terms of a chemical potential driving force for diffusion the differential equation describing absorption without chemical reaction becomes

$$\partial C_A/\partial t = \mathcal{M}\partial^2\mu_A/\partial x^2 \quad . \tag{53}$$

$\mathcal{M}$ is the diffusion coefficient defined in terms of a chemical potential driving force.

$$J = -\mathcal{M}\nabla\mu_A. \tag{54}$$

The chemical potential is defined as

$$\mu_A = \mu_A^\circ + RT \ln \gamma_A C_A \quad . \tag{55}$$

Therefore,

$$\partial\mu_A/\partial t = RT\,\partial\,(\ln \gamma_A C_A)/\partial t = (RT/C_A)\partial C_A/\partial t\ , \tag{56}$$

or

$$\partial C_A/\partial t = (C_A/RT)(\partial\mu_A/\partial t). \tag{57}$$

From Equation (55)

$$C_A = (1/\gamma_A)\exp\,[(\mu_A - \mu_A^{\circ})/RT]. \tag{58}$$

Substituting (57) and (58) into (53)

$$\partial\mu_A/\partial t = \eta\,\gamma_A\,RT\exp\,[(\mu_A^{\circ} - \mu_A)/RT]\partial^2\mu_A/\partial x^2\ . \tag{59}$$

The boundary conditions are:

$$\begin{aligned} &x = 0, \quad t > 0 \quad \mu_A = \mu_{A,e} \\ &t = 0, \quad x > 0 \quad \mu_A = \mu_{A,o} \\ &x = \infty, \quad t \geq 0 \quad \mu_A = \mu_{A,o}\ . \end{aligned} \tag{60}$$

It is convenient to rearrange Equation (59) as follows:

$$\partial\mu_A/\partial t = \left\{\eta\,\gamma_A RT\exp\,[(\mu_A^{\circ} - \mu_{A,e})/RT]\right\}\cdot\exp\,[(\mu_{A,e} - \mu_A)/RT]\cdot \partial^2\mu_A/\partial x^2\ . \tag{61}$$

The solution to Equation (61) appears in Mathematics of Diffusion by Crank (61). The average rate of absorption over the exposure period, t_e, is given as

$$\bar{N}_A = (\mu_{A,e} - \mu_{A,o})\sqrt{\eta\,\gamma_A RT/t_e}\cdot\exp\,[(\mu_A^{\circ} - \mu_{A,e})/2RT]\cdot \left\{1.128/[0.177(\mu_{A,e} - \mu_{A,o})/RT - 1]\right\} \tag{62}$$

The term in the brackets is an empirical interpolation formula given by Cranck for a tabulated function of the exact solution.

In this case, $C_{A,o} = 0$, therefore

$$\mu_{A,o} \longrightarrow -\infty \quad \text{as} \quad C_{A,o} \longrightarrow 0$$

Taking the limit of Equation (62) as $\mu_{A,o} \longrightarrow -\infty$

$$\bar{N}_A \longrightarrow \sqrt{\eta \gamma_A RT/t_e} \cdot \exp\left[(\mu_A^{\circ} - \mu_{A,e})/2RT\right] \cdot 6.38\ RT \qquad (63)$$

Substituting Equation (55) into Equation (63) for $\mu_{A,e}$

$$\bar{N}_A = \sqrt{\gamma_A C_{A,e}} \cdot \sqrt{\eta \gamma_A RT/t_e}\ (6.38\ RT) \qquad (64)$$

Rewriting in the form of Equation (35) and (51)

$$\bar{N}_A = 2\, a_{A,e} \sqrt{31.9\, R^3 T^3 \eta \gamma_A / t_e a_{A,e}} \qquad (65)$$

Equation (65) is the same as Equation (51) where

$$\mathcal{\eta} = (31.9\, R^3 T^3 / a_{A,e})\, \eta \qquad (66)$$

remembering that $a_{A,e}$ is independent of the salt concentration.

Thus, within the limits of the interpolation formula used in solving Equation (59), a chemical potential driving force is equivalent to an activity driving force for physical absorption in solutions where the activity coefficient of the absorbed solute is independent of the concentration. η will correlate with γ_A in the same manner as did $\mathcal{\eta}$.

Discussion of the Thermodynamic Driving Force

From a theoretical viewpoint a thermodynamic driving force is more closely related to the actual causes of mass transport, but from a practical viewpoint the driving force which is most convenient may be used as long as the appropriate transfer coefficient is correctly defined.

The data and calculations presented here do show that the diffusion coefficients defined in terms of a thermodynamic driving force are a less complicated function of the system properties than are the diffusion coefficients defined in terms of a concentration driving force.

It is believed that the complications of a concentration driving force would be more evident if the absorption experiments were carried out at higher pressures where Henry's law was not valid. Then the activity coefficients would be a function of concentration. As a result a concentration defined diffusion coefficient would be an extremely complicated function of the intermolecular forces or of the actual driving force.

ABSORPTION WITH CHEMICAL REACTION

Summary of Runs

A total of forty runs was made with absorbents whose initial pH values ran from one to fourteen. The water was acidified with sulfuric acid and made basic with sodium hydroxide. The runs were made at from three to nine different exposure times at each pH value. The exposure times were from 0.018 to 0.039 second. The purpose of these runs was to clarify the mechanism and to determine the speed of the hydrolysis reaction. The results of these runs are tabulated in Appendix VIII.

The Mechanism of the Hydrolysis Reaction

At each pH value the absorption rates were plotted against the square root of the inverse of the exposure time. The value of the absorption rate at 0.03 second was then determined by interpolation so that the absorption rates could be compared on a common basis. The time of 0.03 second was chosen because it was approximately the median of exposure times used. This rate was then divided by the rate of absorption without chemical reaction to obtain the function, Φ, at 0.03 second.

The rate of absorption without chemical reaction was calculated from either Equation (35) or Equation (51) depending upon whether model or nonmodel behavior existed in the absorbents. With the exception of the concentrated caustic solutions, the absorbents were dilute enough to warrant the assumption of model behavior. When calculating the rate without chemical reaction in the strong caustic solutions, the activity coefficient was determined as described in Appendix IV, and the diffusion coefficient was determined by assuming that $(\mathcal{D}\eta\gamma^{2.5})$ was constant.

The values of Φ at 0.03 second as a function of initial absorbent pH appear in Table IX and in Fig. 14. Values of $\Phi - 1$ are plotted in Fig. 14 so that the log scale will be sensitive at Φ values close to one.

The two mechanisms proposed for the hydrolysis reaction are:

$$Cl_2 + H_2O \rightleftharpoons H^+ + Cl^- + HOCl \qquad (2)$$

and

$$Cl_2 + OH^- \rightleftharpoons Cl^- + HOCl \qquad (27)$$

TABLE IX

THE EFFECT OF THE CHLORINE HYDROLYSIS REACTION ON ABSORPTION RATES AT 25°C.

Absorbent	pH	Absorption Rate With Chemical Reaction, $\bar{N}_A$ g./sec. sq.cm. x 10^4	Absorption Rate Without Chemical Reaction, $\bar{N}^*_A$ g./sec.sq.cm. x 10^4	$\Phi = \bar{N}_A/\bar{N}^*_A$
1.733N NaOH	14.2	27.3	0.647	42.2
1.166	14.1	21.0	0.777	27.0
0.500	13.7	10.5	0.915	11.5
0.244	13.4	6.07	0.979	6.22
0.1268	13.1	3.60	1.023	3.51
0.0603	12.8	2.19	1.056	2.07
0.00610	11.8	1.365	1.059	1.29
Dil. NaOH	10.3	1.275	1.059	1.21
Dil. NaOH	9.7	1.260	1.059	1.19
Dil. NaOH	8.8	1.261	1.059	1.20
H_2O	6.8	1.278	1.059	1.21
Dil. H_2SO_4	4.2	1.267	1.059	1.20
Dil. H_2SO_4	2.7	1.250	1.059	1.17
Dil. H_2SO_4	1.6	1.186	1.058	1.12
0.1N H_2SO_4	1.0	1.152	1.055	1.09

The rate expression for Reaction (2) is

$$-d\,C_{Cl_2}/dt = k_1 C_{Cl_2} - k_2 C_{H^+} C_{Cl^-} C_{HOCl} \qquad (67)$$

and for Reaction (27)

$$-d\,C_{Cl_2}/dt = k_1' C_{Cl_2} C_{OH^-} - k_2' C_{Cl^-} C_{HOCl} \qquad (68)$$

where k_1 and k_2 are the forward and reverse reaction rate constants.

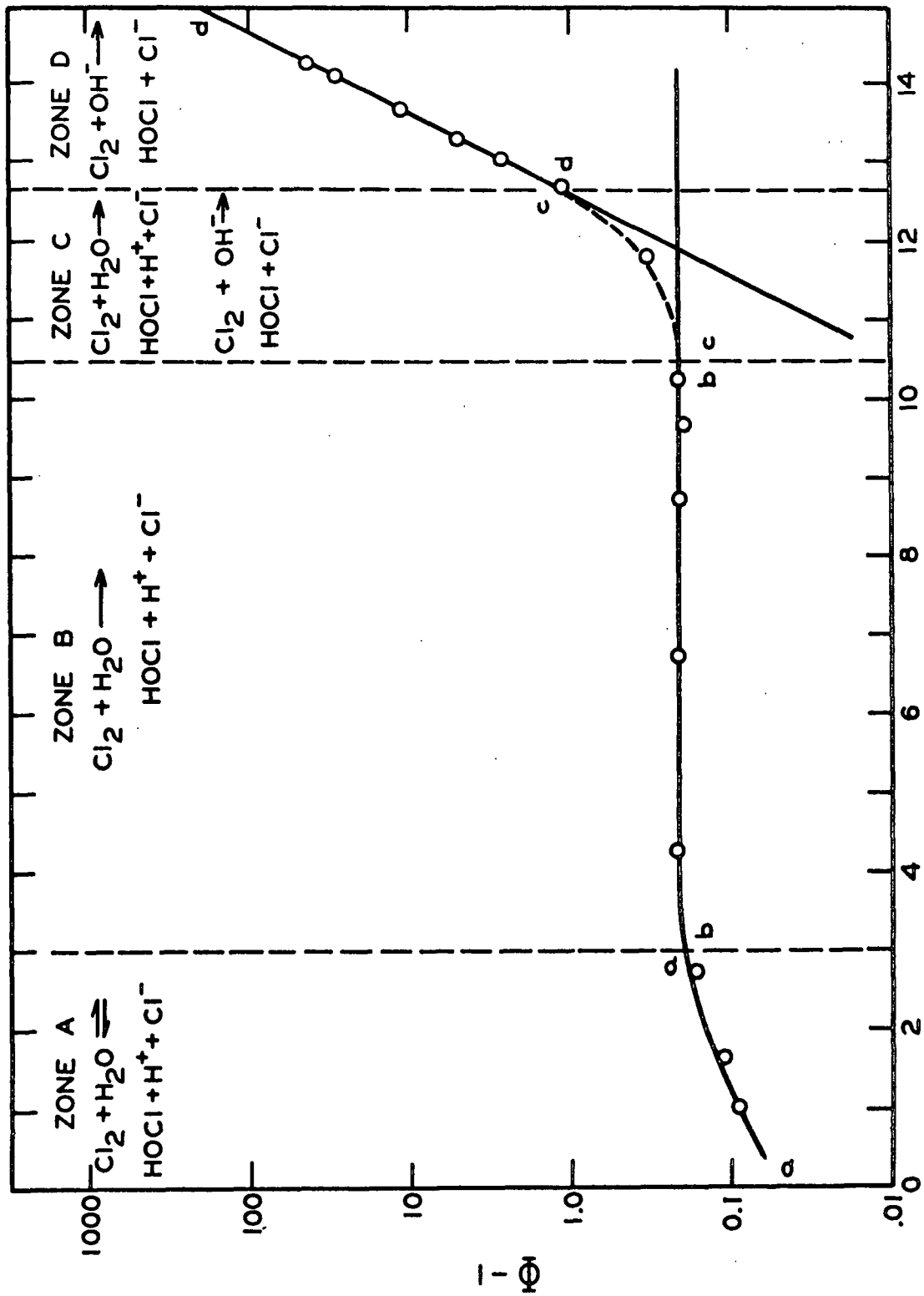

Figure 14. The Effect of Chlorine Hydrolysis on the Chlorine Absorption Rate at 25°C. (t_e = 0.03 sec.)

The proper mechanism can now be deduced from the shape of the curve in Fig. 14 if it is remembered that the function, Φ, is a measure of the effect of the chemical reaction on the rate of absorption. The penetration theory for absorption with chemical reaction shows that the function, Φ, increases as the speed of the chemical reaction increases. Thus, Φ, is an indirect measure of the reaction rate, R.

Upon examining that portion of the curve labeled aa in Zone A of Fig. 14, it is seen that the reaction rate increases as the hydrogen ion concentration decreases. If Reaction (27) were the controlling mechanism in this pH region, an increase in the reaction rate would be expected because of the increase in hydroxyl ion concentration. However, the increase in reaction rate would also be expected to become more and more as at higher pH values the hydroxyl ion concentration is building up faster than the product concentrations. Such an interpretation contradicts the experimental evidence shown by portion bb in Zone B which indicates that the reaction rate is independent of the hydroxyl ion concentration for a wide range. Thus, Reaction (27) does not explain the facts.

The experimental facts up to a pH of 10.5 can be explained in a satisfactory manner if Reaction (2) is considered to be the controlling mechanism. The reaction rate increases and then levels off with decreasing hydrogen ion concentration because the rate of the reverse reaction of Reaction (2) becomes less and less with decreasing hydrogen ion concentration until its influence on the over-all reaction rate is nil (portion bb). During this range the hydrolysis reaction is first order with respect to chlorine concentration and is irreversible.

The reaction rate remains constant with pH until it suddenly begins to increase. The only reason for this increase could be that now the hydroxyl ion concentration is great enough that Reaction (27) begins to influence the over-all reaction rate. In Zone C both reactions show their influence until in Zone D the influence of Reaction (2) is negligible and only Reaction (27) affects the over-all hydrolysis rate.

The rate-controlling reaction in each pH zone is shown in Fig. 14.

The dashed portion of the curve (portion CC) represents the summation of the extensions of lines dd and bb. The data point in this region falls fairly close to this line; thus indicating that if two reactions simultaneously influence the rate of absorption, the total increase in absorption rate is equal to the sum of the increases expected if the reactions took place individually.

These results definitely show that when chlorine is dissolved in water, the chlorine reacts with both the hydroxyl ion and water molecules. The rate at which the chlorine reacts is controlled by one, the other, or both of the reactions depending upon the pH of the solution. For an exposure time of 0.03 second and at pH values less than three the reversible reaction with water is rate controlling. Between pH 3 and pH 10.5 the forward reaction with water is rate controlling. At pH values greater than 12.5 the reaction with the hydroxyl ion is rate controlling. A transition region between the two reactions exists between pH 10.5 and pH 12.5.

The Velocity of the Hydrolysis Reaction

The velocity constant of the reaction between chlorine and water can be determined from the value of Φ during the horizontal portion of the curve of Fig. 14. During this pH range the rate of the hydrolysis is first order with respect to chlorine, and the reaction is irreversible because the reverse reaction does not influence the rate until the pH is less than three. The penetration theory for a first-order irreversible reaction (Appendix I) gives the function, Φ, as

$$\Phi = 1/2 \left[\sqrt{\pi/k_1 t_e}\,(1/2 + k_1 t_e)\,\mathrm{erf}\sqrt{k_1 t_e} + \exp(-k_1 t_e)\right] \quad (69)$$

where k_1 is the reaction rate constant defined by the rate expression,

$$R = k_1 C_{Cl_2} \quad (70)$$

The solutions in this region are so dilute that model behavior exists; and thus, a concentration driving force is used in the rate expression.

The function, Φ, and the exposure time, t_e, were determined from experiment. The first-order reaction rate constant, k_1, can thus be determined from Equation (69) by a trial and error procedure.

The reaction-rate constant was calculated in this manner for several of the runs in the pH range of 3 to 10.5. The results are tabulated in Table X.

During the calculations it was observed that the rate constant, k_1, is rather sensitive to the function, Φ. About a one per cent change in Φ brings about a five per cent change in k_1. This is the major reason for

TABLE X

CALCULATED REACTION RATE CONSTANTS FOR THE FIRST-ORDER REACTION BETWEEN CHLORINE AND WATER AT 25°C.

Run No.	pH	Exposure Time, sec.	k_1, $sec.^{-1}$
91	4.2	.028	21.8
92	4.2	.031	20.2
93	4.2	.036	20.4
49	6.8	.024	24.9
50	6.8	.029	22.7
51	6.8	.031	20.2
83	8.8	.028	19.7
84	8.8	.031	19.4
85	9.7	.028	20.5
80	10.3	.029	20.7
81	10.3	.032	20.0
82	10.3	.036	19.8
			Av. (20.9 ± 1.2)

the six per cent deviation in the average result. Also a slight negative correlation of the rate constant with time is noticed. This trend would arise if the reaction rate constant were not entirely independent of concentration as is assumed when the expression for the reaction rate is written. A similar trend, but to a much greater degree, was noticed by Shilov and Solodushenkov (13). Liftshitz and Perlmutter-Haymen (16) calculated the rate constant from smoothed data and therefore could not observe such a trend. Because the correlation is so slight it is not felt to be a serious limitation on the results.

The value of the rate constant calculated here can be compared with those of Shilov and Solodushenkov (13) and Liftshitz and Perlmutter-Haymen (16) by plotting the results in the form of the familiar Arrhenius Equation.

$$k_1 = A \exp(-E_a/RT) \qquad (71)$$

If it is assumed that the activation energy, E_a, is temperature independent, a plot of log k_1 versus $1/T$ should yield a straight line. Such a plot is shown in Fig. 15. The dashed line is drawn through what is felt to be the two most reliable points, and the solid line represents the best line through all of the points. The slopes of the two lines are approximately the same.

An activation energy value was calculated from the slope of the lines of Fig. 15 and found to be 15,100 cal./mole. The value of A in the Arrhenius Equation was calculated as 2.58×10^{12} sec.$^{-1}$ for the dashed line and 2.31×10^{12} sec.$^{-1}$ for the solid line.

The fact that a fairly good straight line was obtained in Fig. 15 indicates that the rate constant as calculated here is as reliable as those obtained by other workers by more direct methods.

There is no theoretical means of determining whether the actual mechanism of the chlorine hydrolysis is unimolecular or bimolecular. If it were a unimolecular mechanism, some water-chlorine complex would dissociate with a rate constant of 20.9 sec.$^{-1}$ at 25°C. However, if the reaction were bimolecular, it would involve a collision between chlorine and water molecules and would proceed at a rate of 0.377 l./(mole)(sec.) at 25°C. This value was obtained by dividing the apparent first-order rate constant by the molecular concentration of water, i.e., 55.5 moles/l.

If it is assumed that the mechanism is bimolecular, the frequency factor of the Arrhenius Equation, A, becomes 4.65×10^{10} l./(mole)(sec.).

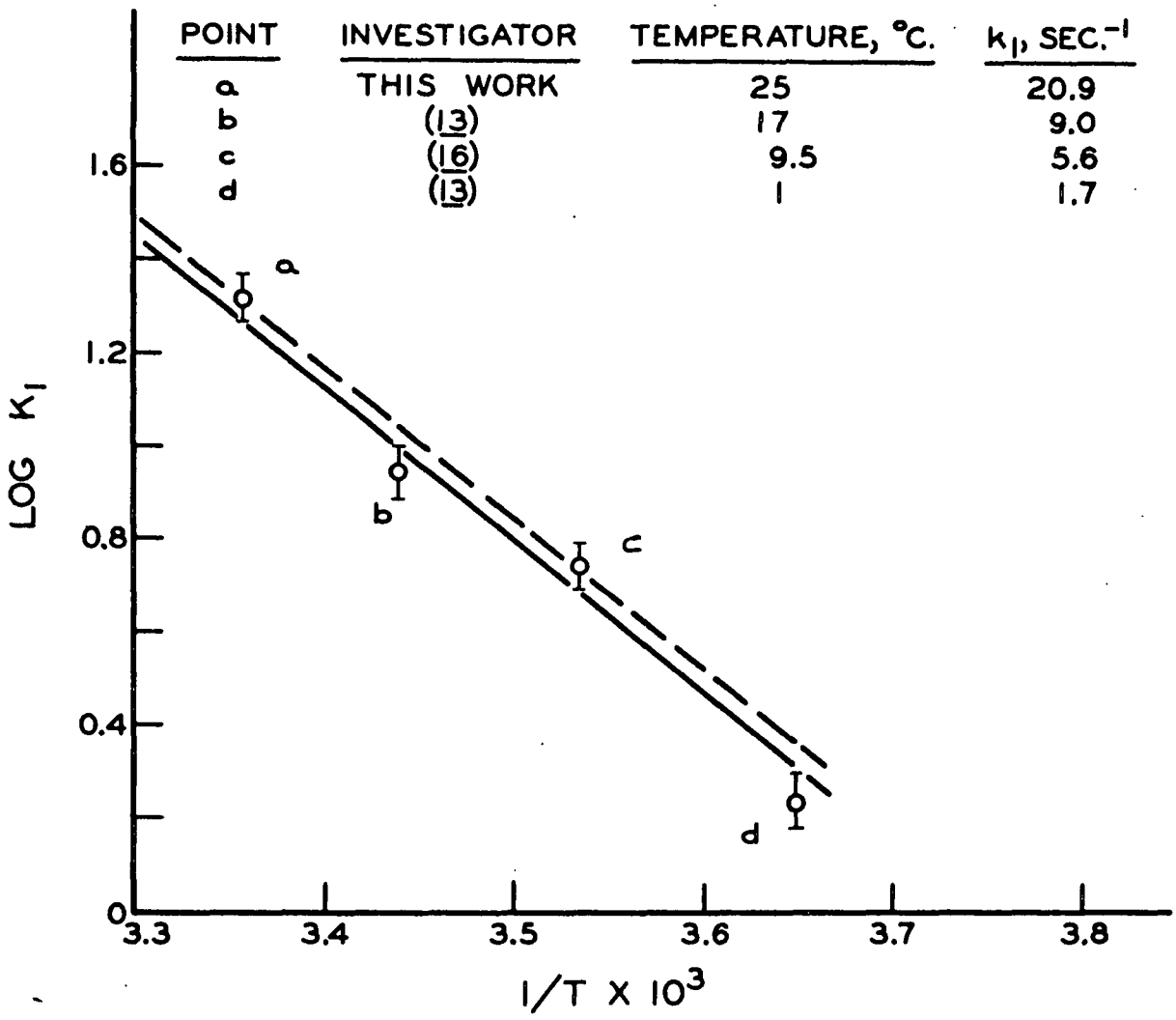

Figure 15. Rate Constant vs. Temperature for Chlorine Hydrolysis Reaction

The collision theory for bimolecular reactions in solution predicts a frequency factor close to 10^{11} l./(mole)(sec.). This value is considered to be the norm. Any value considerably higher is associated with an abnormally fast reaction, and any value considerably lower is associated with an abnormally slow reaction. Thus, if the hydrolysis of chlorine is bimolecular, it proceeds at a normal rate.

In terms of the collision theory, Equation (71) is sometimes written as

$$k_1 = p\ Z \exp(-E_a/RT) \qquad (72)$$

where $\underline{Z}$ is the number of collisions between the reacting molecules per second at unit concentration. The term, $\underline{p} \exp(-\underline{E_a}/\underline{RT})$, then represents the fraction of collisions that result in actual chemical combination. The factor, $\exp(-\underline{E_a}/\underline{RT})$, represents the fraction of colliding molecules which possess the required energy for combination, and $\underline{p}$ represents a steric factor which describes the fraction of colliding molecules with the required energy which are oriented in the proper manner for unity. It is interesting to estimate the order of magnitude of each of these factors for the hydrolysis reaction. The factor, $\exp(-\underline{E_a}/\underline{RT})$, is of the order of 10^{-11}. As was mentioned previously the frequency of collision is about 10^{11} l./(mole)(sec.). Thus, $\underline{p}$ is of the order of 10^{0}.

The steric factor, $\underline{p}$, can be much less than unity even for small inorganic molecules. This arises from the polarity of the molecules or interference from the solvent. These factors are evidently not very prominent for the reaction between chlorine and water.

In terms of the transition state theory, the rate constant is given by

$$k = \epsilon \, e^{\Delta S^{\ddagger}/R} \cdot e^{-\Delta H^{\ddagger}/RT} \qquad (73)$$

where $\underline{H}^{\ddagger} = (\underline{E}_{\underline{a}} - \underline{RT})$ in solution. The entropy of activation, $\Delta \underline{S}^{\ddagger}$, for the hydrolysis reaction is -14 entropy units (standard state of 1 mole/l.). The negative value of entropy arises because of the standard state chosen. This value and the value of the activation energy, 15.1 Kcal./mole, are both in the range listed by Frost and Pearson (62) for ionization of neutral molecules in water solvent reactions.

Thus, the chlorine hydrolysis reaction proceeds at a normal rate and has a normal temperature dependence when compared to similar reactions and when it is considered as bimolecular. These same conclusions can be reached when the reaction is considered to be unimolecular.

The Influence of Solvent Ionic Strength on the Hydrolysis Rate Constant

Three runs were made in each of four sodium sulfate solutions of varying ionic strength. The absorbents were adjusted to a pH of 8.6 with a small amount of sodium hydroxide so that the hydrolysis reaction would be first order with respect to chlorine and irreversible. The average rate of absorption at 0.03 second was determined for each of the salt solutions by interpolating between the three results. The rate of absorption without chemical reaction was calculated by means of Equation (51). The effect of the ionic strength on the diffusion coefficient was accounted for by assuming that $(\underline{m}\,\eta\,\gamma_{\underline{A}}^{2.5})$ was constant. The function, Φ, was then calculated and from this the rate constant, $\underline{k}_1$, was determined. These calculations are illustrated in Appendix VIII, and the results appear in Table XI.

TABLE XI

THE INFLUENCE OF IONIC STRENGTH ON THE RATE OF CHLORINE HYDROLYSIS IN SODIUM SULFATE SOLUTIONS AT pH 8.6 AND 25°C.

Ionic Strength of Na_2SO_4 Solution	Absorption Rate With Chemical Reaction, $\bar{N}_A$ g./(sec.)(sq.cm.) x 10^4	Absorption Rate Without Chemical Reaction, $\underline{N}_A$ g./(sec.)(sq.cm.) x 10^4	Φ	$\underline{k}_1$ $sec.^{-1}$
0	1.268	1.059	1.199	20.9
0.529	1.085	0.974	1.116	11.6
1.057	0.930	0.880	1.058	6.0
2.110	0.704	0.694	1.014	1.4
3.17	0.559	0.560	(1.00--)	--

The form of the dependence of the rate constant on the ionic strength of the solution can be deduced from the transition state theory.

The rate constant $\underline{k}_1$ is given as

$$k_1 = \epsilon K_S^{\ddagger} \gamma_A \gamma_B / \gamma_{M^{\ddagger}} \qquad (74)$$

At zero ionic strength

$$k_{1,o} = \epsilon K_S^{\ddagger} \qquad (75)$$

Therefore,

$$k = k_{1,o} \gamma_A \gamma_B / \gamma_{M^{\ddagger}} \qquad (76)$$

It was previously stated that the dependence of the activity coefficient on ionic strength could be written as

$$\ln \gamma_A = b_A I_s \qquad (77)$$

Thus, the reaction rate constant can be written

$$\ln k_1 = \ln k_{1,o} + (b_A + b_B - b_{M^{\ddagger}})I_s \qquad (78)$$

Whether k_1 increases or decreases with increased ionic strength depends upon the sign of the coefficient $(b_A + b_B - b_{M^{\ddagger}})$. It is not possible to predict the magnitude or sign of this coefficient unless the form of the activated complex is known.

Figure 16 is a plot of the log of $k_1/k_{1,o}$ *versus* the ionic strength, and it is noticed that a fairly good straight line is obtained in accordance with Equation (78).

The slope of this line gives the value of $(b_A + b_B - b_{M^{\ddagger}})$ as -1.26 l./mole. The values of b_A and b_B can be found by plotting the log of the appropriate activity coefficients against the sodium sulfate ionic strength and taking the slope. The activity coefficients of the chlorine, γ_A, can be determined from the equilibrium solubility measurements, and those of the water, γ_B, can be determined from water-vapor pressure data over the salt solutions. The values of b_A and b_B were determined in this way and found to be +0.16 l./mole and -0.001 l./mole, respectively. Thus,

$$b_{M^{\ddagger}} = 1.10 \text{ l./mole} \qquad (79)$$

This value is very much greater and of opposite sign than that predicted by considering just the electrostatic influence of the salt ions on the salting out of the activated complex. See Frost and Pearson (62).

The abnormal decrease in reaction rate constant with increasing solvent ionic strength can be explained if it is assumed that the salt ions complex

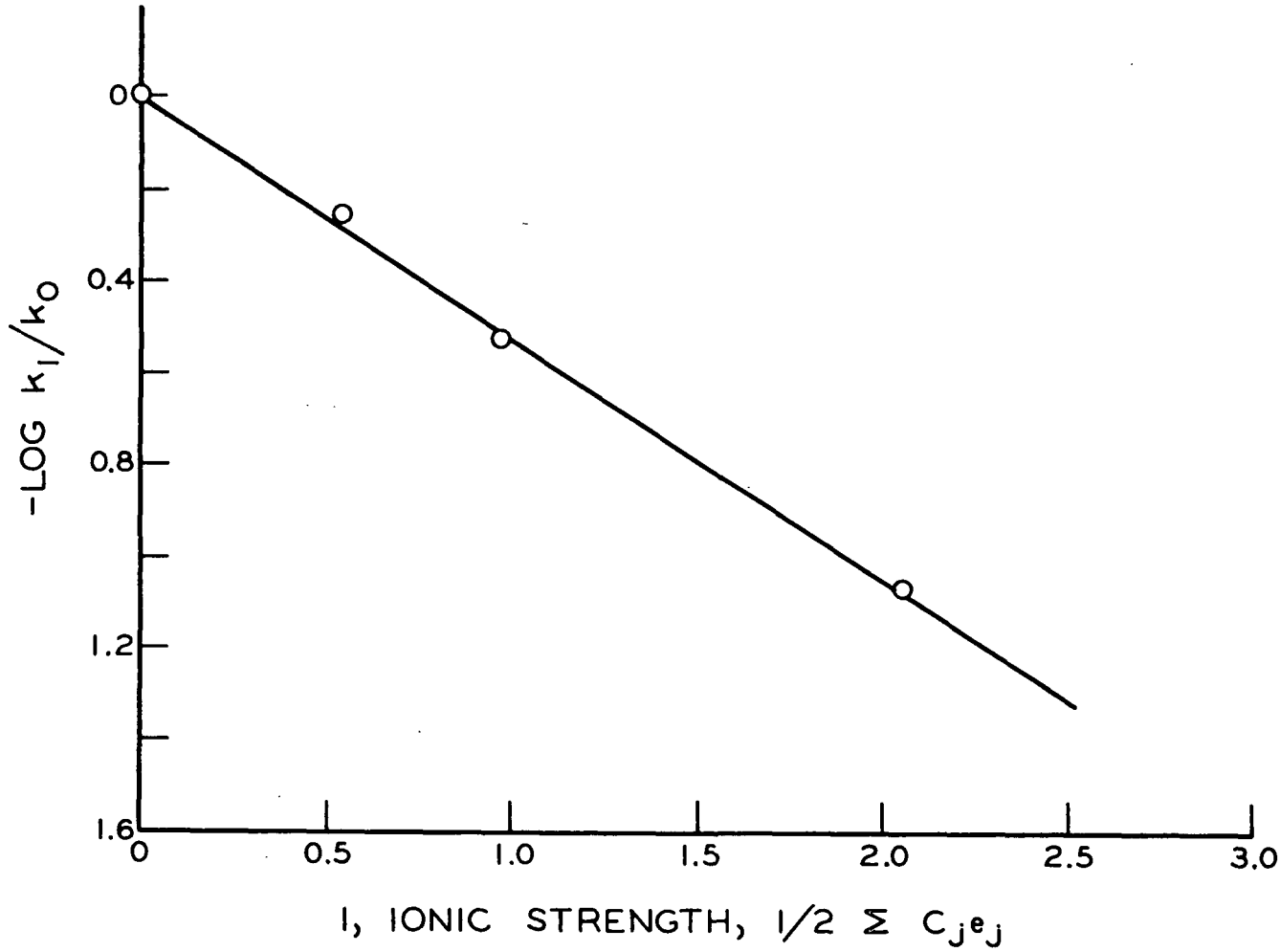

Figure 16. Rate Constant vs. Solution Ionic Strength for Chlorine Hydrolysis Reaction

with the chlorine and the activated species. This complexing could cause a less stable activated species and thus lower the equilibrium constant, $K_{S^{\ddagger}}$, of Reaction (42) which would in turn lower the rate constant. In other words, the actual molecular species of the reactant and activated complex change as the solvent ionic strength increases and causes increased complexing. Such a complexing mechanism was also evident during the diffusion experiments. (Appendix V.)

In terms of the transition state theory it is an arbitrary choice whether a concentration or an activity driving force is used to express the reaction rate. This is only true because for our particular system the activity coefficients of the reactants are independent of their concentration.

It has been found experimentally (40) that many systems do have reaction rates which are readily expressed as

$$R_i = (k_o/\beta)\, a_A a_B \tag{80}$$

where β is a factor which approaches unity as the system approaches model behavior, and k_o is the rate constant in a model system. In terms of the transition state theory it is seen that β represents the activity coefficient of the activated complex.

For the hydrolysis of chlorine in sodium sulfate solutions at 25°C. the rate expression for the forward reaction in terms of activity is

$$R_{Cl_2} = 0.377 \exp(-1.16\, I_s)\, a_{Cl_2} a_{H_2O} \tag{81}$$

whereas in terms of concentration

$$R_{Cl_2} = 0.377 \exp(-1.26\, I_s)\, C_{Cl_2} C_{H_2O} \tag{82}$$

If the activity coefficients were concentration dependent, a rate expression in terms of an activity driving force would be more convenient.

Again, as in the case of diffusion, the rate of entropy increase is the most fundamental factor governing the reaction rate. Ideally, the rate

of the reaction should be in terms of this entropy increase and the molecular mechanical properties of the system. An activity driving force more closely represents this ideal than does a concentration driving force.

The Effect of the Reverse Reaction on the Absorption Rate

At low pH values the reverse reaction begins to influence the hydrolysis rate as is evident in Zone A of Fig. 14. The rate of absorption accompanied by this first-order forward, third-order reverse reaction could be determined from the penetration theory if the differential equations describing the process could be solved. These equations are

$$\partial C_{Cl_2}/\partial t - D_{Cl_2}\partial^2 C_{Cl_2}/\partial x^2 = D_{HCl}\partial^2 C_{HCl}/\partial x^2 - \partial C_{HCl}/\partial t =$$

$$D_{HOCl}\partial^2 C_{HOCl}/\partial x^2 - \partial C_{HOCl}/\partial t =$$

$$k_1 C_{Cl_2} - k_2 C_{H^+} C_{Cl^-} C_{HOCl} \qquad (83)$$

The boundary conditions become

$$\text{at} \quad x = 0, \quad t > 0; \quad C_{Cl_2} = C_{Cl_{2e}}, \quad \partial C_{HCl}/\partial x = \partial C_{HOCl}/\partial x = 0$$

$$x > 0, \quad t = 0; \quad C_{Cl_2} = C_{HCl} = C_{HOCl} = 0$$

$$x = \infty, \quad t \geq 0; \quad C_{Cl_2} = C_{HCl} = C_{HOCl} = 0 \qquad (84)$$

Unfortunately, no analytical solution to this system of equations could be found. A numerical integration of the equations for the specific conditions of the chlorine-water system at 25°C. was carried out using the value of the forward reaction rate constant determined previously, i.e., 20.9 sec.^{-1}.

Details of this integration are given in Appendix IX. The results of the integrations are shown in Fig. 17 which is a plot of the instantaneous absorption rate, $\underline{N}_A$, against the time of exposure at various pH values.

The line for physical absorption, line e, was obtained by making the hydrogen ion concentration 10$\underline{N}$ in the absorbent and thus forcing the numerical solution to represent physical absorption. The average rate of physical absorption was obtained by integrating under line e as follows:

$$\bar{N}_A = 1/t_e \int_0^{t_e} N_A \, dt \qquad (85)$$

The value obtained was 1.048×10^{-4} g./(sq. cm.)(sec.) at 0.03 second. The analytical solution, Equation (35), gives a value of 1.059×10^{-4} g./(sq. cm.)(sec.) for the average rate of physical absorption. This 1% error is the result of truncating errors in the numerical integration method.

The average rate of absorption at 0.03 second for each pH value was obtained by numerically integrating each line according to Equation (85). The function, Φ, was calculated as a function of pH by dividing the rate with chemical reaction by the rate without chemical reaction. The appropriate values are compared to the experimental results in Table XII.

The slight discrepancy at the higher pH values is felt to arise from truncating errors in the numerical integration method and not to deficiencies in the penetration theory.

It is interesting to see that the absorbent must be quite acidic before the reverse reaction has an appreciable effect on the absorption rate.

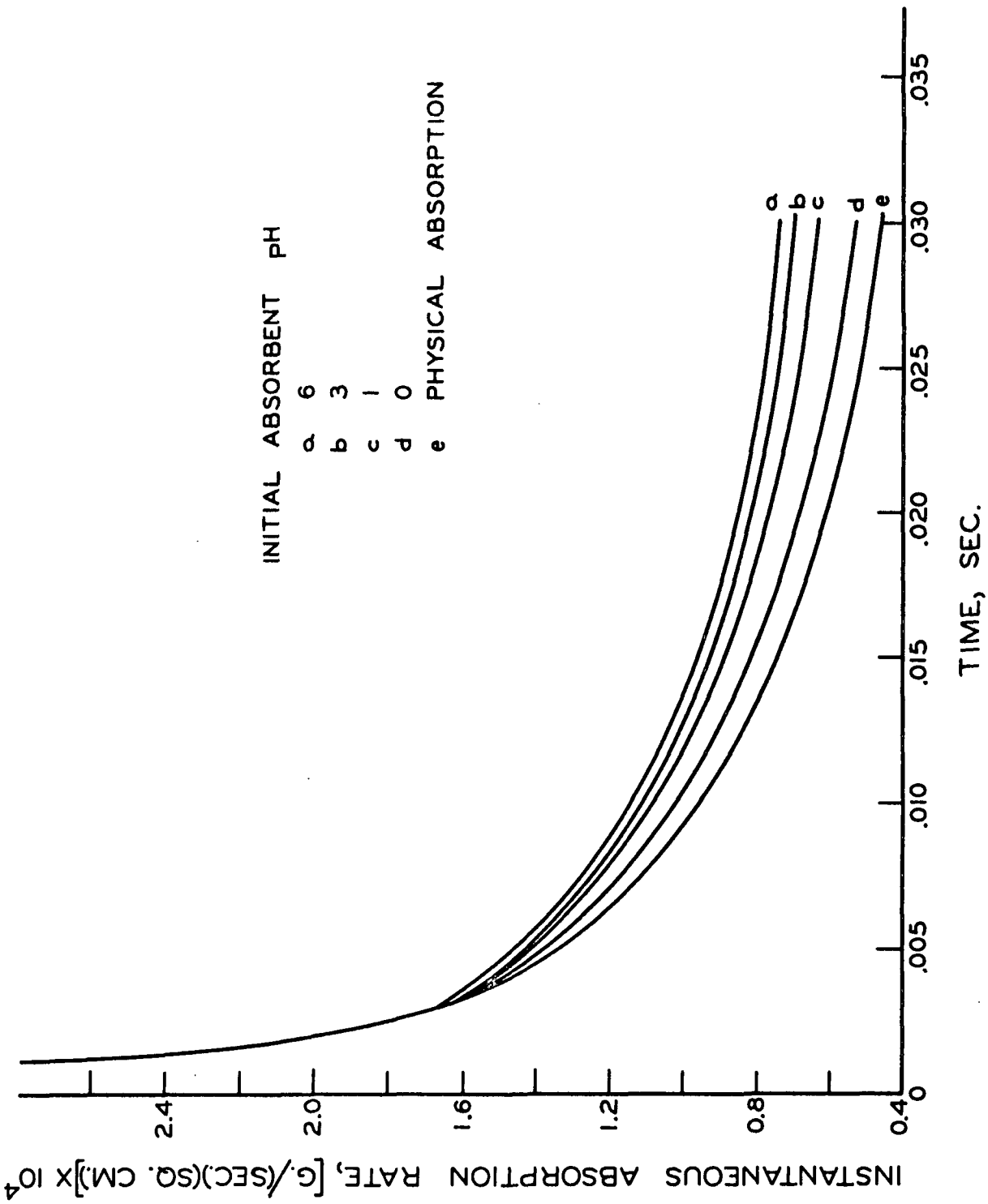

Figure 17. Influence of Reverse Reaction on Chlorine Absorption Rate at 25°C. and P_{Cl_2} = 760 mm. Hg.

TABLE XII

COMPARISON OF Φ VALUES AT 0.03 SECOND

pH	Experimental	Calculated
6	1.20	1.18
2.7	1.17	1.14
1.6	1.12	1.12
1.0	1.09	1.09

This is extremely fortunate because then throughout most of the pH range the reaction rate can be expressed by a first-order irreversible expression which greatly simplifies the penetration theory absorption rate equations.

The Effect of the Reaction with Hydroxyl Ions on the Absorption Rate

As is seen in Fig. 14 the effect of the reaction between hydroxyl ions and chlorine does not become prominent until a pH of 10.5 is reached and does not become dominant until a pH of 12.5 is reached. The very rapid rise in the function Φ with pH beyond this point is an indication that the chemical reaction is very rapid.

The penetration theory differential equations for absorption with an infinitely fast second-order irreversible reaction are capable of being solved analytically. A solution to these equations is presented in Appendix I.

The final result is

$$\overline{N}_A = 2\, C_{Cl_2,e} \sqrt{D_{Cl_2}/\pi t_e} \quad \left(1/\mathrm{erf}(\alpha/\sqrt{D_{Cl_2}})\right) \qquad (86)$$

where α is given by

$$C_{Cl_2,e}\sqrt{D_{Cl_2}}\ \exp(-\alpha^2/D_{Cl_2})\operatorname{erfc}(\alpha/\sqrt{D_{OH^-}}) =$$

$$C_{OH^-}\sqrt{D_{OH^-}}\ \exp(-\alpha^2/D_{OH^-})\operatorname{erf}(\alpha/\sqrt{D_{Cl_2}}) \qquad (87)$$

C_{OH^-} is the concentration of hydroxyl ions in the bulk of the liquid.

The reaction between chlorine and hydroxyl ions is second order and reversible. It is permissible to apply the irreversible equations to the reversible system provided that the equilibrium constant is large when compared to unity. The equilibrium constant for the reaction between chlorine and hydroxyl ions is of the order of 10^{10}.

The function, Φ, was calculated from Equations (86) and (87) for various values of the hydroxyl ion concentration. The diffusion coefficients of sodium hydroxide through water were taken from the International Critical Tables (56). The chlorine diffuses through a solution of sodium hypochlorite and sodium chloride. The diffusion coefficient of chlorine in this mixture was estimated by assuming that $(\mathfrak{m}\eta\gamma_{\underline{A}}^{2.5})$ remained constant. The activity coefficient of chlorine in this mixture was taken as the average between the activity coefficient in a sodium chloride solution and the activity coefficient in a sodium hydroxide solution of the same concentration. The activity coefficient of chlorine in the sodium hydroxide solutions was estimated as is explained in Appendix IV.

The resulting calculated Φ values at 0.03 second exposure time are compared to the appropriate experimental values in Table XIII.

TABLE XIII

THE EFFECT OF HYDROXYL ION CONCENTRATION ON THE ABSORPTION RATE OF CHLORINE INTO WATER AT 0.03 SEC. AND 25°C.-P_{Cl_2} = 760 mm. Hg.

NaOH Concentration, N	Experimental Φ	Calculated Φ
1.733	42.2	52.2
1.166	27.0	30.5
0.500	11.5	11.7
0.244	6.22	5.93
0.127	3.51	3.41
0.0603	2.07	2.17
0.00593	--	1.092
0.000593	--	1.0088
0.0000593	--	1.00087

It is noticed that the agreement between the experimental results and the theory for an infinitely fast reaction is good at the lower hydroxyl ion concentrations and poor at the higher hydroxyl ion concentrations. This can be explained by considering the penetration theory for absorption with a second-order reaction. Nyjsing (63) has shown that for the reaction A + B $\longrightarrow$, where A is the gaseous solute, the solution takes the form shown in Fig. 18. $\underline{C}_{\underline{B},o}$ is the initial concentration of B in the liquid, and $\underline{C}_{\underline{A},\underline{e}}$ is the concentration of A at the interface.

At low values of $\underline{C}_{\underline{B},o}/\underline{C}_{\underline{A},\underline{e}}$ the process follows the theory for an infinitely fast reaction; and at high values of $\underline{C}_{\underline{B},o}/\underline{C}_{\underline{A},\underline{e}}$ where the lines are horizontal, the process behaves as a first-order reaction because the

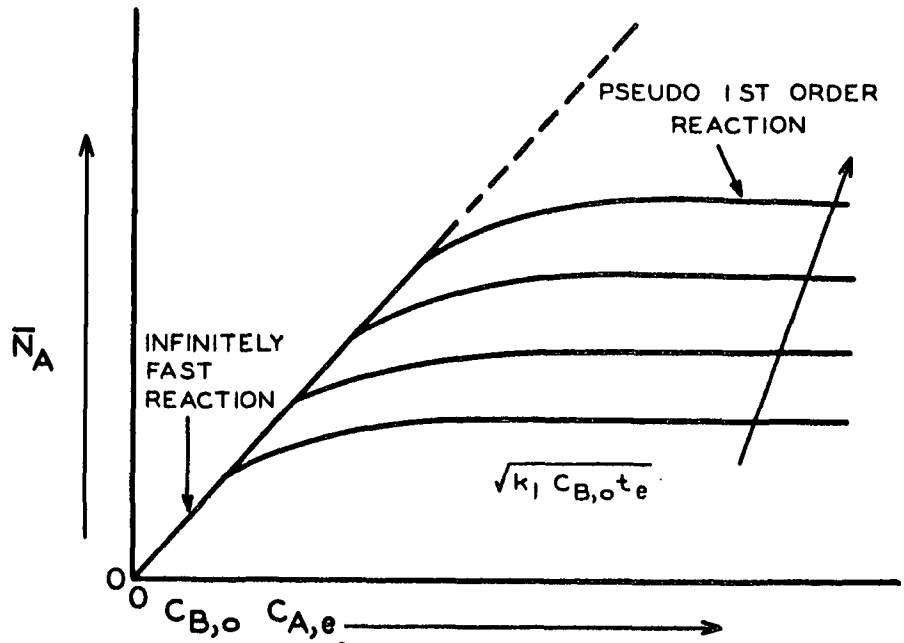

Figure 18. Absorption with Second-Order Chemical Reaction

concentration of B is so great that it is not depleted to an appreciable extent by the reaction. The curved portion of the curves represents the region where the reaction has a finite rate and is second order.

It is felt that the experimental points at 1.733N and 1.166N sodium hydroxide represent points where the absorption rates just begin to deviate from the infinitely rapid reaction line onto the curved portion of the lines. The penetration theory equations for this portion of the curve have not been solved, so an estimate of the rate constant for the reaction between chlorine and the hydroxyl ion cannot be made by this method.

Peaceman (31) presents an approximate solution for absorption accompanied by a second-order irreversible reaction by assuming that the diffusion process is at steady state, i.e., $\partial C_A / \partial t = 0$, and that all the diffusion

and reaction take place in a stagnant film next to the interface.* The function Φ is given by

$$\Phi = \sqrt{\bar{M}[1-q'(\Phi-1)]}/\tanh\sqrt{\bar{M}[1-q'(\Phi-1)]} \qquad (88)$$

where $\bar{M} = k_1 C_{B,o}\, x_f^2/D_A$ (89)

and $q' = (C_{A,e}/C_{B,o})\, D_A/D_B$ (90)

The thickness of the film, x_f, is given as follows:

$$x_f = 1/2\sqrt{\pi D_A t_e} \qquad (91)$$

Values of k_1 were calculated from the above equations and were found to vary from 0.5×10^6 to 5×10^6 l./(mole)(sec.) with hydroxyl ion concentration. It is felt that this variation is the result of using the film theory for the calculations. When the absorption is accompanied by simpler chemical reactions the penetration theory and the film theory predict absorption rates which are fairly close. For this reason it is believed that the order of magnitude of the calculated rate constant is correct even though the actual value cannot be firmly established.

It was indicated by the experimental work that during the transition region, Zone C of Fig. 14, the increase in absorption rate attributed to one reaction is additive to the increase attributed to the other reaction giving the total increase. The experimental points of Zones C and D of Fig. 14 are replotted in Fig. 19 together with the theoretical lines for

* The film theory.

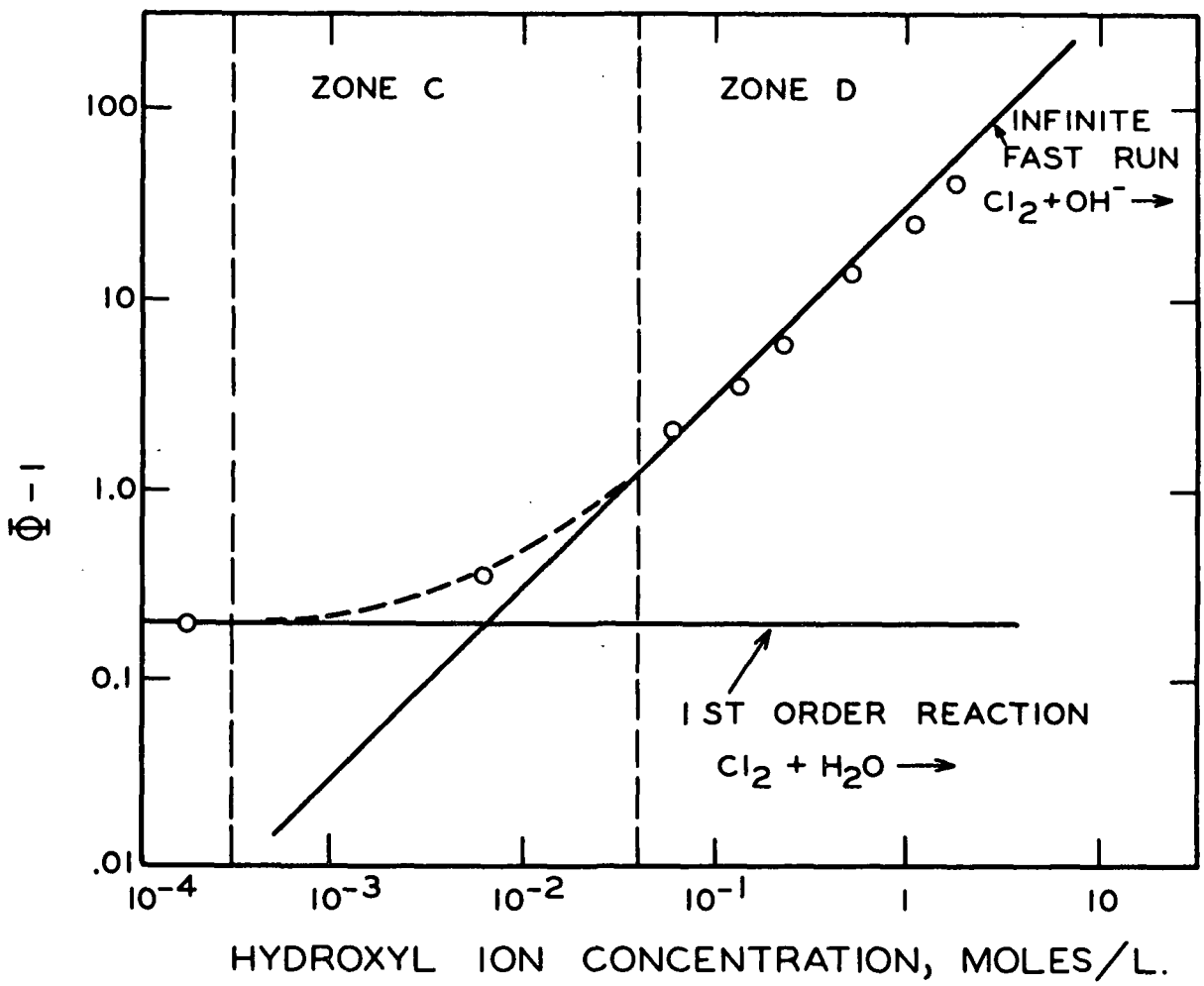

Figure 19. Influence of Reaction with Hydroxyl Ion on Chlorine Absorption Rate at 25°C. and P_{Cl_2} = 760 mm. Hg

the hydrolysis reaction and the infinitely fast reaction between chlorine and the hydroxyl ion. The dashed line in Zone C is the sum of the two theoretical lines. The closeness of the experimental point to the dashed line indicates that the expression

$$\bar{N}_{A_{\text{reaction 1 \& 2}}} = \bar{N}_{A_{\text{no reaction}}} + \Delta\bar{N}_{A_{\text{reaction 1}}} + \Delta\bar{N}_{A_{\text{reaction 2}}}$$

is a good approximation for the absorption rate when two competing reactions occur.

SUMMARY AND CONCLUSIONS

1. The equilibrium solubility of molecular chlorine in solutions of sodium chloride--0.1N hydrochloric acid and of sodium sulfate--0.15N hydrochloric acid was determined so that the penetration theory could be applied to the absorption of chlorine in these solutions. The solubility of unhydrolyzed chlorine in 0.1N hydrochloric acid was measured and found to be 4.22 g./l. at 25°C. and a chlorine partial pressure of 760 mm. Hg which agrees with the calculated solubility of chlorine in water. The addition of a salt always lowers the solubility of molecular chlorine in solution.

2. The diffusion coefficient of unhydrolyzed chlorine in water at 25°C. was measured on a Beckman, Spinco Model-H electrophoresis-diffusion apparatus and found to be 1.48×10^{-5} sq. cm./sec. which is in good agreement with the result of Peaceman (31) by a different technique. The diffusivity of chlorine in salt solutions, however, could not be experimentally determined.

3. Chlorine gas was absorbed into 0.1N hydrochloric acid with a laminar liquid jet apparatus at exposure times ranging from 0.008 to 0.04 second. The rates of absorption at these exposure times were found to be in very good agreement with the penetration theory. This indicated that the experimental apparatus was very suitable for the subsequent study of absorption with simultaneous chemical reaction.

4. Chlorine was absorbed into sodium chloride solutions ranging in concentration from 0 to 200 g./l. These solutions always contained 0.1N

hydrochloric acid to prevent the chlorine hydrolysis reaction from influencing the absorption rates. The purpose of these runs was to establish whether a concentration or activity driving force used in conjunction with the penetration theory best expressed the rates of absorption in systems which do not exhibit model behavior. It was concluded that an activity driving force yielded an absorption transfer coefficient which was a less complicated function of the system properties than did a concentration driving force. It was believed that the activity driving force was more closely related to the actual causes of mass transport.

5. Chlorine was absorbed into aqueous solutions whose initial pH ranged from one to fourteen. Chemical reactions took place resulting in varying absorption rates. The rate of absorption in these solutions was then compared to the rate that would occur if no chemical reaction had taken place. From this comparison it was definitely established that when chlorine comes in contact with water it reacts with both water molecules and hydroxyl ions. Either or both of these reactions controls the rate of chlorine consumption depending upon the pH of the solution. For an exposure time of 0.03 second and at a pH less than three the rate-controlling reaction is the reversible reaction between chlorine and water. Between a pH of 3 and 10.5 the forward reaction of chlorine and water controls the absorption rate. At a pH greater than 12.5 the reaction between chlorine and the hydroxyl ion is rate controlling. Between pH 10.5 and 12.5 a transition zone exists in which both reactions influence the rate of chlorine consumption.

6. By analyzing the chlorine-water absorption data in terms of the penetration theory it was evaluated that the reaction between chlorine and water proceeds with a first-order reaction rate constant of 20.9 $\pm$ 1.2 $sec.^{-1}$ at 25°C. The reaction between chlorine and the hydroxyl ion has a second-order rate constant in the order of 10^6 l./(mole)(sec.) at 25°C. At pH values of less than 13.5 the reaction between chlorine and the hydroxyl ion may be considered as being infinitely fast when used in predicting absorption rates.

7. Chlorine was absorbed into sodium sulfate solutions in the pH range where the reaction between chlorine and water is first order with respect to chlorine. The purpose of these runs was to establish the effect of ionic strength on the rate of the reaction. It was found that the rate constant decreased markedly with ionic strength and in a manner predictable by the transition state theory of reaction rates.

8. The influence on the rate of absorption of the chemical reaction between chlorine and water and between chlorine and the hydroxyl ion was determined, and it was shown that this influence was capable of being predicted by the penetration theory over the entire pH range.

ACKNOWLEDGMENTS

I wish to thank Messrs. S. T Han, R. P. Whitney, and H. D. Wilder of the thesis advisory committee for their guidance and encouragement in this work.

The assistance of R. B. Kesler in developing the analytical procedures, of E. O. Dillingham in running the Spinco Model-H apparatus, and of R. W. Nelson in helping with many mathematical problems is gratefully acknowledged.

The assistance of W. H. Trice, F. J. Vermillion, and R. B. Wasser in carrying out some preliminary experiments is very much appreciated.

I also wish to thank the International Business Machines Corporation and the Kimberly-Clark Corporation for making the IBM 650 Computer available for use.

NOMENCLATURE

a	interfacial area, sq. ft./cu. ft.
a_i	activity of species i
A	frequency factor in Arrhenius equation
A'	constant in Equations (101) through (104)
$A_{m,n}$	concentration of chlorine in numerical integration, moles/l.
b	relative boundary layer thickness, δ/R_o
b_i	constant in Equation (25)
b_j	radius of ion species j
c_1	k_1K in numerical integration
c_2	k_2K in numerical integration
C	initial hydrogen ion concentration in numerical integration
C_i	concentration of species i, moles/l. or g./l.
C_p	heat capacity of solution, cal./(mole)(°K.)
D_i	diffusion coefficient of species i defined in terms of a concentration driving force, sq. cm./sec.
D_s	dielectric constant of solvent
D_o	diameter of nozzle opening, cm.
D	diameter of jet, cm.
e_j	electrical charge of ion species j
E_a	activation energy, cal./mole
$E_{m,n}$	concentration of hypochlorous acid in numerical integration, moles/l.
f_i	fugacity of species i
$F_{m,n}$	concentration of hydrochloric acid in numerical integration, moles/l.
$F_{(s)}$	Laplace integral, Equation (94)

g gravitational constant, cm./sq. sec.

h intermediate jet length, cm.

h' grid spacing in space, cm.

H total jet length, cm.

$\Delta H^{\ddagger}$ enthalpy of activation, cal./mole

I_s ionic strength of solution, $1/2\Sigma C_j e_j^2$

J rate of diffusion per unit area, g./(sec.)(sq. cm.)

k Boltzmann's constant

k_1 rate constant for forward reaction

k_2 rate constant for reverse reaction

k_L liquid-side mass transfer coefficient, cm./sec. or ft./hr.

K grid spacing in time, sec.

K_i Henry's law constant for species i

K_i' $\gamma_i K_i$, Equation (17)

K_T thermal conductivity of solution, cal./(mole)(cm.)(°K.)

$K_S^{\ddagger}$ equilibrium constant for Reaction (42)

L liquid flow rate, lb./(hr.)(sq. ft.)

m constant in Equation (107)

M molecular weight, g./mole

$\overline{M}$ variable in Equation (88)

N_A instantaneous absorption rate, g./(sec.)(sq. cm.)

$\overline{N}_A$ average absorption rate, g./(sec.)(sq. cm.)

p steric factor in collision theory

p_i partial pressure of species i

P total pressure, atm.

q jet flow rate, cc./sec.

q' variable in Equation (88)

R gas constant, cal./(mole)(°K.)

R_i rate of reaction, mole/(sec.)(l.)

R_o nozzle radius, cm.

s Laplace transform variable

S entropy, cal./(mole)(°K.)

$\Delta S^{\ddagger}$ entropy of activation, cal./(mole)(°K.)

t intermediate time, sec.

t_e total exposure time, sec.

T absolute temperature, °K.

T_s temperature at jet surface, °K.

T_o temperature at jet core, °K.

$\overline{U}$ mean velocity of jet, cm./sec.

$\overline{U}_o$ mean velocity of jet at nozzle, cm./sec.

U_s velocity at jet surface, cm./sec.

U_∞ velocity of jet at core, cm./sec.

U velocity vector parallel to bulk flow, cm./sec.

V velocity vector perpendicular to bulk flow, cm./sec.

x direction of mass movement, cm.

x_f film thickness, cm.

x_i mole fraction of species i

X distance in x co-ordinate system

y direction perpendicular to mass movement, cm.

Z collision frequency, l./(mole)(sec.)

α relative concentration, Equation (92)

α' constant in Equation (158)

$\bar{\alpha}$ Laplace transform of α

β constant in Equation (80)

β' heat of solution of molecular chlorine, cal./mole

$\bar{\beta}$ constant in Equation (188)

γ_i activity coefficient of species i

δ boundary layer thickness, cm.

ϵ constant in Equation (43)

λ_i $D_i K/h'^2$, Equations (202)-(204)

η viscosity relative to water

ρ density of solution, g./cc.

χ association parameter, Equation (52)

Φ function defined by Equation (38)

μ viscosity of solution, g./sec. cm.

μ_i chemical potential of species i, cal./mole

ℓ equivalent flat plate length, cm.

ℓ' characteristic nozzle length, cm.

$\mathcal{L}$ Laplace transform operator

$\mathcal{D}$ diffusion coefficient defined in terms of an activity driving force, sq. cm./sec.

$\mathcal{D}$ diffusion coefficient defined in terms of a chemical potential driving force

Subscripts:

A the gaseous solute

B the reactant in solution

e equilibrium at interface

i species i

$\underline{j}$ species $\underline{j}$

$\underline{m}$ the $\underline{m}^{th}$ position in space

$\underline{M}^{\ddagger}$ the activated complex

$\underline{n}$ the n^{th} position in time

$\underline{o}$ pure water or bulk of solution

$\underline{s}$ salt solution

Superscripts:

$\underline{s}$ solution phase

$\underline{v}$ vapor phase

$\underline{o}$ standard value

$*$ absorption without chemical reaction

exp $\underline{z}$ exponential of $\underline{z}$, i.e., $e^{\underline{z}}$

erf $\underline{z}$ error function of $\underline{z}$, i.e., $2/\sqrt{\pi} \int_0^{\underline{z}} e^{-\underline{u}^2} \underline{du}$

erfc $\underline{z}$ 1 - erf $\underline{z}$

LITERATURE CITED

1. Higbie, R., Trans. Am. Inst. Chem. Engrs. 31:365-70(1935).

2. Whitney, R. P., and Vivian, J. E., Ind. Eng. Chem. 33:741-4(1941).

3. Yokota, N., Kagaku Kogaku (Japan) 22:476-82(1958).

4. Yakovin, A. J., Russ. Phys.-Chem. Soc. 32:673(1900); Quoted in Whitney and Vivian (2).

5. Gibbs, J. Willard. The collected works of J. Willard Gibbs, New York, Longmans, Green and Co., 1928. 434 p.

6. Siegler, L., Chem. Ing. Tech. 22:229-35(1950).

7. Pimentol, S. C., and McClellan, A. L., The hydrogen bond. San Francisco, W. H. Freeman, 1960. 475 p.

8. Setchenow, M., Ann. Chim. Phys. 25:226(1892); Quoted in Harned, H. S., and Owen, B. B. The physical chemistry of electrolytic solutions. 3rd ed. p. 531. New York, Reinhold, 1958.

9. Debye, P., and McAuley, J., Physik. Z. 26:22(1925); Quoted in Harned and Owen. p. 80.

10. Connick, R. E., and Chia, Y. T., J. Am. Chem. Soc. 81:1280-1(1959).

11. Latimer, Wendell M., Oxidation potentials, 2nd ed., p. 55. New York, Prentice Hall, 1952.

12. Kielland, Jacob, J. Am. Chem. Soc. 59:1675-8(1937).

13. Shilov, E. A., and Solodushenkov, S. N., Compt. Rend. Acad. Sci. (USSR) 3:15-19(1936); C.A. 31:239.

14. Morris, J. Carrell, J. Am. Chem. Soc. 68:1692-4(1946).

15. Shilov, E. A., and Solodushenkov, S. N., J. Phys. Chem. (USSR) 21: 1159-61(1947); C.A. 42:2495g.

16. Liftshitz, A., and Perlmutter-Haymen, B., J. Phys. Chem. 64:1663-7 (1960).

17. Eigen, M. Discussions Faraday Soc. 17:194-205(1954).

18. Onsager, L., J. Chem. Phys. 2:599-614(1933).

19. Debye, D., Trans. Electrochem. Soc. 82:265(1942).

20. Umberger, J. Q., and La Mer, V. K., J. Am. Chem. Soc. 67:1099-1109(1945).

21. Moelwyn-Hughes, E. A. Kinetics of reaction in solution. Oxford, Clarendon Press, 1942.

22. Eigen, M., and deMaeyer, L., Z. Electrochem. 59:986-93(1955).

23. Pozin, M. E., J. Appl. Chem. (USSR) 20:345-59, 963-75(1947); Quoted in Sherwood, T. K., and Pigford, R. L. Absorption and extraction. p. 346. New York, McGraw-Hill, 1952.

24. Danckwerts, P. V., Trans. Faraday Soc. 46:300-4(1950).

25. Danckwerts, P. V., Trans. Faraday Soc. 46:701-12(1950).

26. Peaceman, Donald W. Liquid-side resistance in gas absorption with and without chemical reaction. p. 140-234. Sc. D. Thesis in Chem. Eng., Mass. Inst. of Tech., 1951.

27. Adair, G. S., Biochem. J. 14:762-79(1920).

28. Vivian, J. E., and Whitney, R. P., Chem. Eng. Progr. 43:691-702(1947).

29. Craig, E. T. The absorption of chlorine in hydrochloric acid solutions. S.M. Thesis in Chem. Eng., Mass. Inst. of Tech., 1951.

30. Whitney, R. P., and Vivian, J. E., Chem. Eng. Progr. 45:323-37(1949).

31. Peaceman, Donald W. Liquid-side resistance in gas absorption with and without chemical reaction. Sc.D. Thesis in Chem. Eng., Mass. Inst. of Tech., 1951. 426 p.

32. Nyjsing, R. A. T. O., Hendriksz, R. H., and Kramers, H., Chem. Eng. Sci. 10:88-104(1959).

33. Andrew, S. P. S., Chem. Eng. Sci. 3:279-86(1954).

34. Lynn, S., Straatemeier, J. R., and Kramers, H., Chem. Eng. Sci. 4:49-57(1955).

35. Cullen, E. J., and Davidson, J. F., Chem. Eng. Sci. 6:49-55(1956).

36. Prigogini, J. Introduction to thermodynamics of irreversible processes. Springfield, Illinois, Charles C. Thomas, Publisher, 1955. 115 p.

37. Harned, Herbert S., Chem. Revs. 40:461-522(1947).

38. Kirkwood, J. G., J. Chem. Phys. 14:180-201(1946).

39. Leaf, B., Phys. Rev. 70:748-58(1946).

40. Denhigh, K. G. The principles of chemical equilibrium. Cambridge, University Press, 1955.

41. Gilliland, E. R., and Sherwood, T. K., Ind. Eng. Chem. 26:516-23(1934).

42. Barnet, W. J., and Kobe, K. A., Ind. Eng. Chem. 33:436-42(1941).

43. Morris, G. A., and Jackson, J. Absorption towers. London, Butterworths, 1953.

44. Johnstone, H. F., and Pigford, R. L., Trans. Am. Inst. Chem. Eng. 38:25-32(1942).

45. Jackson, M. L., and Ceagalske, N. H., Ind. Eng. Chem. 42:1188-97(1950).

46. Stephens, G. A., and Morris, G. A., Chem. Eng. Progr. 47:232-42(1951).

47. Lynn, S., Straatemeier, J. R., and Kramers, H., Chem. Eng. Sci. 4:63-70(1955).

48. Oyama, Y., and Iwase, K., Sci. Papers Inst. Phys. Chem. Research (Tokyo) 35:131-57(1939); C.A. 33:3239.

49. Guyer, A., and Pfister, X., Helv. Chim. Acta 29:1400-12(1946); C.A. 41:4026g.

50. Dixon, B. E., and Swallow, J. E. L., J. Appl. Chem. 4:86-93(1954).

51. Danckwerts, P. V., and Kennedy, A. M., Trans. Inst. Chem. Engrs. (London) 32:S49-S53(1954).

52. Cullen, E. J., and Davidson, J. F., Trans. Faraday Soc. 53:113-20 (1957).

53. Matsuyama, T., Chem. Eng. (Japan) 19:245(1950).

54. Scriven, L. E. Interfacial resistance in gas absorption. Ph.D. Thesis. Univ. of Delaware, 1956.

55. Sherril, M. S., and Izard, E. F., J. Am. Chem. Soc. 53:1667-74(1931).

56. West, C. J. International critical tables. Vol. III. New York, McGraw-Hill, 1933.

57. Chang, P., and Wilke, C. R., A. J. Ch. E. Journal 1:264-70(1955).

58. Olson, R. L., and Walton, J. S., Ind. Eng. Chem. 43:703-6(1951).

59. Othmer, D. F., and Thakar, M. S., Ind. Eng. Chem. 45:589-98(1953).

60. Glasstone, S., Laidler, K. J., and Eyring, H. The theory of rate processes. p. 477. New York, McGraw-Hill, 1941.

61. Cranck, J. The mathematics of diffusion. London, Oxford Press, 1956.

62. Frost, A. A., and Pearson, R. G. Kinetics and mechanism. New York, John Wiley & Sons, 1953.

63. Nyjsing, R. A. T. O. Dissertation, Delft, 1957; Quoted in Pigford, R. L. Diffusion and chemical kinetics. Unpublished manuscript, 1958.

64. Hansen, M. NACA Tech. Memo. No. 585, 1930; Quoted in Schlicting, H. Boundary layer theory. p. 111. New York, McGraw-Hill, 1955.

65. Nikuradse, J. Quoted in Schlicting. p. 219.

66. Goldstein, S., Proc. Cambr. Phil. Soc. 26:Part 1 (1930); Quoted in Schlicting. p. 142.

67. Schiller, L., Phys. Z. 23:14(1922).

68. Rideal, E. K., and Sutherland, K. L., Trans. Faraday Soc. 48:1109-23 (1952).

69. Scriven, L. E., and Pigford, R. L., A. J. Ch. E. Journal 5:397-402 (1959).

70. Danckwerts, P. V., Appl. Sci. Research A3:385-90(1952).

71. Blanch, G., J. Research Natl. Bur. Standards 50:343-56(1953).

72. Stokes, R. H., J. Am. Chem. Soc. 72:763-7(1950).

73. Schachman, H. K., Enzymology 4:32-104(1957).

74. Pierce, W. C., and Haenisch, E. L. Quantitative analysis. 3rd. ed. New York, John Wiley & Sons, 1948.

75. Pitts, J. N., DeFord, D. D., Martin, T. W., and Schmall, E. A., Anal. Chem. 26:268(1954).

76. Rideal, S., and Stewart, G. G., Analyst 26:141-8(1901).

77. Sherwood, T. K., and Holloway F. A. L., Trans. Am. Inst. Chem. Engrs. 36:39-70(1940).

78. Sherwood, T. K., and Pigford, R. L. Absorption and extraction. 2nd. ed. New York, McGraw-Hill, 1952.

79. Grimely, S. S., Trans. Inst. Chem. Engrs. 23:228-35(1945).

80. Campbell, G. A., and Foster, R. M. Fourier integrals for practical applications. New York, D. Van Nostrand Company, 1948.

81. Pigford, R. L. Diffusion and chemical kinetics. Unpublished manuscript, 1958.

APPENDIX I

MATHEMATICAL DETAILS OF THE PENETRATION THEORY

PHYSICAL ABSORPTION

The basis differential equation of the penetration theory describing purely physical absorption is given by Equation (29) as

$$D_A \partial^2 C_A/\partial x^2 - \partial C_A/\partial t = 0 \qquad (29)$$

The appropriate boundary conditions are

$$\text{at} \quad t = 0, \quad x > \delta \qquad C_A = C_{A,o} \qquad (31)$$

$$x = \infty, \quad t \geq 0 \qquad C_A = C_{A,o} \qquad (32)$$

$$x = 0, \quad t > 0 \qquad C_A = C_{A,e} \qquad (33)$$

In solving Equation (29) the following substitution is made

$$\alpha = (C_A - C_{A,o})/(C_{A,e} - C_{A,o}) \qquad (92)$$

Equation (29) and the boundary conditions then become

$$D_A \partial^2\alpha/\partial x^2 - \partial\alpha/\partial t = 0 \qquad (93)$$

$$\text{at} \quad x = 0, \quad t > 0 \qquad \alpha = 1$$

$$t = 0, \quad x > 0 \qquad \alpha = 0$$

$$x = \infty, \quad t \geq 0 \qquad \alpha = 0 \qquad (94)$$

Parabolic partial differential equations like Equation (93) occur frequently in diffusion and heat problems. Solutions to these have been established for many initial and boundary value situations. It has been found that for the initial value problem of interest here, the Laplace transform technique gives a readily available solution.

The Laplace transform of any function, α, is given by:

$$\mathcal{L}(\alpha) = \bar{\alpha} = \int_0^\infty e^{-st}\, \alpha\, dt = F_{(s)} \tag{94}$$

The Laplace transform of many functions have been tabulated (80). Relationships of interest here from these tables are:

$$\mathcal{L}\,(\partial\alpha/\partial x) = \partial\,(\mathcal{L}(\alpha))/\partial x = \partial\bar{\alpha}/\partial x \tag{95}$$

$$\mathcal{L}\,(\partial\alpha/\partial t) = s\,\bar{\alpha} - (\alpha)_{t=0} \tag{96}$$

$$\mathcal{L}\,(t\alpha) = -F'_{(s)} \tag{97}$$

$$\mathcal{L}\left(\int_0^t \alpha\, dt\right) = 1/s\; F_{(s)} \tag{98}$$

The inverse operation is designated as

$$\mathcal{L}^{-1}\,(\bar{\alpha}) = \alpha \tag{99}$$

Inverse operations of interest are

$$\mathcal{L}^{-1}\,(1/s)\,\exp(-A'\sqrt{s}) = \operatorname{erfc}\,(A/2\sqrt{t}) \tag{100}$$

where A' is any constant.

$$\mathcal{L}^{-1}\,(-1/A'\sqrt{s}) = -1/A'\sqrt{\pi t} \tag{101}$$

$$\mathcal{L}^{-1}\,(1/\sqrt{s + A'}) = (1/\sqrt{\pi t})\,\exp(-A't) \tag{102}$$

$$\mathcal{L}^{-1}(1/s\sqrt{s + A'}) = (1/\sqrt{A'})\,\operatorname{erf}\sqrt{A't} \tag{103}$$

$$\mathcal{L}^{-1}\,(1/s^2\sqrt{s + A'}) = (t/\sqrt{A'})\,\operatorname{erf}\sqrt{A't} - 1/2[(1/A'^{3/2})\operatorname{erf}\sqrt{A't} - (2\sqrt{t}/A'\sqrt{\pi})\exp(-A't) \tag{104}$$

Operating on Equation (93) gives

$$D_A \, d^2 \bar{\alpha}/dx^2 - s \, \bar{\alpha} = 0 \tag{105}$$

The function, s, is only a function of t; and the function, $\bar{\alpha}$, is only a function of x and s; therefore, s may be regarded as a constant in Equation (105) and the total second derivative of $\bar{\alpha}$ is permissible. Operating on the boundary conditions gives

$$\begin{aligned} &\text{at} \quad x = 0, && \bar{\alpha} = 1/s \\ &\qquad x = \infty, && \bar{\alpha} = 0 \end{aligned} \tag{106}$$

The initial condition, $t = 0, \alpha = 0$, has been used in Equation (96) when obtaining Equation (105). Equation (105) may be solved in substituting

$$\bar{\alpha} = e^{mx} \tag{107}$$

Equation (105) then becomes

$$e^{mx} \left[m^2 - s/D_A\right] = 0 \tag{108}$$

The auxiliary equation has the roots

$$m = \pm\sqrt{s/D_A} \tag{109}$$

Thus, the general solution of Equation (105) is

$$\bar{\alpha} = C_1 \exp(\sqrt{s/D_A}\, x) + C_2 \exp(-\sqrt{s/D_A}\, x) \tag{110}$$

The constants C_1 and C_2 can be evaluated from the boundary conditions (106).

$$C_1 = 0 \tag{111}$$

$$C_2 = 1/s \tag{112}$$

Thus,

$$\bar{\alpha} = 1/s \exp(-\sqrt{s/D_A}\, x) \tag{113}$$

From Equation (100)

$$\alpha = \text{erfc}\ (x/2\sqrt{D_A t}) \tag{114}$$

or

$$(C_A - C_{A,o})/(C_{A,e} - C_{A,o}) = 1 - \text{erf}(x/2\sqrt{D_A t}) \tag{115}$$

It is desired to obtain the rate of absorption which is equal to the rate of diffusion away from the interface.

$$N_A = -D_A(\partial C_A/\partial x)_{x=0} = -D_A(C_{A,e} - C_{A,o})(\partial\alpha/\partial x)_{x=0} \tag{116}$$

$$\partial\alpha/\partial x = \mathcal{L}^{-1}(\partial\bar{\alpha}/\partial x) \tag{117}$$

Differentiating Equation (113)

$$\partial\bar{\alpha}/\partial x = -1/\sqrt{sD_A}\ \exp(-\sqrt{s/D_A}\, x) \tag{118}$$

therefore,

$$(\partial\bar{\alpha}/\partial x)_{x=0} = -1/\sqrt{sD_A} \tag{119}$$

From Equation (101)

$$\mathcal{L}^{-1}(\partial\bar{\alpha}/\partial x)_{x=0} = (\partial\alpha/\partial x)_{x=0} = -1/\sqrt{D_A \pi t} \tag{101}$$

Therefore, from Equation (116)

$$N_A = (C_{A,e} - C_{A,o})\sqrt{D_A/\pi t} \tag{34}$$

The average rate of absorption over a given time period, t_e, is given by:

$$1/t_e \int_o^{t_e} N_A\, dt = \sqrt{D_A/\pi}\ (C_{A,e} - C_{A,o}) \int_o^{t_e} t^{-1/2} dt \tag{120}$$

$$\bar{N}_A = 2(C_{A,e} - C_{A,o})\sqrt{D_A/\pi t_e} \tag{35}$$

ABSORPTION WITH SIMULTANEOUS FIRST-ORDER IRREVERSIBLE CHEMICAL REACTION

For the case of absorption with first-order irreversible chemical reaction the differential Equation (37) reduces to

$$D_A \, \partial^2 C_A/\partial x^2 - \partial C_A/\partial t = k_1 C_A \tag{121}$$

and the boundary conditions become:

$$\begin{aligned} &\text{at} \quad x = 0, \quad t > 0, && C_A = C_{A,i} \\ &\qquad t = 0, \quad x > 0, && C_A = C_{A,o} \\ &\qquad x = \infty, \quad t \geq 0, && C_A = C_{A,o} \exp(-k_1 t) \end{aligned} \tag{122}$$

The last boundary condition results from the fact that at an infinite distance from the interface a concentration change takes place because of the chemical reaction and not from diffusion. Thus, at $\underline{x} = \infty$

$$-d \, C_A/dt = k_1 C_A \tag{123}$$

Integrating,

$$\int_{C_{A,o}}^{C_A} d \, C_A/C_A = -k_1 \int_o^t dt \tag{124}$$

$$\ln (C_A/C_{A,o}) = -k_1 t \tag{125}$$

$$C_A = C_{A,o} \exp(-k_1 t) \tag{126}$$

Operating on Equation (121) and the boundary conditions (122) with the Laplace transform gives

$$D_A \, d^2\overline{C}_A/dx^2 - (s \, \overline{C}_A - C_{A,o}) = k_1 \overline{C}_A \tag{127}$$

where

$$\bar{C}_A = \mathcal{L}(C_A) \tag{128}$$

and at $x = 0$ $$\bar{C}_A = C_{A,e}/s \tag{129}$$

$x = \infty$ $$\bar{C}_A = C_{A,o}/(s + k_1) \tag{130}$$

Rearranging Equation (127)

$$d^2 \bar{C}_A/dx^2 - \bar{C}_A(s + k_1)/D_A = -C_{A,o}/D_A \tag{131}$$

A solution to the reduced equation of Equation (131) is obtained as is Equation (110) and is

$$\bar{C}_A = C_1 \exp[\sqrt{(s + k_1)/D_A}\ x] + C_2 \exp[-\sqrt{(s + k_1)/D_A}\ x] \tag{132}$$

A particular solution to the completed equation is

$$\bar{C}_A = C_{A,o}/(s + k_1) \tag{133}$$

Thus, the complete solution is

$$\bar{C}_A = C_1 \exp[\sqrt{(s + k_1)/D_A}\ x] + C_2 \exp[-\sqrt{(s + k_1)/D_A}\ x] + C_{A,o}/(s + k_1) \tag{134}$$

From the boundary conditions (129) and (130)

$$C_1 = 0$$
$$C_2 = C_{A,e}/s - C_{A,o}/(s + k_1) \tag{135}$$

Thus,

$$\bar{C}_A = -[C_{A,e}/s - C_{A,o}/(s + k_1)] \exp[-\sqrt{(s + k_1)/D_A}\ x] + C_{A,o}/(s + k_1) \tag{136}$$

Differentiating Equation (136)

$$d\bar{C}_A/dx = -[C_{A,e}/s - C_{A,o}/(s + k_1)] \cdot \sqrt{(s + k_1)/D_A} \quad \exp[-\sqrt{(s + k_1)/D_A}\ x] \quad (137)$$

at $\underline{x} = 0$

$$(d\bar{C}_A/dx)_{x=0} = 1/\sqrt{D_A}\ [(C_{A,o}-C_{A,e})/\sqrt{s + k_1} - C_{A,e}\ k_1/s\sqrt{s + k_1}] \quad (138)$$

From Equations (102) and (103)

$$(\partial C_A/\partial x)_{x=0} = 1/\sqrt{D_A}\ \left\{[(C_{A,o}-C_{A,e})/\sqrt{\pi t}]\ \exp(-k_1 t) - C_{A,e}\sqrt{k_1}\ \ \text{erf}\ \sqrt{k_1 t}\right\} \quad (139)$$

$$N_A = -D_A\ (\partial C_A/\partial x)_{x=0} \quad (140)$$

Substituting Equation (139) into (140)

$$N_A = \sqrt{D_A}\ \left\{[(C_{A,e}-C_{A,o})/\sqrt{\pi t}]\ \exp(-k_1 t) + C_{A,e}\sqrt{k_1}\ \text{erf}\ \sqrt{k_1 t}\right\} \quad (141)$$

The average absorption rate in time, $\underline{t_e}$, is

$$\bar{N}_A = 1/t_e \int_o^{t_e} N_A\ dt = -D_A/t_e \int_o^{t_e} (\partial C_A/\partial x)_{x=0}\ dt \quad (142)$$

From Equations (138) and (98)

$$\mathcal{L} \int_o^{t_e} (\partial C_A/\partial x)_{x=0} dt = 1/\sqrt{D_A}\ \left\{[(C_{A,o}-C_{A,e})/s\sqrt{s + k_1}] - C_{A,e}k_1/s^2\sqrt{s + k_1}\right\} \quad (143)$$

Applying Equations (103) and (104) to Equation (143)

$$\int_o^{t_e} (\partial C_A/\partial x)_{x=0} dt = -1/\sqrt{D_A} \left\{ [(C_{A,o}-C_{A,e})/\sqrt{k_1}] \cdot \right.$$

$$\operatorname{erf}\sqrt{k_1 t_e} - C_{A,e} t_e \sqrt{k_1} \operatorname{erf}\sqrt{k_1 t_e} +$$

$$\left. (C_{A,e}/2\sqrt{k_1} \operatorname{erf}\sqrt{k_1 t_e} - C_{A,e}\sqrt{t_e/\pi} \cdot \exp(-k_1 t_e) \right\} \qquad (144)$$

Substituting Equation (144) into (142) and rearranging

$$\bar{N}_A = C_{A,e}\sqrt{D_A/\pi t_e} \left\{ \sqrt{\pi/k_1 t_e} \quad [1/2-(C_{A,o}/C_{A,e}) + k_1 t_e] \right.$$

$$\left. \operatorname{erf}\sqrt{k_1 t_e} + \exp(-k_1 t_e) \right\} \qquad (145)$$

When $\underline{C_{A,o}} = 0$

$$\Phi = \bar{N}_A/\bar{N}_A{}^* = \bar{N}_A/2C_{A,e}\sqrt{D_A/\pi t_e} =$$

$$1/2[\sqrt{\pi/k_1 t_e} \ (1/2 + k_1 t_e) \operatorname{erf}\sqrt{k_1 t_e} + \exp(-k_1 t_e)] \qquad (146)$$

ABSORPTION WITH SIMULTANEOUS SECOND ORDER, INFINITELY RAPID, IRREVERSIBLE REACTION

The solution to this problem is based on Danckwerts' (61) treatment of the more general problem of diffusion with a moving boundary. If we consider a gas, A, in contact with a liquid containing a reactant, B, such that the reaction between A and B is second order, infinitely rapid and irreversible, there will exist a plane within the liquid where the chemical reaction takes place. At this reaction plane the concentrations of A and B will be zero, because they cannot exist together. The rate of absorption or the rate of diffusion of A from the liquid surface is governed by the rate of diffusion of A to the reaction plane which is in turn controlled by the rate of diffusion of reactant B to the other side of the plane.

Above the reaction plane only the gaseous solute exists; this is designated as medium A. Position in medium A is designated by a co-ordinate in the $\underline{x}_A$ system. Below the reaction plane only solute reactant B exists; this is designated as medium B. Position in medium B is designated by a co-ordinate in the $\underline{x}_B$ system. Figure 20 depicts the two co-ordinate systems.

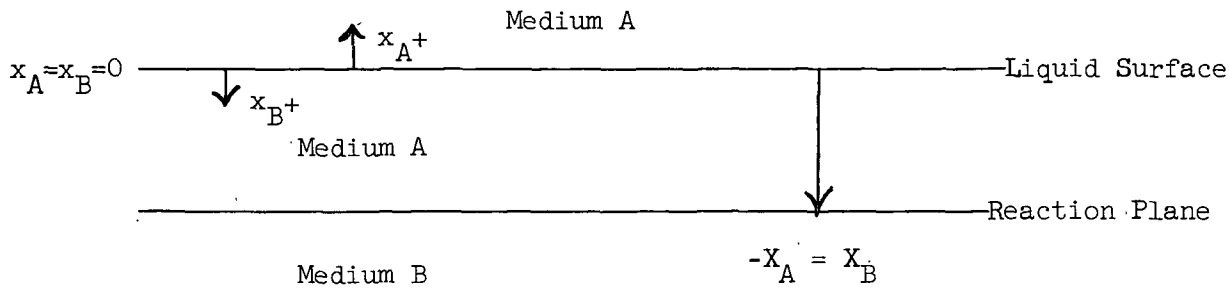

Figure 20. The Co-ordinate Systems

The surface of the liquid remains permanently at $\underline{x}_A = \underline{x}_B = 0$ so that the distance of the reaction plane from the surface is the same in both co-ordinate systems, i.e.,

$$-X_A = X_B$$

The equations governing the diffusion of A and B in their respective media are as follows:

$$\partial C_A/\partial t = D_A \partial^2 C_A/\partial x^2 \qquad (148)$$

$$\partial C_B/\partial t = D_B \partial^2 C_B/\partial x^2 \qquad (149)$$

For the time being each medium will be considered separately and also be considered as infinite. Then, in medium A a solution takes the form

$$(C_{A(-\infty)}-C_A)/(C_{A(-\infty)}-C_{A,e}) = 1 + \text{erf}\ (x_A/2\sqrt{D_A t}) \qquad (150)$$

when the initial boundary conditions are

$$x_A < 0, \qquad t = 0 \qquad C_A = C_{A(-\infty)} \qquad (151)$$

$$x_A = 0, \qquad t > 0 \qquad C_A = C_{A,e} \qquad (152)$$

Likewise in medium B a solution is

$$(C_{B(\infty)}-C_B)/(C_{B(\infty)}-C_{B,o}) = 1 - \text{erf}\ (x_B/2\sqrt{D_B t}) \qquad (153)$$

when the initial conditions are

$$x_B < 0, \qquad t = 0 \qquad C_B = C_{B(\infty)} \qquad (154)$$

$$x_B = 0, \qquad t > 0 \qquad C_B = C_{B,o} \qquad (155)$$

The solutions apply to an infinite media but can be applied to a region bounded by one or two $\underline{x}$-planes either stationary or moving, provided that (a) the initial concentration at every point in the bound region is the same as in the infinite medium at the same value of $\underline{x_A}$ or $\underline{x_B}$; and (b) the concentration at the boundary planes is at all times the same as for the same value of $\underline{x_A}$ or $\underline{x_B}$ in the infinite medium. In other words, the presence of restricting planes does not alter the general shape of the concentration-distance curves; however, the discontinuity at these restriction planes does affect the position of the concentration-distance curves. The position of the curves can be determined by considering an infinite medium with a boundary value such that concentration at the position of the restriction plane is the same as if the plane was actually there. In this case the boundary value concentrations associated with the infinite media lie outside of the actual media and are negative. Thus, they have no physical meaning. Figure 21 shows this situation. $\underline{C_{A(-\infty)}}$ and $\underline{C_{B,o}}$ are the

hypothetical boundary value concentrations associated with their respective infinite media which must be chosen so that A = B = 0 at the reaction plane at all times.

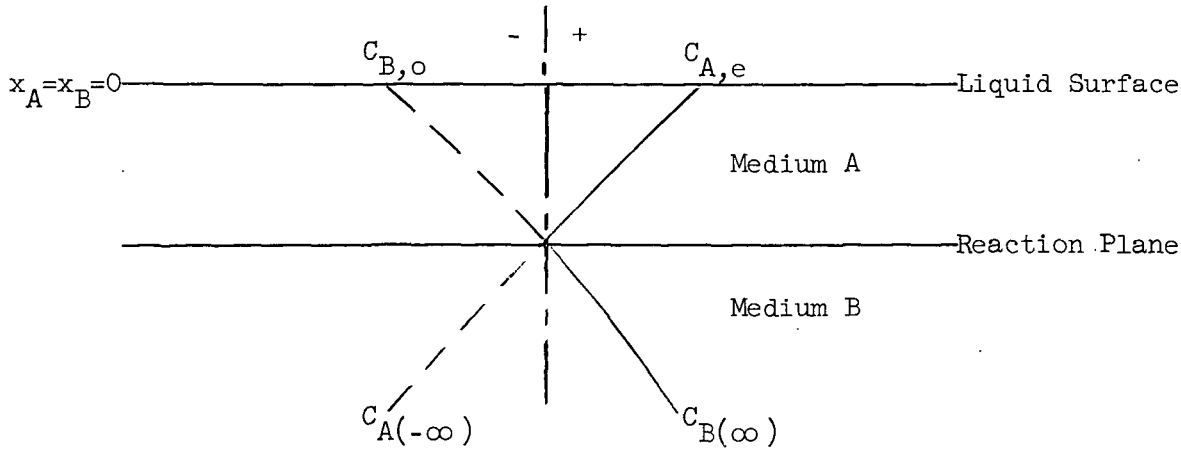

Figure 21. Concentration Gradients of A and B

In this case one mole of A reacts with one mole of B, and there is no accumulation of A or B at the reaction plane. Thus,

$$D_A(\partial C_A/\partial x_A)_{x_A=-X_A} = D_B(\partial C_B/\partial x_B)_{x_B=X_B} \qquad (156)$$

Substituting (150) and (153) into (156) gives

$$\left(C_{A,e}-C_{A(-\infty)}\right)\ (D_A/\pi t)^{1/2}\ \exp\ (-X^2/\ 4\ D_A t)\ -$$

$$\left(C_{B(\infty)}-C_{B,o}\right)\ (D_B/\pi t)^{1/2}\ \exp\ (-X^2/\ 4\ D_B t) = 0 \qquad (157)$$

It is seen that this is true for all values of t only if $X/t^{1/2}$ is a constant. After putting

$$X = 2\ \alpha\ t^{1/2} \qquad (158)$$

Equation (157) becomes

$$\left(C_{A,e}-C_{A(-\infty)}\right) \quad D_A \exp(-\alpha^2/D_A) =$$

$$\left(C_{B(\infty)}-C_{B,o}\right) \quad D_B \exp(-\alpha^2/D_B) \tag{159}$$

From (150) and (153) at the reaction plane

$$C_{A(-\infty)} = -C_{A,e} \text{ erfc } (X/2\sqrt{D_A t})/\text{erf } (X/2\sqrt{D_A t}) \tag{160}$$

and

$$C_{B,o} = -C_{B(\infty)} \text{ erf } (X/2\sqrt{D_B t})/\text{erfc } (X/2\sqrt{D_B t}) \tag{161}$$

Substituting (160) and (161) into (159) gives

$$C_{A,e}\sqrt{D_A} \exp(-\alpha^2/D_A) \text{ erfc } (\alpha/\sqrt{D_B}) =$$

$$C_{B(\infty)}\sqrt{D_B} \exp(-\alpha^2/D_B) \text{ erf}(\alpha/\sqrt{D_A}) \tag{162}$$

The rate of diffusion away from the liquid surface can be found by differentiating Equation (150) just as was done for physical absorption.

$$\bar{N}_A = [C_{A(-\infty)}-C_{A,e}] \, 2\sqrt{D_A/\pi t} \tag{163}$$

Substituting (160) into (163)

$$\bar{N}_A = 2 \, C_{A,e}\sqrt{D_A/\pi t_e}/ \text{ erf } (\alpha/\sqrt{D_A}) \tag{164}$$

Equations (162) and (164) comprise the solution to the problem.

APPENDIX II

DESCRIPTION OF THE ABSORPTION APPARATUS AND AUXILIARY EQUIPMENT

The general design of the absorption apparatus was taken from that employed by Scriven (54). A few modifications were made to allow for the corrosive and toxic nature of chlorine gas. The basic considerations in the design of the apparatus are as follows:

1) To provide a means for suddenly terminating the jet without entraining any gas or losing any absorbent.
2) To provide a nonfluctuating flow to the jet nozzle.
3) To provide a means for obtaining an accurate sample of the liquid after absorption.

THE LIQUID SUPPLY SYSTEM

The liquid supply system comprised: 1) 3 storage tanks, 2) a centrifugal pump, 3) 2 rotameters, 4) teflon needle valves, 5) a cooling coil, 6) a surge tube, and 7) connecting pipe and tubing.

The storage tanks were 16-liter glass bottles which were interconnected with rubber and glass tubing.

The centrifugal pump was an Eastern, Model D-11, Type 100, 316 stainless steel pump operated by an 1/8 h.p. motor at 3450 r.p.m.

The liquid rotameters were purchased from the Scientific Glass App. Co. (tube No. 0532-150). Their floats were 5/32-inch diameter stainless steel balls which gave a flow range of 10 to 450 cc. of water per minute.

Rotameters were placed before and after the surge tube so that the flow rate to the nozzle could be adjusted quickly and easily. The rotameters were used for adjustment purposes only.

The surge tube was a length of 80-mm. tubing with a rubber stopper at one end. It was placed in the flow line by means of a glass tee. This surge tube did an excellent job of dampening any variations in the liquid flow.

The cooling coil was made of a 10-ft. length of 1/4-inch stainless steel tubing which was coiled into an eight-inch diameter.

Most of the connecting pipe was 1/4-inch schedule 40 polyvinyl chloride plastic pipe. The remainder was rubber and glass tubing.

THE LIQUID TAKE-OFF SYSTEM

The leveling device, a sampling pipet, and a stay tube made up the liquid take-off system. The leveling device is shown in Fig. 22.

The sampling pipet, shown in Fig. 23, was constructed from Pyrex glass by the Scientific Apparatus Corporation of Chicago. The curved tube in the lower bulb was to prevent channeling and insure complete mixing in the delivered sample. It delivered 111.3 ml. of sample.

A stay tube was placed immediately after the absorption chamber. Its function was to provide an escape for any bubbles of chlorine that were entrained in the liquid stream during adjustment. A few bubbles of gas were found to cling to the sides of the take-off tube. These were knocked off

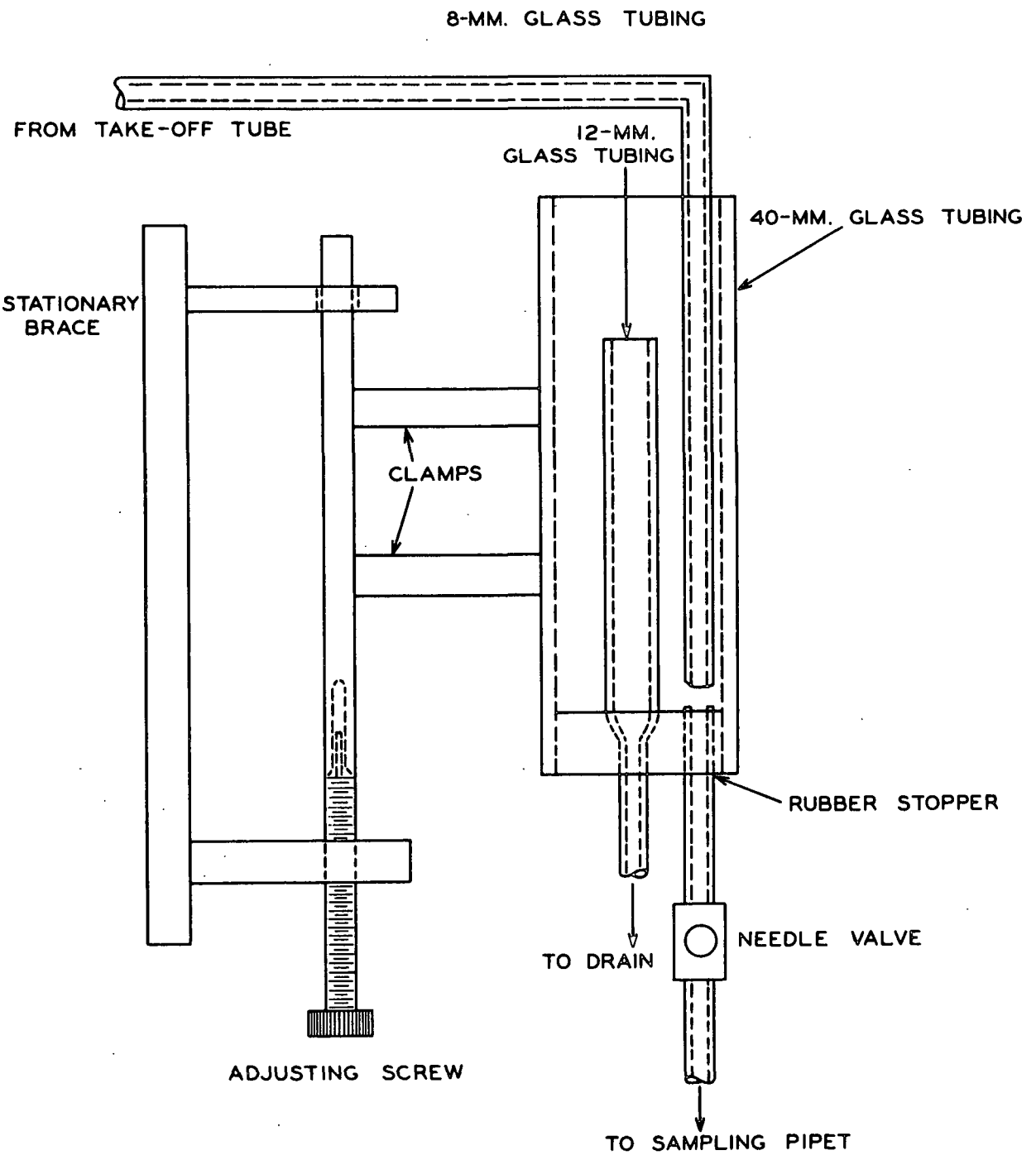

Figure 22. Leveling Device

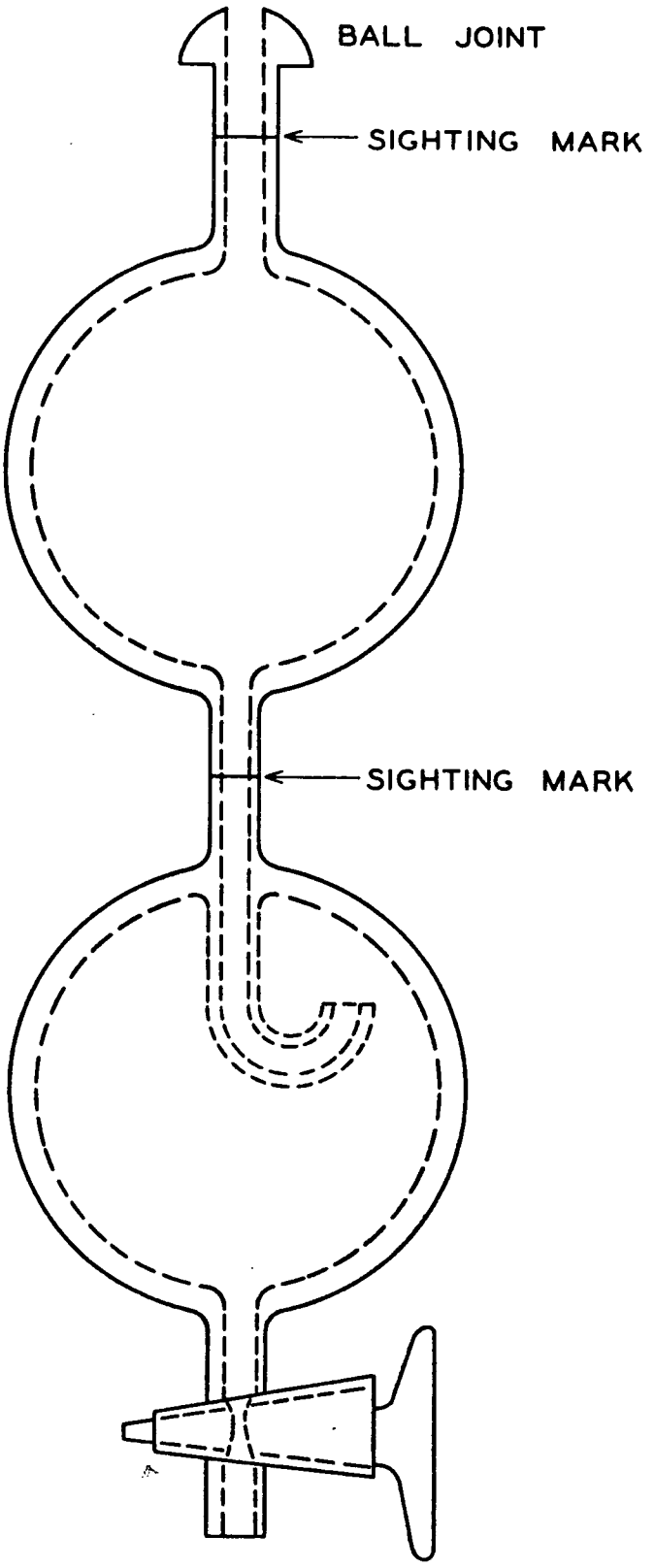

Figure 23. Sampling Pipet

during the adjustment period by a plastic-coated wire that ran down the stay tube and then up into the take-off tube.

THE GAS SUPPLY AND EXHAUST SYSTEM

The gas supply system consisted of a gas cylinder, a rotameter, a cooling coil, a saturater, and a filter. The gas cylinders were five-pound chlorine cylinders purchased from The Matheson Company, Inc., of Joliet, Illinois. The flow of chlorine from these cylinders was controlled by a Matheson chlorine control valve attached to the cylinder.

The chlorine gas was metered through a Fischer and Porter Co. rotameter (tube No. 08F-1/16-16-4/38) with a glass float. This combination gave a flow range from 1000 to 8000 std. cc./min. of air metered at 14.7 p.s.i. abs. pressure and 70°F.

The cooling coil was constructed from twenty 2-ft. lengths of 8-mm. glass tubing joined end to end by rubber tubing.

The gas was saturated with water vapor by bubbling it through a test tube full of water with a very fine nozzle to create small bubbles.

The chlorine gas was passed through a long glass tube filled with fiberglass. The purpose of this filter was to remove any entrained grease or oil that might be in the gas stream.

The connecting piping was made from tygon and rubber tubing. The chlorine attacked these materials initially and formed a protective coating on the walls which then minimized further attack.

When the chlorine gas left the absorption chamber, it was exhausted by bubbling it through five successive 2-liter bottles filled with 25% sodium hydroxide solution. Potassium iodide solution in a small Erlenmeyer flask was placed at the end of the line to act as an indicator.

THE ABSORPTION CHAMBER, JET NOZZLE, TAKE-OFF TUBE, AND ALIGNING MECHANISM

The absorption chamber is shown in Fig. 24. It was constructed from Pyrex glass by the Scientific Apparatus Corporation and is 11-inches long and 2-inches in diameter. The chamber was suspended into the constant temperature bath by means of a clamp which was made from 1/2-inch brass plate. The chamber and clamp were isolated from the bath to prevent vibrational interference with the jet operation.

The jet nozzle, shown in Fig. 25, was fabricated by the Fox River Tool Company of Menasha, Wisconsin. The nozzle itself was made of Lucite methyl methacrylate polymer which is adequately resistant to the chemicals used at the temperature encountered. The approach tube was constructed from a piece of 1/4-inch polyvinyl chloride schedule 40 pipe which also resists attack by the chemicals encountered.

The take-off tube (Fig. 26) was constructed by joining a piece of 2-mm. capillary glass tubing to a piece of 4-mm. regular glass tubing and then grinding the capillary tubing down to a very thin disk. This assemblage was then joined to the end of a 10/30 ground-glass male joint. The top and inner surfaces of the disk were made nonwetting by coating them with paraffin. This aided the stability of the jet at the termination point a great deal.

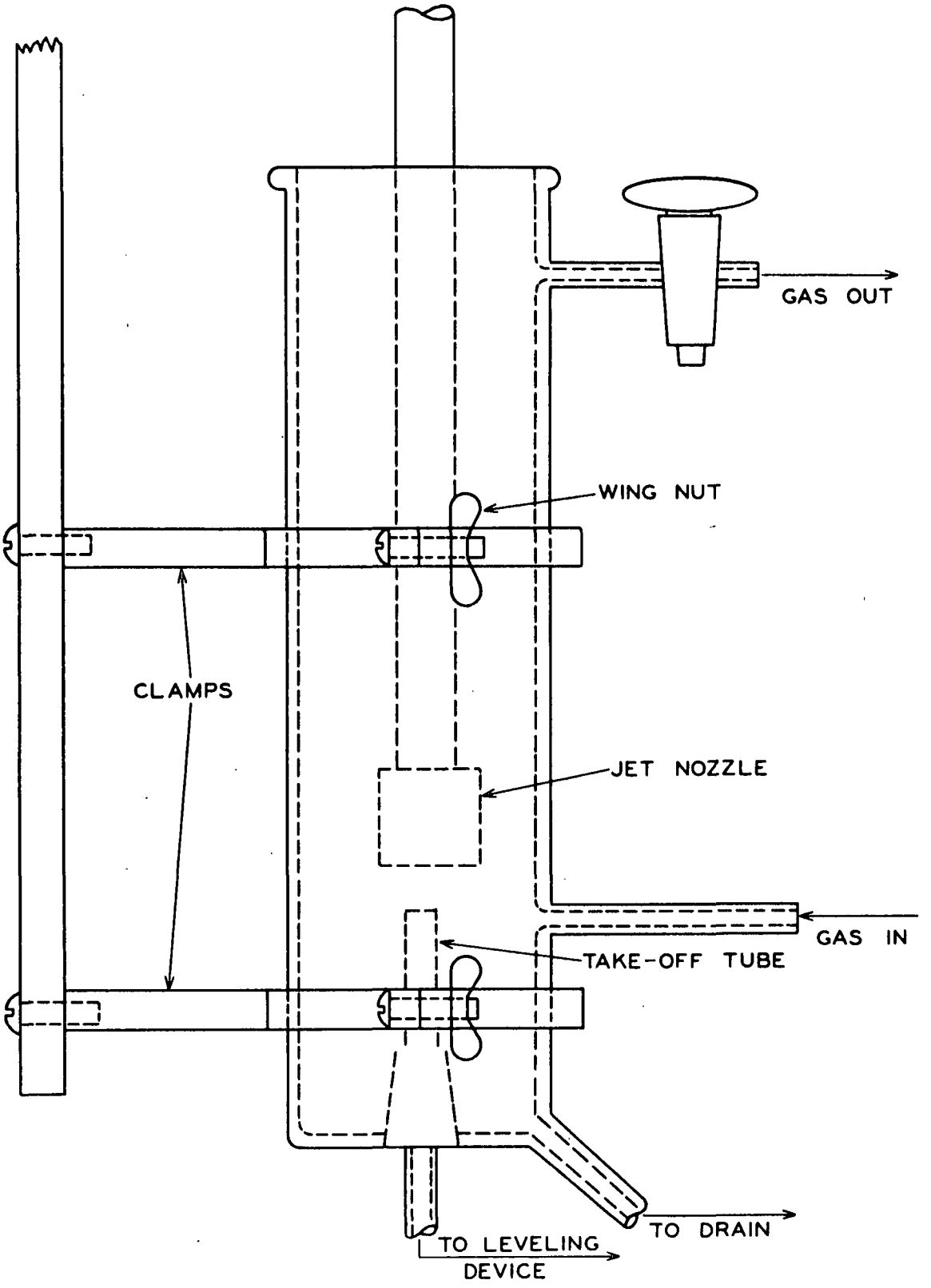

Figure 24. Absorption Chamber

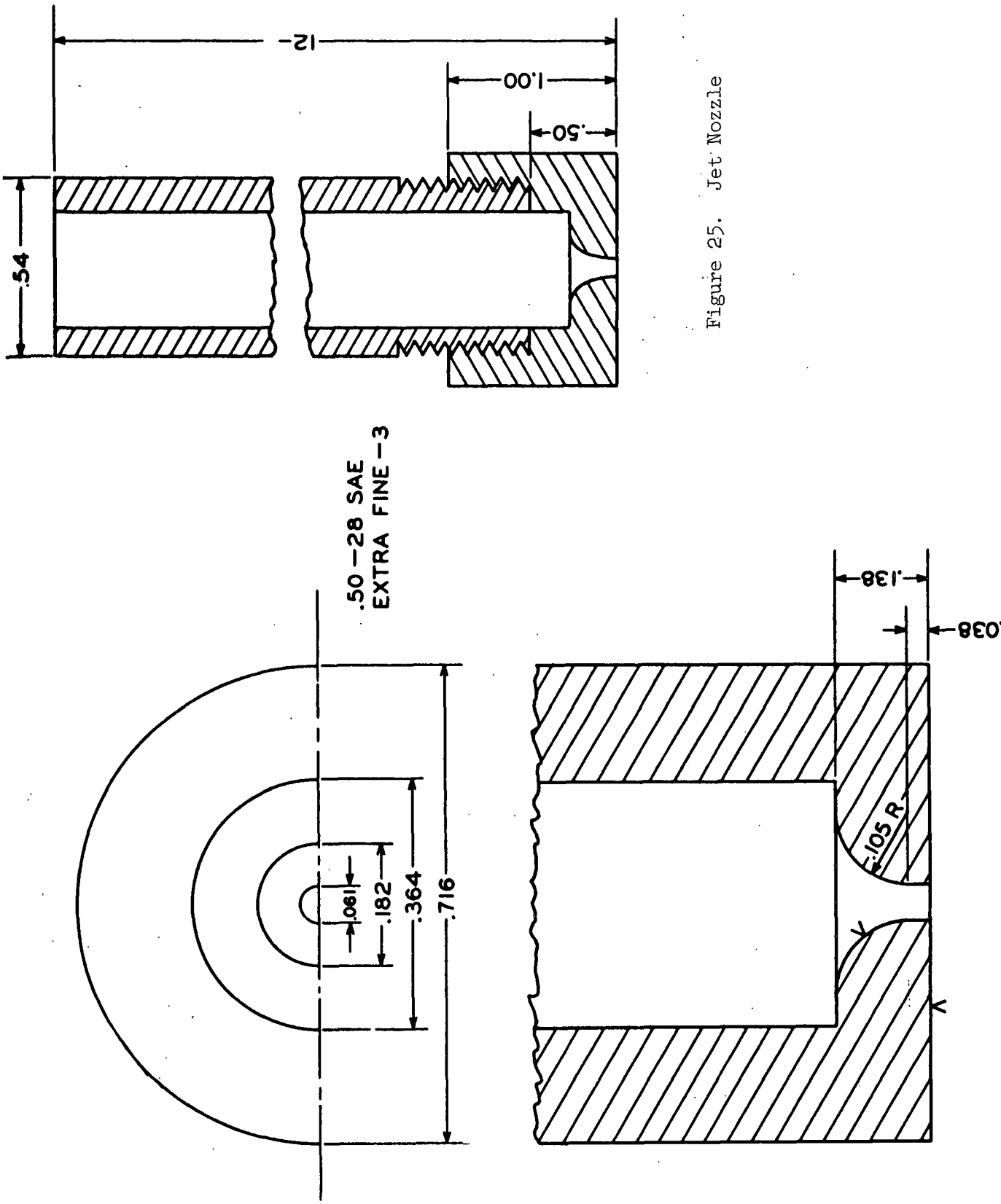

Figure 25. Jet Nozzle

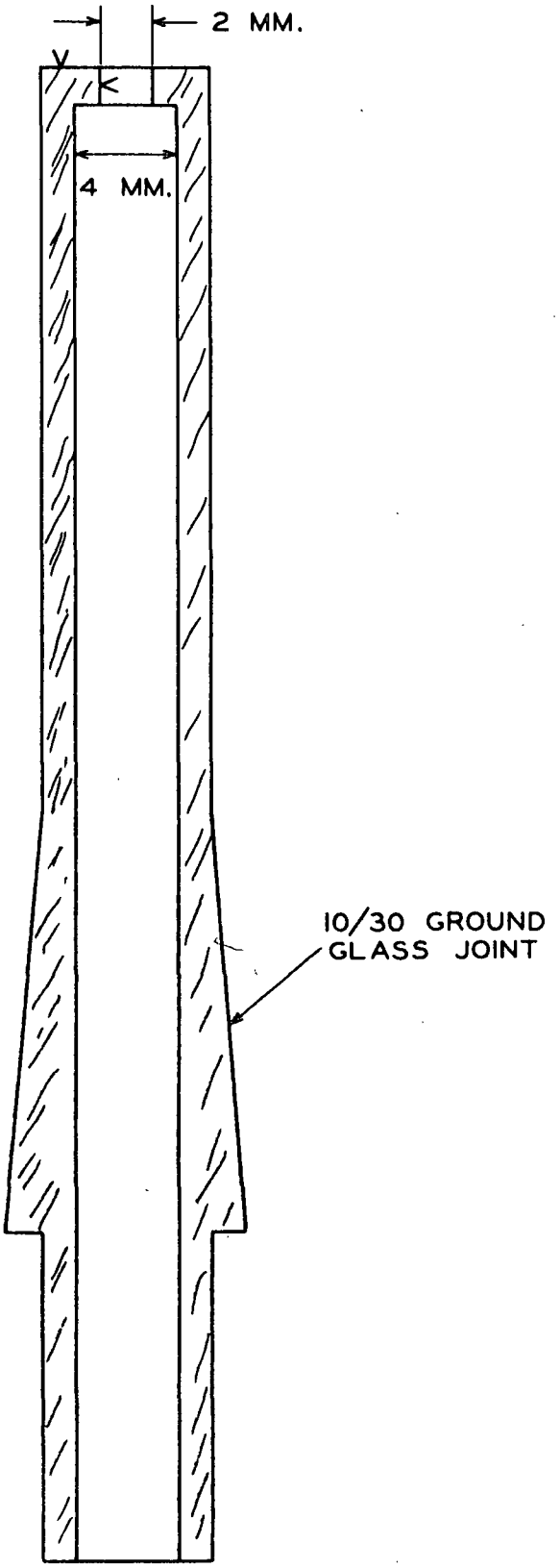

Figure 26. Take-off Tube

The aligning mechanism and nozzle holder are depicted in Fig. 27. The aligning mechanism was made by adapting a Bauch and Lomb microscope slide aligner to the nozzle tube holder. The nozzle holder was constructed of Lucite, the pieces being joined together by using a 1,2 dichloroethane solution of the methyl methacrylate monomer as the bonding agent.

The length of the jet was adjusted by sliding the nozzle tube up and down through its holder. During a run the three brass screws on top of the tube holder were tightened down, expanding the rubber O-ring within the holder and forming a good seal between the slide tube and its holder.

The tube holder was joined to the absorption chamber by means of a flexible rubber connector. This arrangement prevented leakage of the chlorine while still allowing alignment of the jet nozzle. The tube holder was bolted to the aligning mechanism, which in turn was bolted to the chamber brace as shown in Fig. 27. When the aligning knobs were turned, the tube holder and tube moved about within a 3-inch hole in the brace.

THE CONSTANT TEMPERATURE BATH

The inner dimensions of the constant temperature bath were 30 inches by 20 inches by 20 inches. The walls were made of two layers of type 304 stainless steel sheeting between which was a layer of fiberglass insulation one inch thick. There was a Lucite window on each side of the bath for viewing. The bath held 52 gallons of water which was externally circulated by a Goulds type 316 s.s. centrifugal pump (20 g.p.m. capacity at 20 ft. head, 1150 r.p.m.). There were four 200-watt heaters in the bottom of the bath which were operated by relays connected to a bimetallic temperature

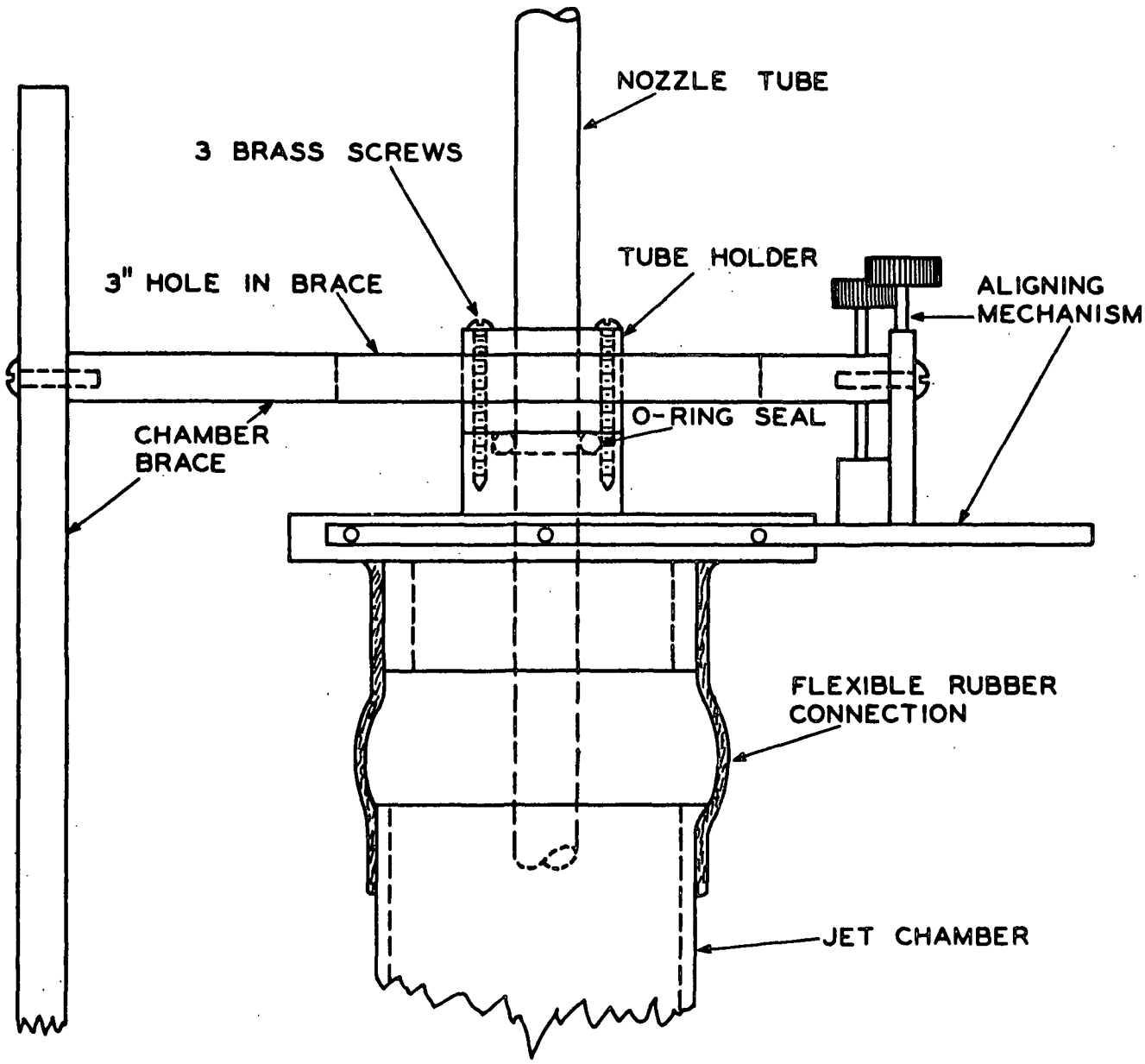

Figure 27. Tube Holder and Aligning Mechanism

regulator. The output of two of the heaters could be varied by a Variac. Cooling water was run through copper coils also located in the bottom of the bath. Five thousand parts per million of sodium dichromate were used in the bath water to prevent corrosion and slime growth. The temperature of the bath water was held at 25°C. $\pm$ 0.1°, and there existed no detectable temperature gradients within the bath due to its excellent circulation and insulation.

THE DEGASSING UNIT

The absorbent water was degassed in the unit shown in Fig. 28. The water was stored in a 16-liter glass bottle. The water ran from this bottle to the top of a Graham condenser, the outside chamber of which was connected to a steam line. At the bottom of the condenser a nozzle issued into a 10-liter spherical glass flask. A vacuum was applied to the receiving flask with an aspirator. This caused water to come from the storage bottle through the steam condenser and to spray fine drops into the receiving flask where it continued to boil. When the receiving flask was full, the water was boiled for a few minutes and then siphoned into another storage bottle. The degassed water entered the storage bottle under a layer of n-heptane to prevent absorption of air.

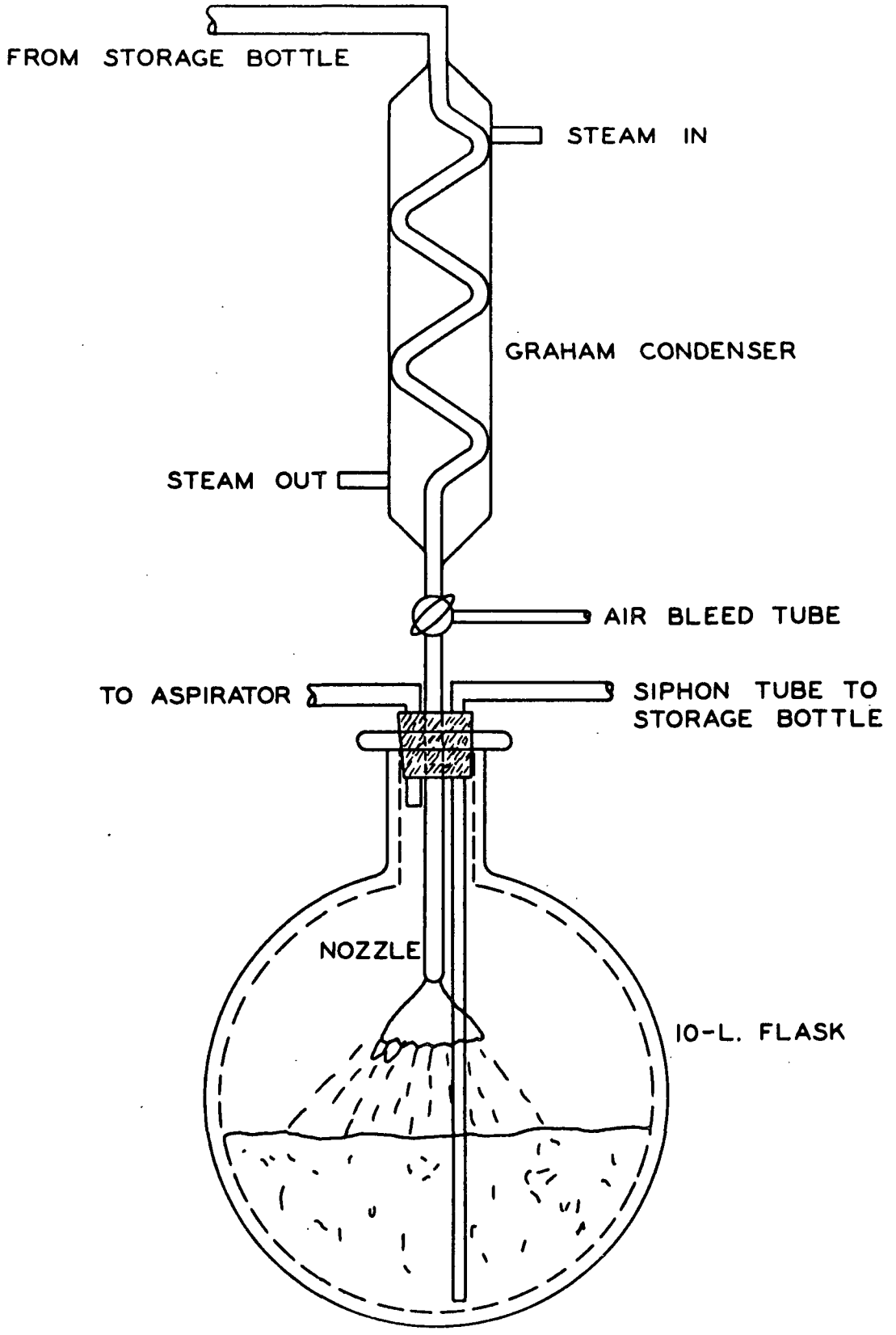

Figure 28. Degassing Unit

APPENDIX III

DETAILS OF THE LAMINAR LIQUID JET

LAMINAR FLOW

In the development of the absorption equations it is assumed that the absorbent flow is laminar in character; therefore laminar flow in the jet boundary layer must be confirmed. The measurements of B. G. van der Hegge Zijnen and M. Hansen (64) indicate that transition from laminar to turbulent flow in the boundary layer of a fluid flowing past a flat plate occurs at a Reynolds number of 300,000 based on the flat plate length. The Reynolds number for the jets employed in this work range from 1800 to 4000 based on the total nozzle exit length. Even though the flow characteristics over a flat plate and in a pipe are not the same, this is a good indication of the existence of a laminar boundary layer in the jets. Also the bell-shaped nozzle design employed in this work increases the stability of laminar flow because of the favorable pressure gradients present.

GRAVITATIONAL ACCELERATION OF JET

When the jet emerges from the nozzle the fluid velocity increases because of gravitational acceleration and, as a result, the jet diameter decreases. This effect must be taken into account when calculating the interfacial areas and the exposure times.

If it is assumed that energy is conserved within the jet and that the kinetic energy flowing past any cross section of the jet can be calculated

from the mean velocity at that cross section, a mechanical energy balance (neglecting surface forces) can be written as follows:

$$\bar{U}_o^2/2 + gh = \bar{U}_1^2/2 \qquad (165)$$

where $\bar{U}_o$ is the mean velocity at the nozzle exit and $\bar{U}_1$ is the mean velocity in a plane downstream from the nozzle exit.

The equation of continuity gives

$$D_o^2\bar{U}_o = D_1^2\bar{U}_1 \qquad (166)$$

where D is the diameter of the jet.

Combining Equations (165) and (166) gives

$$D_1/D_o = \left(1 + \frac{\pi^2 g D_o^4 h}{8q^2}\right)^{-1/4} \qquad (167)$$

where

$q = \bar{U}_o \pi D_o^2/4$ = absorbent flow rate, cc./sec.

The measurement of the jet diameters at various jet lengths and flow rates is described in Appendix VII. The measured diameters are in accordance with Equation (167), thereby validating the assumptions made.

When calculating the interfacial areas and fluid velocities the effect of gravitational acceleration was accounted for by assuming that the effect could be superimposed on the other effects. In calculating the interfacial area the mean diameter of the jet was used, $\bar{D}$.

$$\bar{D} = 1/H \int_o^H D \, dh \qquad (168)$$

In calculating the mean jet velocity the mean diameter squared was used, $\overline{D}^2$.

$$\overline{D}^2 = 1/H \int_0^H D^2 \, dh \qquad (169)$$

BOUNDARY LAYER CONSIDERATIONS

The velocity at the surface of the jet at the nozzle exit is zero because of the development of a boundary layer by the viscous drag forces within the nozzle. As the fluid proceeds from the nozzle exit, the viscous shear forces within the boundary layer cause the surface velocity to increase and finally approach the velocity at the jet core at a point downstream from the nozzle exit. Figure 29 depicts this situation.

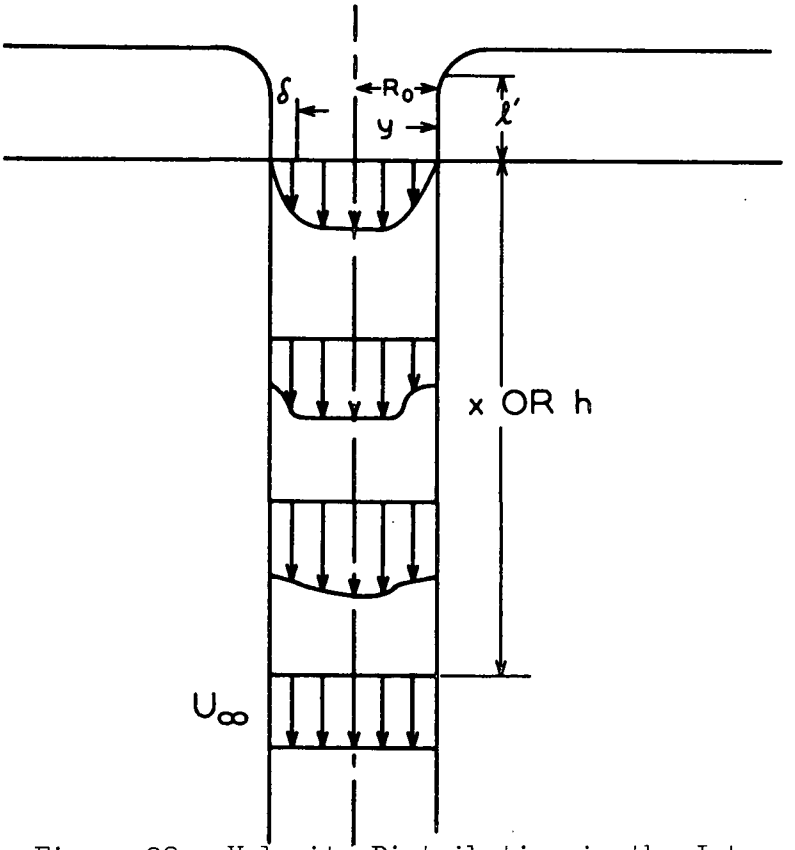

Figure 29. Velocity Distribution in the Jet

The time that the jet surface is exposed to the absorbing gas is clearly given by

$$t_e = \int_o^H dh/U_s \qquad (170)$$

where U_s is the velocity at the jet surface. It is necessary, therefore, to obtain an estimate of the surface velocity as a function of jet length.

FLOW WITHIN THE NOZZLE

The first step in obtaining this function is to examine the development of the boundary layer within the nozzle itself. The measurements of Nikuradse (65) on the velocity distribution in the inlet portion of a pipe for laminar flow were analyzed, and the following empirical equation for the relative boundary layer thickness, b, was determined:

$$b = \delta/R_o = 2.42\ (\nu \ell'/R_o^2 \bar{U})^{0.391} \qquad (171)$$

where δ is the boundary layer thickness, ℓ' is the length of pipe over which the boundary layer developed, and ν is the kinematic viscosity.

The Reynolds numbers encountered in the work here range from 1600 to 3600 based on the nozzle diameter. Even though some of these numbers are above the so-called "critical" Reynolds number of 2000 it is felt that the flow within the whole nozzle remains laminar because of the absence of initial disturbances and because of the extremely short nozzle exit length. With this assumption the boundary layer thickness at the nozzle exit can be calculated from Equation (171).

FLOW WITHIN THE JET

Although the jet is cylindrical the boundary layer problem is treated as a two-dimensional problem because the distances from the surface of the jet which are involved are small when compared with the jet radius.

The boundary layer equation for two-dimensional motion without the pressure term is:

$$U(\partial U/\partial x) + V(\partial U/\partial y) = (\partial^2 U/\partial y^2) \qquad (172)$$

where U is the x component of the velocity vector and V is the y component.

Boundary conditions for the problem can be found by assuming that at the jet surface the surrounding gas exerts no drag force on the jet. Therefore,

$$\text{at } y = 0 \qquad \partial U/\partial y = 0 \qquad (173)$$

Other boundary conditions can be obtained by considering the equation of continuity.

$$(\partial U/\partial x) + (\partial V/\partial y) = 0 \qquad (174)$$

From the calculus for a differential function

$$dV = (\partial V/\partial x)dx + (\partial V/\partial y)dy \qquad (175)$$

Substituting Equation (174)

$$dV = (\partial V/\partial x)dx - (\partial U/\partial x)dy \qquad (176)$$

Integrating,

$$\int_{x,0}^{x,y} dV = -\int_{0}^{y} (\partial U/\partial x)dy \tag{177}$$

or

$$V = -d\left[\int_{0}^{y} U\, dy\right]/dx \tag{178}$$

But,

$$\partial U/\partial y \cong 0 \qquad \text{at } y = 0 \tag{173}$$

Therefore,

$$V \cong -(dU/dx) \int_{0}^{y} dy \tag{179}$$

$$V \cong -y(dU/dx) \tag{180}$$

Thus, the boundary conditions for Equation (172) become:

$$y = 0; \quad \partial U/\partial y = 0, \quad V = 0 \tag{181}$$

$$Y = \infty; \quad U = U_{\infty}, \quad V = 0 \tag{182}$$

where U_{∞} is the velocity of the jet core.

The same equation and boundary conditions apply to the flow in the wake of a flat plate; the only difference between that case and this one being the nature of the boundary layer developed at the solid surface. Goldstein (66) presents a solution to this situation which is based upon the fact that the initial boundary layer was developed on a flat plate. He uses Blasius' solution for flow past a flat plate to describe the initial boundary layer.

Schiller (67) has shown that Nikuradse's measurements for the velocity distribution at the entrance of a pipe for laminar flow can be predicted by assuming a parabolic velocity distribution in the boundary layer. It is well known that Blasius' solution for the velocity distribution over a flat plate can be approximated to a good degree by a variety of functions. A parabolic function can be fitted to Blasius' solution very well. Therefore, it is concluded that the initial boundary layers in the two cases are enough alike to permit the use of Goldstein's solution as an approximation to the flow in a jet. This analogy was pointed out by Rideal and Sutherland (68) and was used by Scriven and Pigford (69) in the same manner used here.

Figure 30 shows Goldstein's solution to this problem. The parameter x/ℓ is the distance from the edge of the flat plate divided by the length of flat plate which developed the initial boundary layer. In this work an equivalent flat plate length was used. It was defined as that length of flat plate which would develop a boundary layer of the same thickness as developed in the nozzle.

Blasius' solution relates boundary layer thickness and flat plate length by

$$\ell = (1/25)(U_\infty/\nu)\delta^2 \qquad (183)$$

Thus, the equivalent flat plate length can be calculated by finding the boundary layer thickness from Equation (171) and substituting this into Equation (183). The equivalent flat plate lengths turn out to be slightly higher than the characteristic nozzle length used in Equation (171) and are

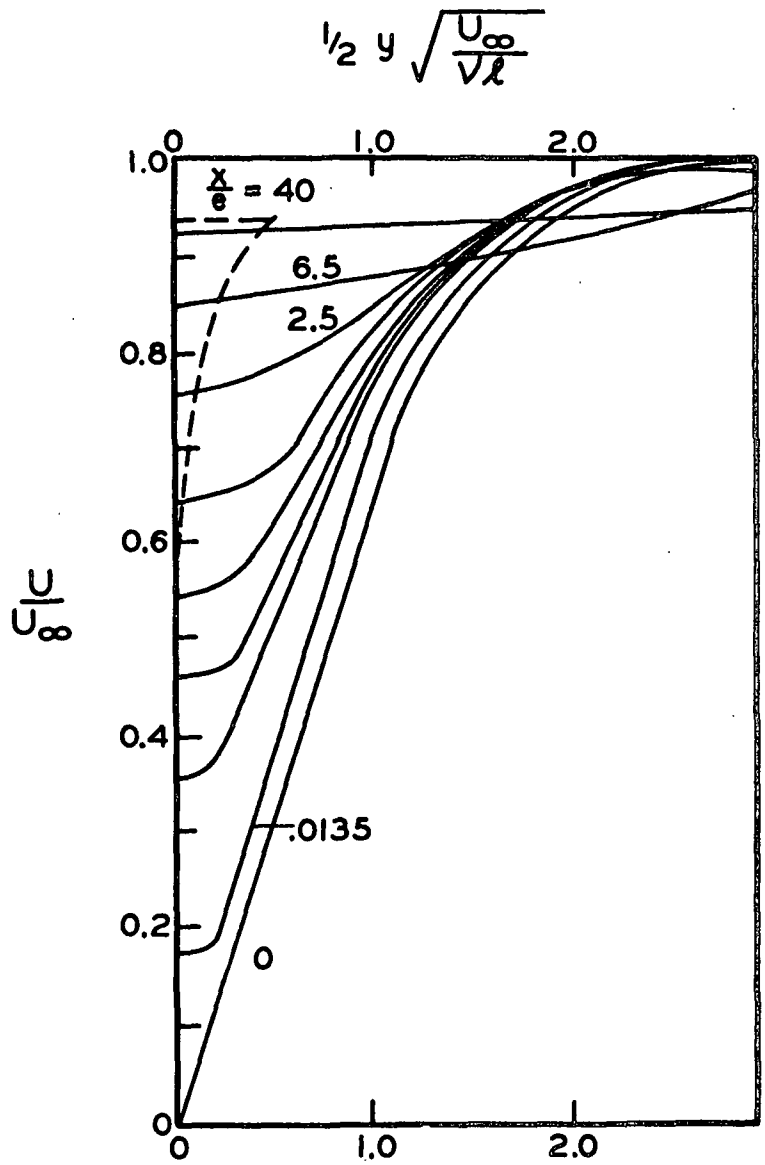

Figure 30. Velocity Distribution in the Laminar Wake Behind a Flat Plate at Zero Incidence. Goldstein's Solution

very slight functions of the flow rate and kinematic viscosity of the absorbent. This is to be expected because of the differences in flow patterns between flow over a flat plate and in a pipe.

The core velocity, $\underline{U}_{\infty}$, is obtained from the mean velocity, $\underline{\bar{U}}$, by a material balance across the jet.

$$U_{\infty} = \bar{U}/(1-3b/4-b^2/5) \qquad (184)$$

Equation (184) is based upon Blasius' flat plate velocity distribution. The effect of gravity is superimposed over all this by using mean diameters to calculate $\underline{\bar{U}}$. Actually, the calculation of the core velocity is immaterial because the ratio $\underline{\ell}/\underline{U}_{\infty}$ is used in calculating the exposure time as will be seen. Equation (184) is presented, however, because it represents an approximation to the velocity the jet attains when the velocity profile is flat.

Figure 31 is a plot of the velocity at the jet surface relative to the core velocity, $\underline{U}_s/\underline{U}_{\infty}$, as a function of $\underline{h}/\underline{\ell}$. This plot was obtained from Fig. 30 at $\underline{y} = 0$.

Thus, the exposure time can be calculated by obtaining the boundary layer thickness at the nozzle exit from Equation (171). From this an equivalent flat plate length is calculated from Equation (183). The surface velocity is then obtained as a function of jet length from Goldstein's solution (Fig. 31). This function is placed in Equation (170) and the exposure time results.

$$t_e = \int_0^H dh/U_s = \ell/U_{\infty} \int_0^{H/\ell} (U_{\infty}/U_s)\,d(h/\ell) \qquad (185)$$

A sample calculation appears in Appendix VIII.

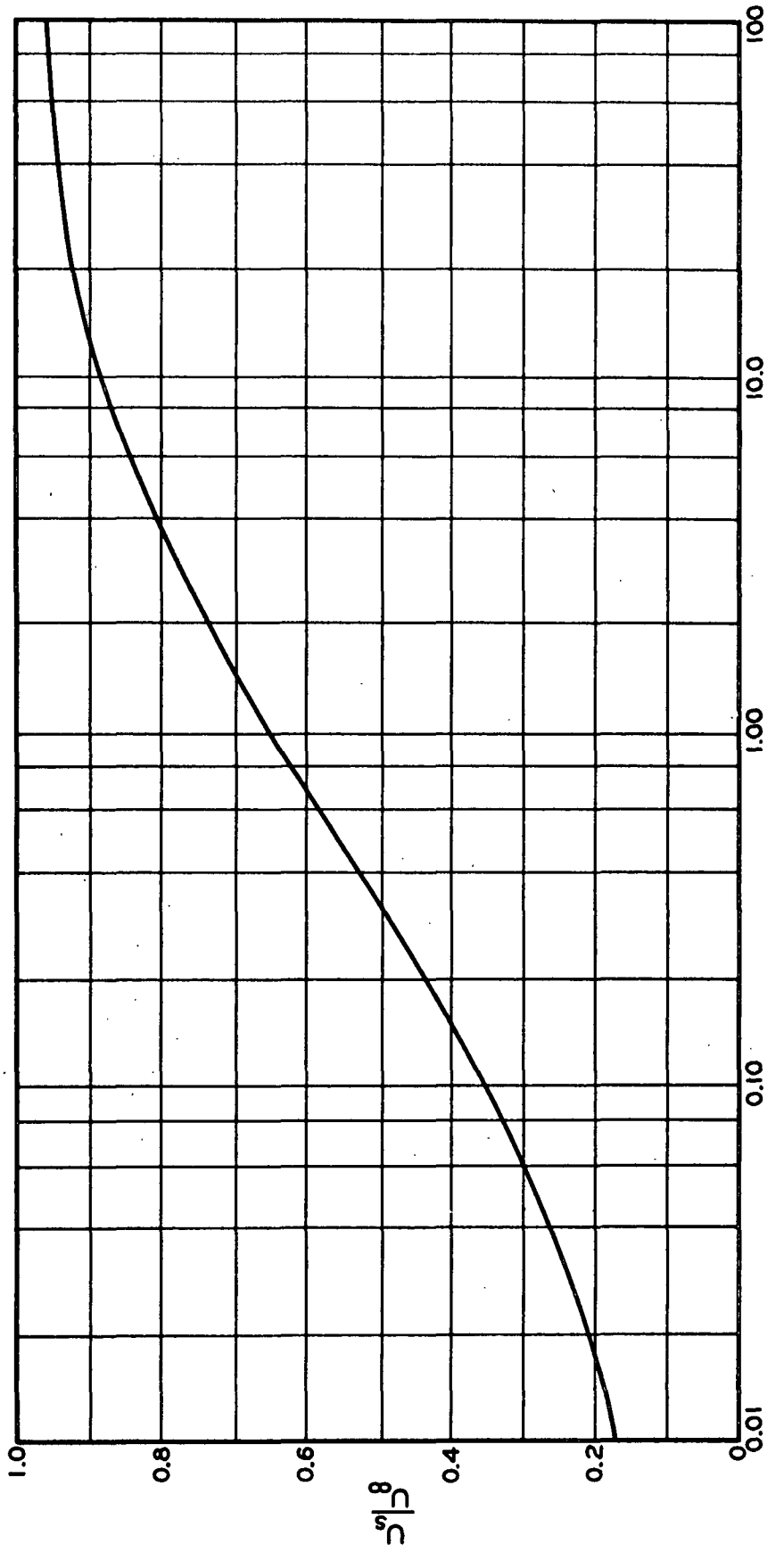

Figure 31. Surface Velocity of Jet as a Function of Jet Length--
Goldstein's Solution

For an ideal jet, i.e., no boundary layer, the exposure time would be given by

$$t_e = H/U \qquad (186)$$

At the longer jet lengths the exposure times calculated from Goldstein's solution differ from Equation (186) by only a few per cent. The difference is quite appreciable for jet lengths of less than 3 cm. as would be expected.

When the boundary layer thickness as calculated by Equation (171) is arbitrarily halved, the resulting calculated exposure times change by about 3% at the shorter jet lengths and do not change at longer jet lengths. This indicates that the final results are quite insensitive to some of the assumptions made during their calculation.

OTHER CONSIDERATIONS

SURFACE DRAG

Scriven (54) attempts to estimate the effect of drag at the jet surface caused by the surrounding gas, by analyzing the shear forces within an assumed gas boundary layer. He estimates that the drop in surface velocity caused by surface drag can be no more than 0.6%.

EFFECT OF FINITE MEDIA AND CURVED SURFACES

The absorption and fluid flow equations are derived for plane surfaces and for a semi-infinite media. These equations would not be expected to apply to a cylindrical jet unless the maximum depth of penetration of the solute molecules is small when compared to the jet radius. The maximum penetration depth occurs during physical absorption as shown in Fig. 2.

If the penetration depth is arbitrarily defined as that point where $\underline{C}_{\underline{A}}/\underline{C}_{\underline{A},\underline{e}} = 0.01$, the greatest depth encountered in this work is calculated by Equation (115) as being 0.0028 cm. This is about 1/30 of the jet radius. For the great majority of runs this ratio is several times as much.

It should be realized that this calculated penetration depth is an instantaneous value at the very bottom of the longest jet, i.e., it is the greatest penetration depth obtained during this work. Although the penetration depth at this extreme is as much as 3.5% of the jet radius, it is felt that this will not affect the rate of absorption appreciably because the solute molecules are at a negligible depth for almost the whole exposure period. Thus, it may be concluded that the depth of penetration is shallow enough to allow the use of the equations presented.

OTHER MEANS OF SOLUTE TRANSPORT

It is assumed in the penetration theory that the only means of solute transport is by molecular diffusion. For this to be the case there should be no relative motion within the jet. There are four means by which relative motion can occur: 1) the velocity gradient within the boundary layer, $\partial\underline{U}/\partial\underline{y}$; 2) the velocity gradient along the jet, $\partial\underline{U}/\partial\underline{x}$; 3) the radial velocity component, $\underline{V}$; and 4) bulk motion caused by density differences.

The dotted line in Fig. 30 represents the maximum depth to which penetration occurs as one proceeds down the jet. It is readily seen that the velocity gradient, $\partial\underline{U}/\partial\underline{y}$, is extremely small in the penetration region especially during the greatest part of the jet length. From this it is assumed that the velocity gradient, $\partial\underline{U}/\partial\underline{y}$, is never large enough in the regions of penetration to affect the rates of absorption.

The velocity gradient, $\partial \underline{U}/\partial \underline{x}$, does not affect the absorption rates because it has no effect on the original differential equations employed in the derivation of the penetration theory. This arises because the relative motion described by $\partial \underline{U}/\partial \underline{x}$ is not in the same direction as the diffusion process and because the concentrations are unaffected. The effect on concentration can be pictured by considering a differential parallelepiped of the jet with a volume of $1 \times d\underline{x}_o \times d\underline{y}_o$. Because of the gradient, $\partial \underline{U}/\partial \underline{x}$, the differential volume is stretched out in the $\underline{x}$-direction; however, the equation of continuity states that $\partial \underline{U}/\partial \underline{x} = -(\partial \underline{V}/\partial \underline{y})$. Therefore, the volume at the same time is thinned in the $\underline{y}$-direction in an amount which makes the volume remain constant. The volume will remain a parallelepiped because $\partial \underline{U}/\partial \underline{y} = 0$. Therefore, the concentration in that volume is unaffected by $\partial \underline{U}/\partial \underline{x}$ even though it has changed dimensions.

The gradient, $\partial \underline{U}/\partial \underline{x}$, does give rise to a radial velocity component, $\underline{V}$, however, which could affect the absorption rates if its magnitude is appreciable compared with the rate of advancement of absorbing molecules. It is seen from Equation (180) that at distances very close to the jet surface $\underline{V}$ is very small, while the rate of advancement of solute is quite large. At the maximum penetration depths, $\underline{V}$ may be appreciable, but the concentration of solute is so small that the effect is negligible.

The concentrations of Cl_2 encountered in this work are so small that one would not expect appreciable density gradients within the jet, and for this reason no bulk motion should result.

LONGITUDINAL DIFFUSION

The effect of diffusion in the direction of flow has been analyzed by Peaceman (31). He estimates that at a flow rate of 0.9 cm./sec. the rate of diffusion in the longitudinal direction is about 10^{-2} times the rate in the radial direction. The effect becomes smaller as the flow rate increases. The minimum flow rates used in this work are around 150 cm./sec. so that the effect of longitudinal diffusion is considered to be negligible.

SURFACE TEMPERATURE

The temperature of the surface of the system is raised during the absorption process because of the heat of solution and the heat of reaction evolved when the solute gas comes in contact with the solution. Danckwerts (70) derived an expression which related the surface temperature for physical absorption to the heat of solution of the solute. This expression is given below:

$$(T_s - T_o) = \beta' \, (C^*_{A,e} - C_{A,o}) \sqrt{D/K_T C_p \rho} \qquad (187)$$

where

T_s = surface temperature

T_o = bulk temperature

β' = heat of solution

K_T = thermal conductivity of solution

C_p = heat capacity of solution

ρ = density of solution

Similar expressions involving the heat of reaction can be derived for the case of absorption with chemical reaction. The most striking aspect of Equation (187) is that it is independent of the exposure time. This indicates that like the surface concentration, the surface temperature reaches an equilibrium value after short times.

The rise in temperature occurring at the surface for the physical absorption of chlorine is estimated to be 0.013°C. by Equation (187). The presence of a chemical reaction should not change the order of magnitude of this temperature rise because the heat of the reaction is slight and the heat of solution of the products is only a few times greater than that of molecular chlorine.

Because of the opposite effects temperature has on the solubility and diffusivity of gases in water a large temperature change is needed in the system before the absorption rate is affected appreciably. It is estimated that a one degree Centigrade temperature rise is needed to raise the absorption rate 1%. Thus, it is felt that the temperature changes resulting from heats of solution and reaction do not affect the absorption rates appreciably.

The countercurrent thermal diffusion of the gaseous solute resulting from the slight rise in surface temperature is estimated to be 10^{-4} as much as the molecular diffusion (assuming a Soret coefficient of 1.0).

The very good agreement between the experimental and theoretical physical absorption rates indicates that the above assumptions and conclusions concerning the hydrodynamic and thermal behavior of the jet are valid.

APPENDIX IV

THE DETERMINATION OF THE EQUILIBRIUM SOLUBILITY OF CHLORINE INTO THE ABSORBENTS

The first attempts to measure the equilibrium solubility of chlorine in the aqueous absorbents were made by the dynamic method. In this method a mixture of chlorine and nitrogen was continually bubbled through the appropriate solution until it was felt that equilibrium had been reached. At this time both the solution and gas stream were sampled and analyzed. At low partial pressures of chlorine this method gave results that were reproducible. At higher partial pressures of chlorine (around 1 atm.) reproducibility could not be obtained, and the results gave solubilities that were too high. This behavior was attributed to the development of a supersaturated state which periodically broke down and reappeared in a cyclic process. The existence of supersaturation was demonstrated by shaking the solutions in a closed vessel and observing the evolution of chlorine gas until equilibrium was reached. As a result of this behavior a static method of attaining equilibrium was used.

APPARATUS AND PROCEDURES

Most of the determinations were made with the total pressure of the system being atmospheric. This was done by placing 25 ml. of the absorbent into a 250-ml. two-necked spherical bulb and introducing saturated chlorine gas under a slight pressure over the solution. The bulb was then sealed off and placed in the constant temperature bath. Equilibrium was attained with intermittent shaking. The pressure in the bulb was then relieved by quickly opening and closing the bulb valve to the atmosphere. Equilibrium was again

obtained, building up the pressure within the bulb. The relieving and equilibrium processes were repeated until finally no pressure build up occurred in the bulb. Then the solution was in equilibrium with saturated chlorine gas at a total pressure equal to that of the atmosphere. The existence of a positive pressure within the bulb was tested with a soap film. When the soap film failed to move with the opening and closing of the valve, final equilibrium had been established.

The solution was then sampled by tilting the bulb so that one of the bulb necks was beneath the surface of the liquid and the other was above the surface. Nitrogen was then introduced in the neck above the liquid surface, forcing the solution out of the other neck into a double-bulbed pipet. The pipet was double bulbed so that during the delivering of the sample no loss of chlorine from the delivered sample would occur. The sample was then analyzed.

A few runs were made at reduced pressures. This was done by introducing the chlorine over the solution and then reducing the total pressure with an aspirator. The bulbs were connected to manometers to measure the total pressure over the solutions. Equilibrium was attained when the bulb pressures became constant. The mercury manometers were protected from the chlorine gas by a layer of silicone oil. The manometer leg connected to the bulbs had a cross-sectional area 10,000 times larger than the atmospheric leg so that virtually no movement of the mercury-silicone oil interface occurred. When equilibrium had been attained, the solutions were sampled and analyzed.

RESULTS

The results of the equilibrium solubility runs are shown in Table XIV. These results show that Henry's law is applicable in the solutions where the hydrolysis reaction is suppressed. The solubility at a chlorine partial pressure of 1 atm. was calculated from these results and is shown in Table IV.

TABLE XIV

THE SOLUBILITY OF CHLORINE IN THE AQUEOUS ABSORBENTS AT 25°C.

Solution	P_{Cl_2}, atm.	Chlorine Solubility, g./l.
H_2O	.947	6.09
0.1N HCl	.945	4.04
	.503	2.13
0.15N HCl	.946	3.99
50 g./l. NaCl & 0.1N HCl	.936	3.30
	.652	2.30
100 g./l. NaCl & 0.1N HCl	.947	2.91
150 g./l. NaCl & 0.1N HCl	.934	2.49
200 g./l. NaCl & 0.1N HCl	.936	2.17
	.437	1.03
25 g./l. Na_2SO_4 & 0.15N HCl	.947	3.58
	.532	2.02
50 g./l. Na_2SO_4 & 0.15N HCl	.935	2.76
100 g./l. Na_2SO_4 & 0.15N HCl	.935	2.76
200 g./l. Na_2SO_4 & 0.15N HCl	.942	2.32
	.478	1.17

The activity coefficient of chlorine in each of the absorbents was calculated by Equation (24) and is shown as a function of absorbent ionic strength in Fig. 32.

It is believed that the static method as used here is free from the errors associated with the dynamic method. In the static method equilibrium is approached by desorption and the sampling and analyzing procedures are all such that no loss of chlorine from the solution could occur. Thus, if appreciable errors were present the results would be too high. The solubilities calculated here are either the same or slightly lower than the results of the dynamic method, which indicated that the supersaturation effect had been eliminated.

ACTIVITY COEFFICIENT OF CHLORINE IN SODIUM HYDROXIDE SOLUTIONS

The activity coefficient of chlorine in the sodium hydroxide absorbents cannot be measured because of the reaction taking place. It can be estimated, however, by considering the Debye-McAulay equation for the activity coefficient of a neutral molecule in an ionic solution. The equation is

$$\ln \gamma_i = \ln(C_{i,o}/C_{i,s}) = \bar{\beta}/2kTD_s \sum_1^s n_j e_j^2/b_j \qquad (188)$$

where γ_i = activity coefficient of neutral molecule

$C_{i,o}$ = the solubility of the neutral molecule in pure water

$C_{i,s}$ = the solubility of the neutral molecule in the salt solution

$\bar{\beta}$ = a constant characteristic of the neutral molecule

k = Boltzmann's Constant

T = temperature

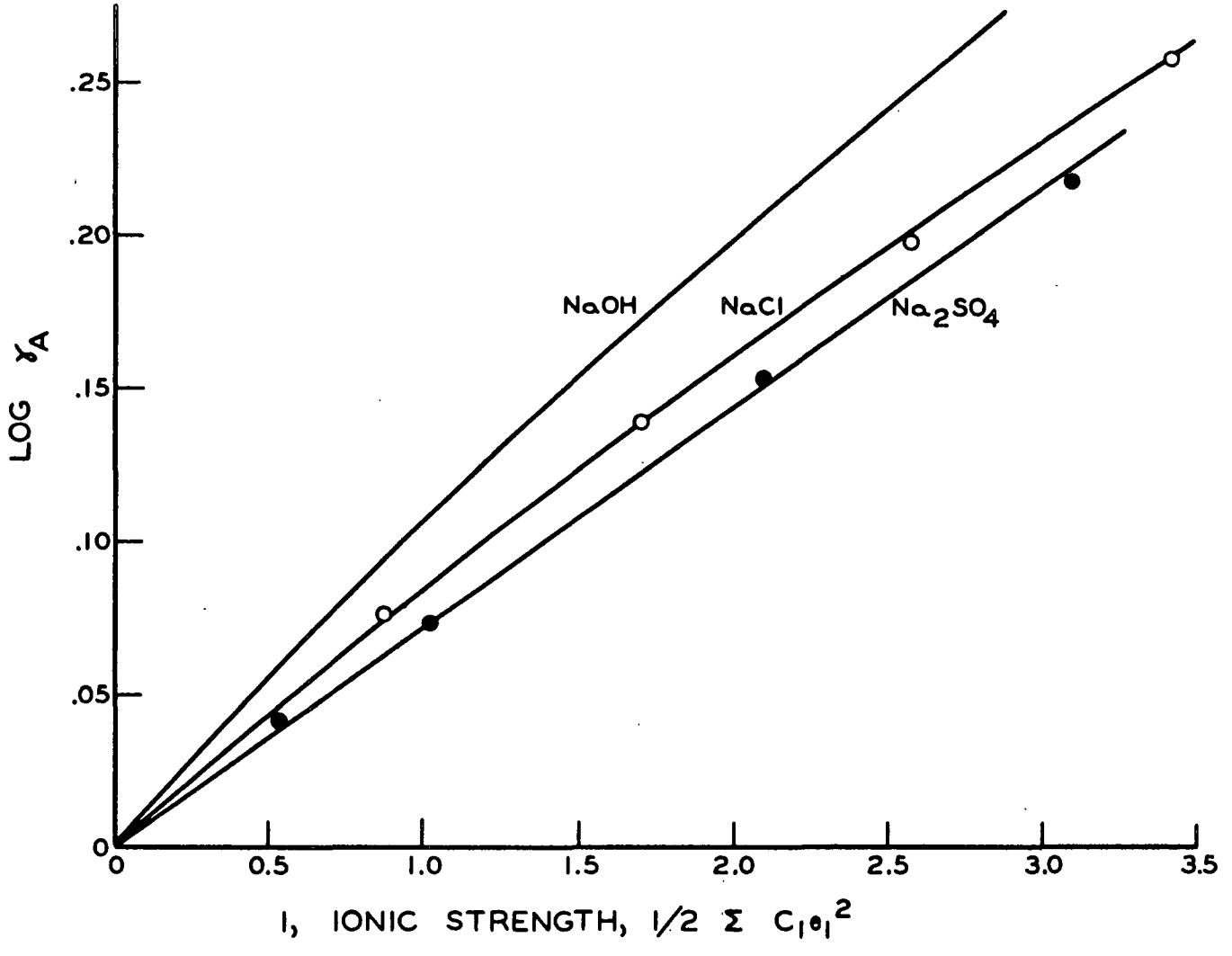

Figure 32. The Activity Coefficient of Chlorine in the Absorbents at 25°C.

D_s = Dielectric constant of solvent

n_j = number of ions of species j

e_j = total electrical charge of ion of species j

b_j = radius of ion of species j

Harned and Owen (8) state that this equation has the same form as that which is obtained empirically from experiment, i.e., that the log of the activity coefficient of the neutral molecule is proportional to the ionic strength of the electrolyte. If Equation (188) is written for a gas dissolved in sodium hydroxide and in sodium chloride solutions, and one divided by the other, the result is as follows:

$$[\ln \gamma_s]_{(NaOH)} / [\ln \gamma_s]_{NaCl} = \sum_1^s (n_j e_j^2 / b_j)_{NaOH} \Big/ \sum_1^s (n_j e_j^2 / b_j)_{NaCl} \qquad (189)$$

It is seen that the right-hand side of Equation (189) is a constant which should be independent of the neutral molecule and independent of the salt concentrations because both sodium hydroxide and sodium chloride are 1-1 electrolytes. The ratio of the log of the activity coefficient of oxygen in sodium chloride and sodium hydroxide solutions was calculated at 25°C. from data in the International Critical Tables at various salt concentrations and found to be:

Salt Concentration, Molality	$\left[\ln \gamma_{(O_2)}\right]_{NaOH} / \left[\ln \gamma_{(O_2)}\right]_{NaCl}$
0.5	1.27
1.0	1.26
2.0	1.25
	Av. 1.26 ± 0.01

Thus, in calculating the activity coefficient of chlorine in sodium hydroxide it is assumed that

$$\left[\ln \gamma_{(Cl_2)}\right]_{NaOH} = 1.26 \left[\ln \gamma_{(Cl_2)}\right]_{NaCl} \qquad (190)$$

The appropriate line is shown in Fig. 32.

APPENDIX V

THE DETERMINATION OF THE DIFFUSION COEFFICIENT OF CHLORINE IN AQUEOUS MEDIA

Initially, attempts were made to measure the diffusion coefficient of chlorine in a porous disk diffusion cell similar to that used by Stokes (72). The cell consisted of a sintered glass diaphragm on each side of which was a closed volume of about 100 ml. The solvent was placed on one side of the diaphragm and the solution on the other, thus causing diffusion to take place through the diaphragm. The solution on each side of the diaphragm was stirred with a magnetic stirrer arrangement so that concentration gradients would occur only in and near the diaphragm. The cells were calibrated with solutions of potassium chloride for which accurate determinations of the diffusion coefficient have been made. Attempts to run the cells with chlorine as the solute and 0.15N hydrochloric acid as the solvent resulted in erratic data.

It was noticed that the diffusion coefficients calculated in each cell were a function of the resistance to diffusion in that cell. The cells with the most resistance gave the lowest apparent diffusion coefficients. The results were then extrapolated to zero resistance and a value of 1.50×10^{-5} sq. cm./sec. was obtained for the diffusion coefficient which is very close to the value obtained by Peaceman (31). It was then hypothesized that during the calibration runs the potassium chloride moved through the diaphragm by a surface transport phenomenon which was a function of the ion charge and the glass surface area in the diaphragm. Stokes (72) found such a phenomenon in his work and gave evidence for its existence.

Extrapolating the data taken here to zero resistance is essentially the same as extrapolating to zero glass surface area and eliminating the transport effect. This is felt to be the reason for the agreement with Peaceman's work.

Because of the uncertain nature of these experiments the diffusion coefficient of chlorine in 0.15N hydrochloric acid was measured on a Beckman Spinco Model-H electrophoresis-diffusion apparatus.

APPARATUS AND PROCEDURES

The Model-H apparatus consists of a constant temperature bath, an optical system for viewing and photographing index of refraction gradients, and timing and control devices which aid in carrying out the experiments. For diffusion experiments, an 11-ml. quartz cell was loaded with the appropriate solvent and solution and placed in the constant temperature bath. A free boundary was formed between solvent and solution and diffusion allowed to take place. The cell was aligned so that the changes in index of refraction in the cell could be viewed and photographed at various time intervals.

The quartz, free diffusion cell of the Model-H apparatus is shown in Fig. 33. The bottom of the cell is capable of being moved back and forth to seal off the two legs as is shown in A. In loading the cell the bottom section was filled with solution and then moved to seal off the legs. Then one side was filled with solution and the other with solvent as shown in A. The cell was placed in the constant temperature bath and aligned with the optical system of the apparatus. A siphoning needle was placed in the

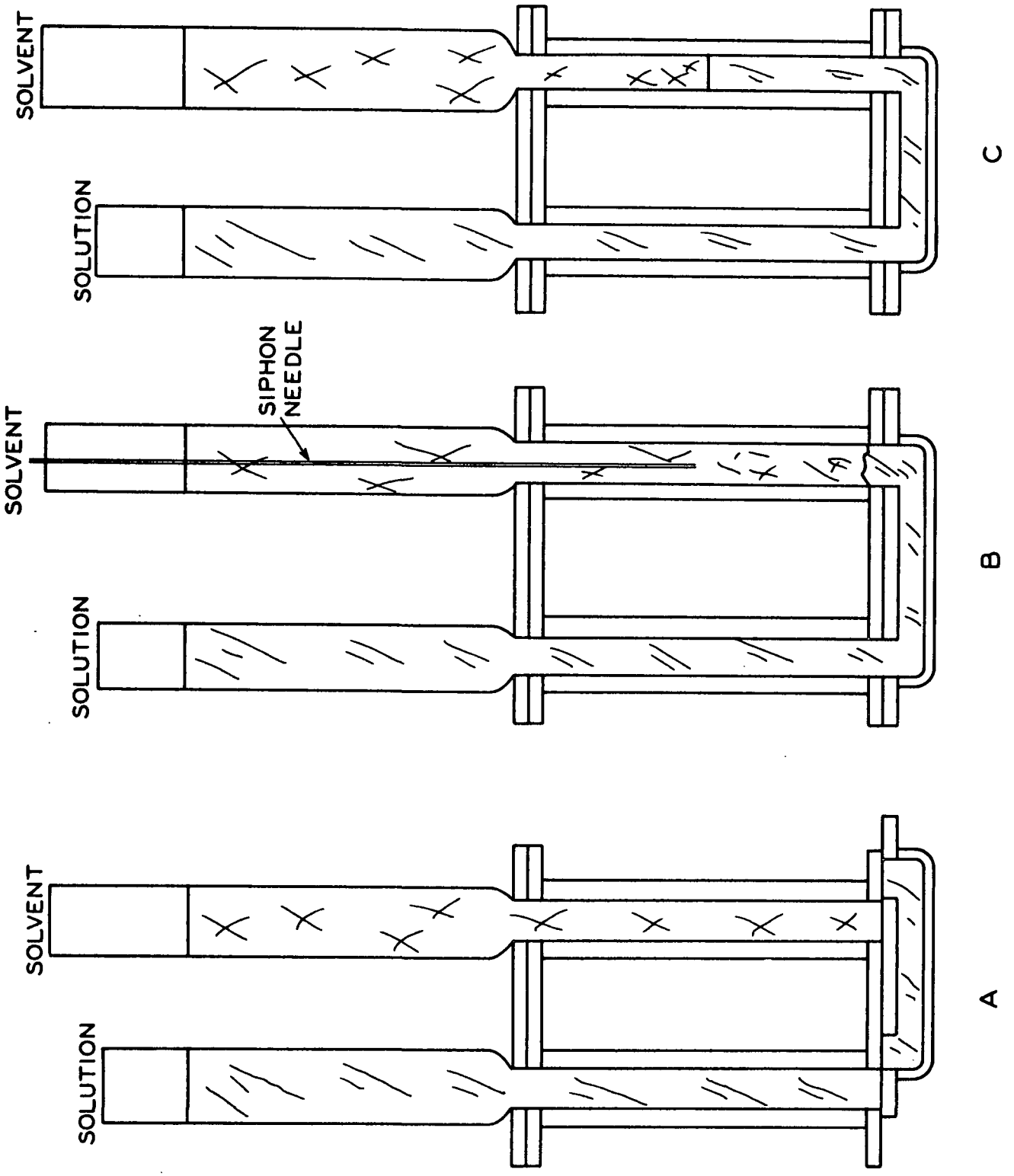

Figure 33. Loading and Boundary Formation in the Free Diffusion Cell

solvent side of the cell, and the bottom section was moved so that both cell legs were joined. Solvent was siphoned from the cell, moving the solution-solvent boundary toward the needle (see B). When the boundary reached the needle, siphoning was continued at a rate fast enough to prevent much solute from diffusing past the needle tip, but not fast enough to cause convection currents that would disturb the boundary. The boundary was then sharpened by carefully moving the needle up a small amount while siphoning. When the boundary was as sharp as could be made, the siphoning was stopped and the needle removed (see C). This point was taken as zero time.

The solute then began to freely diffuse into the solvent causing index of refraction gradients. These gradients were photographed in the form of both schlieren and Rayleigh patterns as shown in Fig. 34. The schlieren peak is a plot of the index of refraction gradient versus distance in the cell, while the Rayleigh interference fringes represent the actual index of refraction as a function of cell distance.

RESULTS

The calculations of the diffusion coefficients were made from the Rayleigh fringes in accordance with the method outlined by Schachman (73). It was assumed that the index of refraction of the solution is a linear function of the chlorine concentration.

One run was made at 0.4°C. with 0.1411N hydrochloric acid as the solvent to suppress the hydrolysis reaction. The diffusivity was calculated and corrected to 25°C. by assuming that $D_A\mu/T$ was a constant. This is a good assumption when the solvent remains the same.

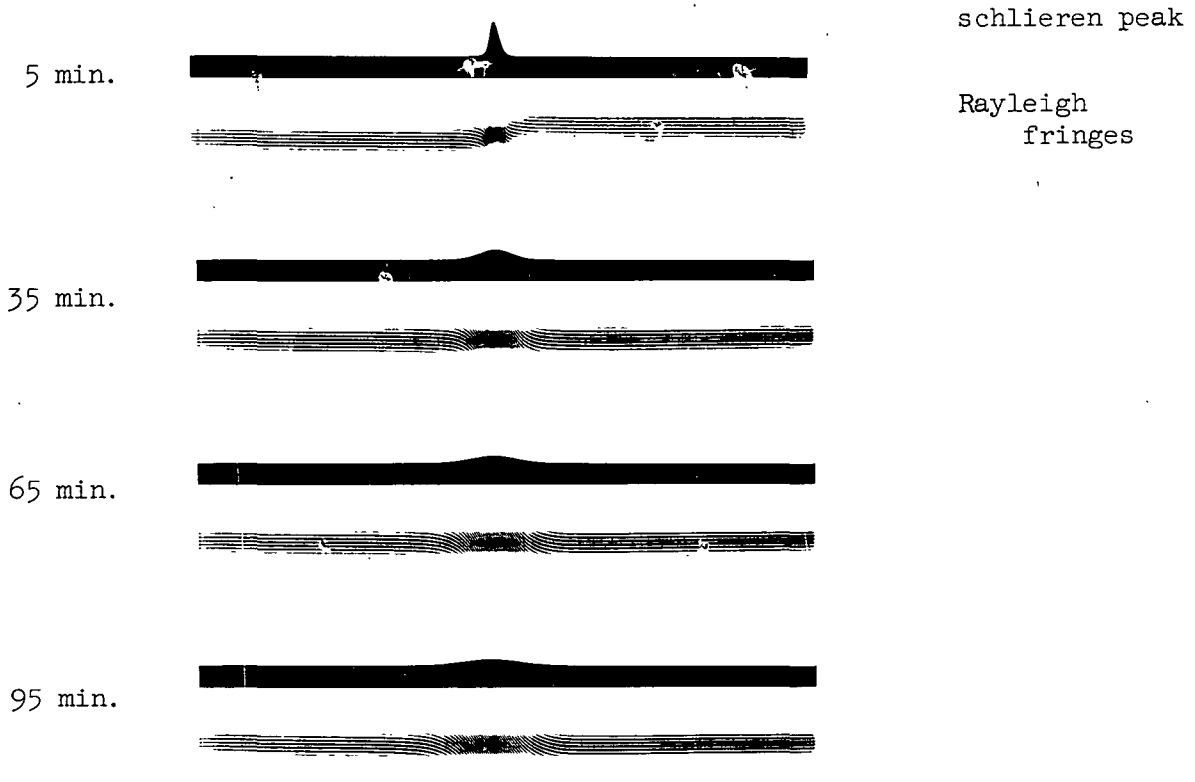

Figure 34. Schlieren Peak and Rayleigh Fringes for Diffusion of Cl_2 in 0.1411N HCl

The value of the diffusion coefficient of chlorine in pure water was then estimated by correcting the calculated value in 0.141N hydrochloric acid by again assuming that $D_A\mu/T$ was constant. The final value for the diffusion coefficient of chlorine in pure water at 25°C. was 1.45×10^{-5} sq. cm./sec.

Another run was made at 20.4°C. with the same solvent. The same calculation and corrections were made yielding a diffusion coefficient of 1.49×10^{-5} sq. cm./sec.

A slight skewness in the concentration gradient was noticed during the calculations. This could be caused by any of three things:

1. A concentration dependent diffusion coefficient.
2. Heterogeneity in the diffusing species.
3. The initial boundary not being sharp.

It is known that the initial boundary of the runs was not perfectly sharp, and it is felt that this is the major reason for the skewness. If the other two effects were present their combined effect on the diffusion coefficient could not be greater than 4% because the skewness was that slight.

The attempts to measure the diffusion coefficient of chlorine in the salt solutions were unsuccessful. In both the sodium chloride and sodium sulfate solutions the total number of Rayleigh fringes did not remain constant. In other words the total index of refraction difference between solution and solvent became less with time. No explanation for this behavior could be found other than that a complexing mechanism between the chlorine and the salt ions slowly altered the index of refraction of the solution, solvent, or both.

APPENDIX VI

ANALYTICAL PROCEDURES

This thesis made use of four different chemical determinations: 1) the determination of chlorine and hypochlorous acid in solution; 2) the estimation of total dissolved oxygen in water; 3) the determination of sodium hydroxide in solution; and 4) the determination of hydrochloric and sulfuric acid in solution.

The first two determinations are based on iodimetry which, in this case, involves the liberation of free iodine from potassium iodide and then subsequent titration with standard sodium thiosulfate solution. The other determinations also involve common volumetric methods of analysis whose procedures are covered in most standard analytical chemistry textbooks, such as that of Pierce and Haenisch (74).

PREPARATION AND STANDARDIZATION OF SODIUM THIOSULFATE SOLUTIONS

The sodium thiosulfate solutions were prepared by dissolving a weighed portion of reagent-grade sodium thiosulfate into degassed, distilled water. Approximately 2 to 3 grams of borax crystals were added per liter of solution to act as a buffer, and approximately 0.001 gram per liter of mercuric iodide were added as a preservative against bacteriological decomposition. The solutions were stored in glass bottles which had previously been cleaned with chromic acid cleaning solution and rinsed with boiling water. The air above the solution in the bottles was kept free from carbon dioxide by using an ascarite filter. The solutions prepared and stored in this manner were very stable.

The sodium thiosulfate solutions were standardized by a coulometric titration technique involving the electrolytic formation of iodine from a potassium iodide electrolyte. The generating cell employed was the design of Pitts, DeFord, Martin, and Schmall (75). The current source was rectified a.c.; the current was integrated by means of a low-inertia integrating motor to which was attached a counter. The current source and motor counter were calibrated by using a silver coulometer of the porous cup type. The efficiency of the generating cell was checked by titrating standard arsenite solutions with electrolytically generated bromine and iodine.* The precision and accuracy of the instruments were found to be excellent.

The titrations were begun by running the potassium iodide electrolyte through the generating cell into an aliquot of the thiosulfate solution at a rate of one drop per second. Then the current was turned on and iodine generation begun. Prior to the end point, starch indicator was added. As the end point was approached the current was turned off and the titration continued by means of a tapping key which permitted short pulses of current to pass through the generating cell. The titration was stopped at the very first sight of the familiar purple starch-iodine complex. From the number of motor counts the equivalents of iodine generated could be determined and the normality of the thiosulfate solution calculated.

---

* The calibration of the counter and checking of the generating cell was done by Mr. R. B. Kesler in connection with an Institute co-operative project. Mr. Kesler also designed the instrument and developed the procedures.

DETERMINATION OF MOLECULAR CHLORINE AND HYPOCHLOROUS ACID IN SOLUTION

The samples of chlorine-water were introduced underneath the surface of a solution of 10% potassium iodide in an Erlenmeyer flask. If it was necessary the resulting solutions were then made acidic by the addition of acetic acid. Nitrogen was then run into the flask to prevent the air-oxidation of the potassium iodide to iodine. The samples were set aside from 1/2 to 2 hours. Then they were titrated with standard sodium thiosulfate solution under a blanket of nitrogen. Starch indicator was added just prior to the end point, and the titration was continued until the characteristic purple color disappeared. The reactions taking place are as follows:

1) $H^+ + Cl^- + HOCl \rightleftharpoons H_2O + Cl_2$

2) $Cl_2 + 2KI(\text{excess}) \rightleftharpoons 2KCl + I_2$

3) $2S_2O_3^{=} + I_2 \longrightarrow S_4O_6^{=} + 2I^-$

THE ESTIMATION OF TOTAL DISSOLVED OXYGEN IN WATER

The Winkler method (76) for the volumetric analysis of dissolved oxygen in water is used in this thesis. This method involves the oxidation of manganeous hydroxide to manganic acid by the dissolved oxygen. The manganic acid then oxidized iodide ions to iodine which is subsequently titrated with standard sodium thiosulfate. The reactions are:

1) $MnSO_4 + 2NaOH \rightleftharpoons Mn(OH)_2 + Na_2SO_4$

2) $Mn(OH)_2 + 1/2O_2 \longrightarrow H_2MnO_3$

3) $H_2MnO_3 + 2H_2SO_4 + 2KI \longrightarrow MnSO_4 + 3H_2O + K_2SO_4 + I_2$

The water samples were taken in clean, dry, 250-ml. Erlenmeyer flasks. The flasks were filled to the very top and then stoppered so that no oxygen from the air could be absorbed. Two milliliters of each of the following reagents were then added in order: 1) $MnSO_4$ solution--363 g. of $MnSO_4 \cdot 4H_2O$ per liter; 2) alkaline-iodide solution--700 g. of KOH and 150 g. of KI per liter; and 3) concentrated sulfuric acid. Two hundred milliliters of the solution were then drawn and titrated with standard sodium thiosulfate.

THE DETERMINATION OF SODIUM HYDROXIDE IN SOLUTION

The strength of the sodium hydroxide absorbents was determined by using the absorbent to titrate a known amount of dissolved potassium acid phthalate (KHP) to a phenolphthalein end point. From 0.5 to 0.9 g. of dried, pure KHP were accurately weighed and dissolved in 50 ml. of water and a drop of phenolphthalein indicator added. The titration then proceeded until a slight pink color appeared.

THE DETERMINATION OF HYDROCHLORIC AND SULFURIC ACID IN SOLUTION

The sodium carbonate method was used to standardize the acid stock solutions from which the acidic absorbents were made.

In the sodium carbonate method, from 0.5 to 1.0 g. of dried reagent-grade sodium carbonate were dissolved in 50 ml. of water in an Erlenmeyer flask. One drop of methyl orange indicator was added, and the solution was titrated with the unknown acid until a definite pink color appeared. Approximately 1 ml. of acid was then added in excess. The solutions were then boiled for one minute to expel most of the carbon dioxide. After

cooling to room temperature, three drops of bromcresol green-methyl red mixed indicator were added. The solutions were then titrated with standard sodium hydroxide solution until a green color appeared. Next a back titration with the acid to a pink color was made. Then standard base was carefully added a drop at a time until a sharp change to green occurred. The equivalents of standard base used were added to the equivalents of sodium carbonate to calculate the normality of the unknown acid.

APPENDIX VII

MEASUREMENT OF JET DIAMETERS

The diameter of the nozzle opening was determined by observing it under a microscope with a glass slide graduated in 0.05-mm. divisions. Measurements were made at several different angles to insure that the opening was perfectly round. The opening measured 1.65 mm. at every angle.

The diameter of the jet issuing from the nozzle was measured by projecting it onto a screen and measuring the width of its image with a micrometer. The projection system used is shown in Fig. 35. The diameters were measured in this manner at various jet lengths and flow rates. The length of the jet was measured with a cathetometer. The results of these measurements appear in Fig. 36. It is seen that the diameters seem to follow Equation (167). These results were also observed for a bell-shaped nozzle by Scriven (54) and Cullen and Davidson (52).

The mean jet diameter, $\bar{D}$, and the mean of the diameter squared, $\bar{D}^2$, were needed to calculate the proper exposure time and interfacial area of the jet to the gas. These can be evaluated from the following equations:

$$\bar{D} = 1/H \int_0^H \bar{D}\, dh \qquad (191)$$

$$\bar{D}^2 = 1/H \int_0^H \bar{D}^2\, dh \qquad (192)$$

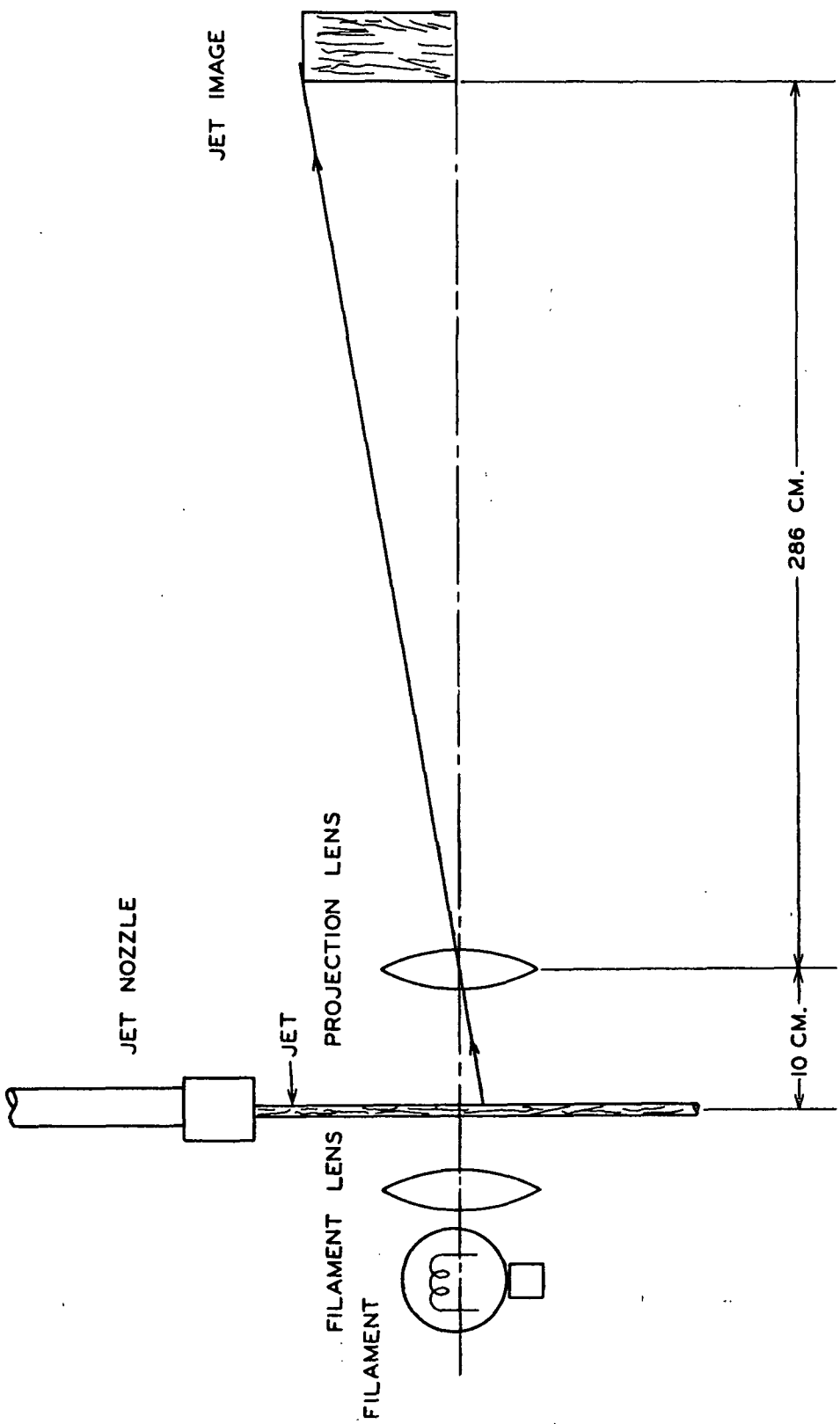

Figure 35. Projection System Used to Measure Jet Diameters

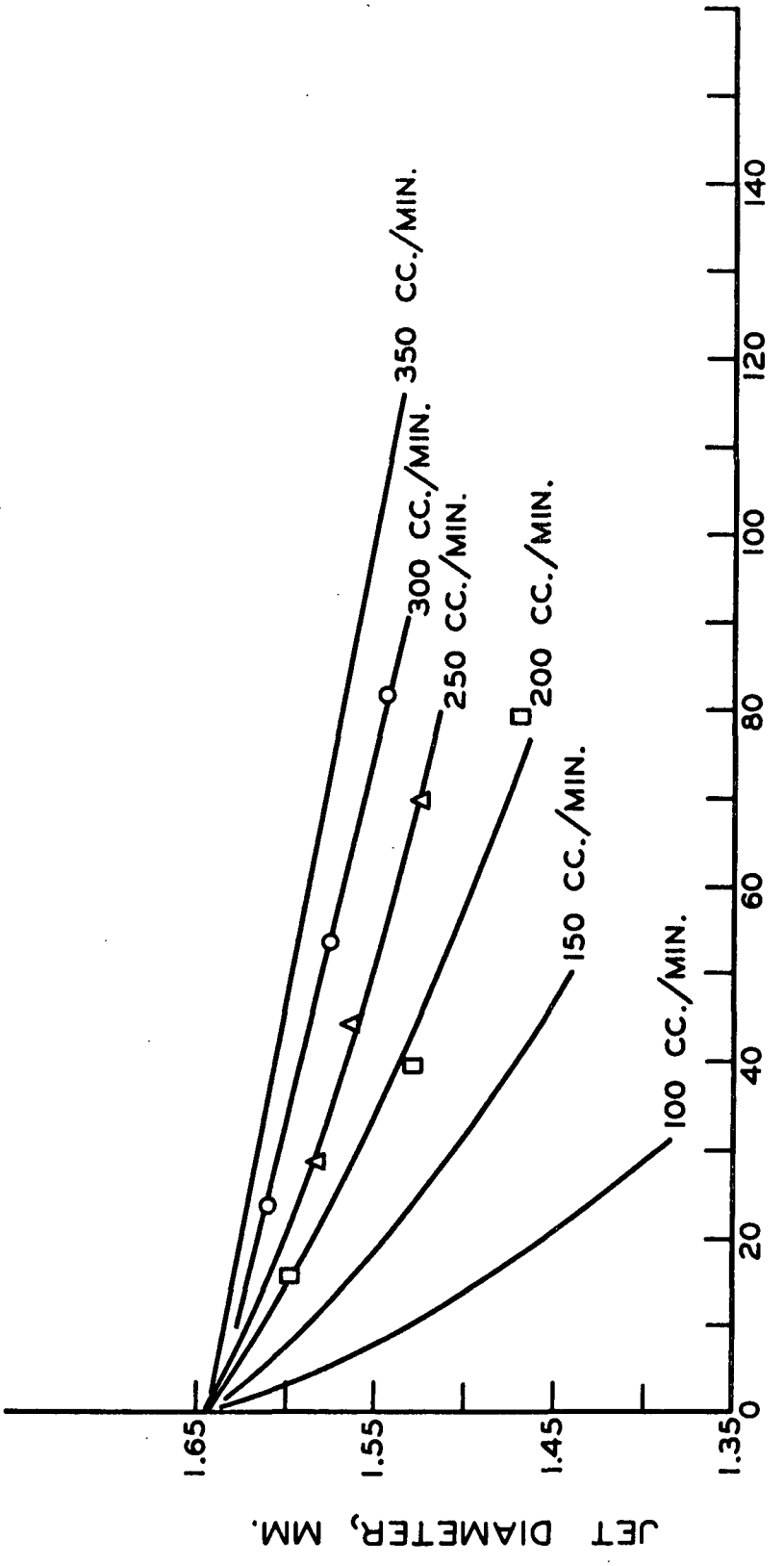

Figure 36. Actual Jet Diameter as a Function of Jet Length and Flow Rate

When Equation (167) is substituted into Equation (191) and (192) and the integrations carried out, the results are:

$$\bar{D} = \frac{32q^2}{3\pi^2 g D_o^3 H} \left[\left(1 + \frac{\pi^2 g D_o^4}{8q^2} H\right) - 1 \right] \qquad (193)$$

and

$$\bar{D}^2 = \frac{16q^2}{\pi^2 g D_o^2 H} \left[\left(1 + \frac{\pi^2 g D_o^4}{8q^2} H\right)^{1/2} - 1 \right] \qquad (194)$$

APPENDIX VIII

SAMPLE CALCULATIONS AND SUMMARY OF ABSORPTION RUNS

CALCULATION OF EXPERIMENTAL ABSORPTION RATE

Run No. 81 Data:

Absorbent: pH 10.3 NaOH

Temperatures: Absorbent--25.09°C.
Chlorine gas--25.00°C.

Pressures: Atmospheric: 737.0 mm. Hg
Jet chamber: 576.0 mm. silicone oil
ρ = 1.006 g./ml.

Absorbent flow rate: 4.41 ml. sec.

Nozzle diameter: 0.1645 cm. = $\underline{D}_o$

Jet length: 7.33 cm.

Titration of 111.3 ml. samples in 10% KI with 0.01263 N thiosulfate solution.
Sample A--25.51 ml. thiosulfate
" B--25.34 " "
" C--25.10 " "

Calculations:

a. Grams of chlorine absorbed/ml. of absorbent =

$$\frac{\text{Av. ml. thiosulfate x normality x equivalent wt.}}{\text{Sample size x 1000}} = \underline{W}$$

$$\frac{25.32 \times .01263 \times 35.5}{111.3 \times 1000} = 1.025 \times 10^{-4} \text{ g./ml.} = \underline{W}$$

b. Rate of chlorine absorption = $\underline{W}$ x absorbent flow rate

1.025×10^{-4} g. Cl_2/ml. x 4.41 ml./sec. =

4.52×10^{-4} g. Cl_2/sec. = $\underline{G}$

c. Interfacial area = $\pi \bar{D}$ x jet length

$$\text{where } \bar{D} = \frac{32q^2}{3\pi^2 gD_o^3 H}\left[\left(1 + \frac{\pi^2 gD_o^4}{8q^2} H\right)^{3/4} - 1\right] \qquad (193)$$

$$= \frac{32 \times 4.41^2}{3 \times 3.14^2 \times 980 \times .1645^3 \times 7.33}\left[\left(1 + \frac{(3.14)^2 \times 980 \times (.1645)^4}{8 \times 4.41^2} 7.33\right)^{3/4} - 1\right]$$

$$= 0.657 \times .242 = .1590 \text{ cm.}$$

Interfacial area = π x .1590 x 7.33 = 3.67 sq. cm. = $\underline{a}$

d. Average absorption rate = $\underline{G}/\underline{a}$

$= 4.52 \times 10^{-4}/3.67 = 1.230 \times 10^{-4}$ g./sec. sq. cm.

e. Correction to $\underline{P}_{Cl_2}$ = 760 mm. Hg

Total pressure in chamber = atmospheric pressure + chamber pressure

$$= 737.0 + \frac{1.006}{13.56} 576 = 779.8 \text{ mm. Hg}$$

$\underline{P}_{Cl_2}$ = total pressure - vapor pressure of absorbent

= 779.8 - 23.8 = 756.0 mm. Hg

Absorption rate at $\underline{P}_{Cl_2}$ = 760 mm. Hg = $1.230 \times 10^{-4} \times \frac{760}{756}$ = 1.236×10^{-4} g./sq. cm. sec. = $\underline{\bar{N}}_{\underline{A}}$

CALCULATION OF EXPOSURE TIME

a. Average velocity of jet, $\bar{U}$

$$\bar{U} = \frac{4q}{\pi \bar{D}^2}$$

$$\text{where } \bar{D}^2 = \frac{16q^2}{\pi^2 gD_o^2 H}\left[\left(1 + \frac{\pi^2 gD_o^4}{8q^2} H\right)^{1/2} - 1\right] \qquad (194)$$

$$= \frac{16 \times 4.41^2}{3.14^2 \times 980 \times .1645^2 \times 7.33} \cdot \left[\left(1 + \frac{3.14^2 \times 980 \times .1645^4}{8 \times 4.41^2} \times 7.33\right)^{1/2} - 1 \right]$$

$= 0.1620 \times .155 \qquad = 0.0251$ sq. cm.

$\therefore \bar{U} = \frac{4 \times 4.41}{3.14 \times .0251} \qquad = 224$ cm./sec.

b. Boundary layer thickness at nozzle exit,

$$= 2.42\, R_o \left(\frac{\nu \ell'}{R_o^2 \bar{U}_o} \right)^{0.391} \tag{171}$$

where $\bar{U}_o$ is average velocity in nozzle.

$$\bar{U}_o = \frac{4q}{\pi D_o^2} = \frac{4 \times 4.41}{\pi \times (1.645)^2} = 208 \text{ cm./sec.}$$

$$\delta = 2.42 \times .0823 \left(\frac{.00895 \times .0181}{.0823^2 \times 208} \right)^{0.391}$$

$$\delta = 2.42 \times .0823 \times .0780 = .01552 \text{ cm.}$$

$$b = \frac{\delta}{R_o} = \frac{.01552}{.0823} = .1890$$

c. Velocity at center of jet, U_∞

$$U_\infty = \frac{\bar{U}}{1-(3b/4)-(b^2/5)} \tag{184}$$

$$U_\infty = \frac{224}{1 - (3/4)(.189) - \frac{(.189)^2}{5}} = 263 \text{ cm./sec.}$$

d. Equivalent flat plate length, ℓ

$$\ell = \frac{1}{25} \frac{U_\infty}{\nu} \delta^2 \qquad (183)$$

$$= \frac{1}{25} \frac{263}{.00895} (.01552)^2 = .284 \text{ cm.}$$

e. Exposure time

$$t_e = \int_0^H \frac{dh}{U_s} = \frac{\ell}{U_\infty} \int_0^{\frac{H}{\ell}} \frac{U_\infty}{U_s} \, d\left(\frac{h}{\ell}\right)$$

$\frac{U_s}{U_\infty}$ is given as a function of $\frac{h}{\ell}$ in Fig. 31.

The line of Fig. 31 was fitted to an empirical equation and integrated. The result is

$$\int_0^{\frac{H}{\ell}} \frac{U_\infty}{U_s} \, d\,\frac{h}{\ell} = 2.90(1 - e^{-0.262(\frac{H}{\ell})}) + 1.061(\frac{H}{\ell})$$

$$= 2.90\,(1-e^{-0.262(\frac{7.33}{.284})}) + 1.061\,(\frac{7.33}{.284})$$

$$= 2.89 + 27.1 = 30.0$$

Therefore,

$$t_e = \frac{0.284}{263} \times 30.0 = .0323 \text{ sec.}$$

CALCULATION OF THEORETICAL ABSORPTION RATE WITHOUT CHEMICAL REACTION, AND OF Φ

$$\overline{N_A^*} = 2\, C_{A,e} \sqrt{\frac{D_A}{\pi t_e}}$$

$D_A = 1.48 \times 10^{-5}$ sq. cm./sec.

$$C_{A,e} = 4.22 \times 10^{-3} \text{ g. } Cl_2/\text{cc.}$$

$$t_e = 0.0323 \text{ sec.}$$

$$\therefore \overline{N}_A^* = 2 \times 4.22 \times 10^{-3} \sqrt{\frac{1.48 \times 10^{-5}}{3.14 \times .0323}}$$

$$\overline{N}_A^* = 1.043 \times 10^{-4} \text{ g./sq. cm./sec.}$$

$$\therefore \Phi = \frac{\overline{N}_A}{\overline{N}_A^*} = \frac{1.236 \times 10^{-4}}{1.043 \times 10^{-4}} = 1.19$$

CALCULATION OF FIRST-ORDER REACTION RATE CONSTANT FROM Φ

$$= 1/2\left[\sqrt{\frac{\pi}{k_1 t_e}}\,(1/2 + k_1 t_e)\,\text{erf}\sqrt{k_1 t_e} + \exp(-k_1 t_e)\right] \qquad (146)$$

A trial and error procedure was used to calculate $\underline{k}_1$ from Equation (146). Values of $\underline{k}_1$ were chosen until Φ equaled the experimental value.

For $\Phi = 1.19$ and $\underline{t}_e = 0.0323$, $\underline{k}_1 = 20.0 \text{ sec.}^{-1}$.

CALCULATION OF THEORETICAL Φ WITH INFINITELY FAST REACTION

From Equation (164)

$$\Phi = 1/\text{erf}\left(\frac{\alpha}{\sqrt{D_A}}\right) \qquad (195)$$

where α is given by

$$C_{A,e}\sqrt{D_A}\ \exp\left(-\frac{\alpha^2}{D_A}\right)\text{erfc}\,\frac{\alpha}{\sqrt{D_B}} =$$

$$C_{B_{(\infty)}}\sqrt{D_B}\ \exp\left(-\frac{\alpha^2}{D_B}\right)\cdot\text{erf}\left(\frac{\alpha}{\sqrt{D_A}}\right) \qquad (162)$$

Therefore,

$$\Phi = \frac{C_{B_\infty} \sqrt{D_B} \exp\left(-\frac{\alpha^2}{D_B}\right)}{C_{A,e} \sqrt{D_A} \exp\left(-\frac{\alpha^2}{D_A}\right) \operatorname{erfc}\left[\frac{\alpha}{\sqrt{D_B}}\right]} \qquad (196)$$

Values of α were chosen until Φ as calculated from Equation (195) equaled Φ as calculated from Equation (196).

TABLE XV

SUMMARY OF ABSORPTION RUNS AT 25°C.
AND P_{Cl_2} OF 760 mm. Hg

Run No.	Absorbent	Absorption Rate, g./sec. sq.cm. x 10^4	Exposure Time, sec.	Absorbent Flow Rate, ml./sec.	Jet Length, cm.
1	0.1N HCl	1.326	.0203	5.19	5.12
2	"	1.351	.0202	5.21	5.12
7	"	1.340	.0203	5.19	5.12
8	"	1.198	.0248	4.08	5.12
9	"	1.085	.0302	3.17	5.12
10	"	1.672	.0123	5.22	2.83
11	"	1.520	.0151	4.11	2.83
12	"	1.382	.0191	3.08	2.83
13	"	2.115	.00805	5.37	1.75
14	"	1.819	.0102	4.11	1.75
15	"	1.550	.0128	3.13	1.75
16	"	1.018	.0326	5.17	8.78
17	"	.938	.0394	4.07	8.78
	50 g./l. NaCl &				
19	0.1N HCl	1.141	.0194	5.17	4.85
20	"	1.000	.0243	3.93	4.85
21	"	.892	.0295	3.06	4.85
22	"	.890	.0303	5.39	8.43
23	"	.816	.0361	4.34	8.43
	100 g./l. NaCl &				
27	0.1N HCl	.756	.0310	5.41	8.72
28	"	.659	.0388	4.07	8.72
29	"	.944	.0210	5.19	5.36
30	"	.806	.0269	3.83	5.36

TABLE XV (Continued)

SUMMARY OF ABSORPTION RUNS AT 25°C.
AND P_{Cl_2} OF 760 mm. Hg

Run No.	Absorbent	Absorption Rate, $g./sec.\ sq.cm. \times 10^4$	Exposure Time, sec.	Absorbent Flow Rate, ml./sec.	Jet Length, cm.
	100 g./l. NaCl &				
31	0.1N HCl	.699	.0333	2.88	5.36
32	"	1.313	.00989	5.35	2.26
33	"	1.177	.0122	4.17	2.26
34	"	.989	.0163	2.96	2.26
	150 g./l. NaCl &				
35	0.1N HCl	.759	.0209	5.24	5.44
36	"	.663	.0262	3.99	5.44
37	"	.565	.0338	2.84	5.44
38	"	1.124	.0104	5.41	2.46
39	"	1.040	.0127	4.30	2.46
40	"	.782	.0176	2.89	2.46
41	"	.663	.0293	5.36	8.17
42	"	.557	.0385	3.78	8.17
	200 g./l. NaCl &				
43	0.1N HCl	.536	.0301	5.15	8.17
44	"	.464	.0381	3.80	8.17
45	"	.681	.0210	5.02	5.27
46	"	.567	.0269	3.70	5.27
48	"	.727	.0176	3.70	3.17
49	H_2O	1.398	.0244	5.55	6.74
50	"	1.291	.0295	4.41	6.74
51	"	1.243	.0312	5.20	8.37
52	"	1.122	.0379	4.06	8.37

TABLE XV (Continued)

SUMMARY OF ABSORPTION RUNS AT 25°C.
AND P_{Cl_2} OF 760 mm. Hg

Run No.	Absorbent	Absorption Rate, g./sec. sq.cm. x 10^4	Exposure Time, sec.	Absorbent Flow Rate, ml./sec.	Jet Length, cm.
55	H_2O	1.299	.0290	3.14	4.83
56	"	1.567	.0187	5.40	4.83
57	"	1.448	.0223	4.37	4.83
65	0.500N NaOH	11.35	.0268	5.23	7.15
66	"	10.38	.0314	4.31	7.15
67	"	9.50	.0371	3.46	7.15
68	0.244N NaOH	6.50	.0266	5.30	7.15
69	"	6.00	.0306	4.47	7.15
70	"	5.51	.0354	3.70	7.15
71	0.127N NaOH	3.63	.0269	5.24	7.15
72	"	3.55	.0309	4.42	7.15
73	"	3.31	.0353	3.72	7.15
74	0.0603N NaOH	2.23	.0270	5.22	7.15
75	"	2.12	.0304	4.53	7.15
76	"	2.05	.0356	3.69	7.15
77	0.0061N NaOH	1.460	.0269	5.26	7.15
78	"	1.348	.0309	4.42	7.15
79	"	1.272	.0359	3.65	7.15
80	pH 10.3 NaOH	1.284	.0289	4.93	7.33
81	"	1.236	.0323	4.41	7.33
82	"	1.182	.0361	3.72	7.33

TABLE XV (Continued)

SUMMARY OF ABSORPTION RUNS AT 25°C.
AND P_{Cl_2} OF 760 mm. Hg

Run No.	Absorbent	Absorption Rate, $g./sec.\ sq.cm. \times 10^4$	Exposure Time, sec.	Absorbent Flow Rate, ml./sec.	Jet Length, cm.
83	pH 8.7 NaOH	1.274	.0290	4.93	7.33
84	"	1.229	.0319	4.37	7.33
85	pH 7.7 NaOH	1.292	.0282	5.10	7.33
86	1.166N NaOH	22.50	.0289	4.85	7.33
87	"	19.94	.0325	4.17	7.33
88	"	18.39	.0374	3.45	7.33
89	1.733N NaOH	28.74	.0295	4.63	7.33
90	"	25.38	.0370	3.44	7.33
91	pH 4.2 H_2SO_4	1.317	.0282	5.10	7.33
92	"	1.236	.0311	4.52	7.33
93	"	1.158	.0364	3.70	7.33
94	50 g./l. Na_2SO_4	.934	.0296	4.76	7.33
95	"	.901	.0332	4.11	7.33
96	"	.865	.0372	3.53	7.33
97	100 g./l. Na_2SO_4	.704	.0300	4.61	7.33
98	"	.690	.0330	4.10	7.33
99	"	.670	.0377	3.41	7.33
100	150 g./l. Na_2SO_4	.542	.0307	4.42	7.33
101	"	.528	.0339	3.89	7.33
102	"	.511	.0391	3.24	7.33

TABLE XV (Continued)

SUMMARY OF ABSORPTION RUNS AT 25°C.
AND P_{Cl_2} OF 760 mm. Hg

Run No.	Absorbent	Absorption Rate, $g./sec.\ sq.cm. \times 10^4$	Exposure Time, sec.	Absorbent Flow Rate, ml./sec.	Jet Length, cm.
103	25 g./l. Na_2SO_4	1.110	.0289	4.92	7.33
104	"	1.050	.0324	4.26	7.33
105	"	.974	.0370	3.58	7.33
106	pH 2.7 H_2SO_4	1.282	.0283	5.07	7.33
107	"	1.222	.0313	4.48	7.33
108	"	1.154	.0356	3.80	7.33
109	pH 1.6 H_2SO_4	1.204	.0281	5.11	7.33
110	"	1.161	.0311	4.52	7.33
111	"	1.094	.0353	3.83	7.33
112	pH 1.0 H_2SO_4	1.188	.0285	5.02	7.33
113	"	1.131	.0310	4.53	7.33
114	"	1.069	.0349	3.88	7.33

APPENDIX IX

THE NUMERICAL INTEGRATION OF THE PENETRATION THEORY EQUATIONS DESCRIBING THE ABSORPTION OF CHLORINE IN ACID MEDIA

The differential equations describing the absorption of chlorine accompanied the reaction

$$Cl_2 + H_2O \rightleftharpoons HOCl + H^+ + Cl^-$$

are written as follows

$$D_A \frac{\partial^2 A}{\partial x^2} - \frac{\partial A}{\partial t} = \frac{\partial E}{\partial t} - D_E \frac{\partial^2 E}{\partial x^2} = \frac{\partial F}{\partial t} - D_F \frac{\partial^2 E}{\partial x^2} =$$

$$k_1 A = k_2 (E)(F)(F+C) \qquad (197)$$

where $\underline{A}$, $\underline{E}$, and $\underline{F}$ are the concentrations of chlorine, hypochlorous acid, and hypochloric acid, respectively; where $\underline{C}$ is the initial concentration of hydrogen ions, and $\underline{k}_1$ and $\underline{k}_2$ are the forward and reverse reaction rate constants. The boundary conditions are:

$$\begin{aligned} &\text{at} \quad x = 0, \quad t > 0; \quad A = A_e, \ \partial E/\partial x = \partial F/\partial x = 0 \\ &\qquad x > 0, \quad t = 0; \quad A = 0, \ E = 0, \ F = 0 \\ &\qquad x = \infty, \quad t \geq 0; \quad A = 0, \ E = 0, \ F = 0 \end{aligned} \qquad (198)$$

It is desired to obtain $(\partial \underline{A}/\partial \underline{x})_{\underline{x}=0}$

The three equations expressed as first approximate difference equations become

$$D_A/h'^2 (A_{m+1,n} - 2A_{m,n} + A_{m-1,n}) = (1/K)(A_{m,n+1} - A_{m,n}) =$$

$$k_1 A_{m,n} - k_2 E_{m,n} F_{m,n} (F_{m,n} + C) \qquad (199)$$

$$D_E/h'^2 \left(E_{m+1,n} - 2E_{m,n} + E_{m-1,n}\right) - (1/E)\left(E_{m,n+1} - E_{m,n}\right) =$$

$$k_2 E_{m,n} F_{m,n} (F_{m,n} + C) - k_1 A_{m,n} \qquad (200)$$

$$D_F/h'^2 \left(F_{m+1,n} - 2F_{m,n} + F_{m-1,n}\right) - (1/K)\left(F_{m,n+1} - F_{m,n}\right) =$$

$$k_2 E_{m,n} F_{m,n} (F_{m,n} + C) - k_1 A_{m,n} \qquad (201)$$

where:

h' is the spacing of the grid points in space

K is the spacing of the grid points in time

subscript m denotes the position in space

subscript n denotes the position in time

If Equations (199), (200), and (201) are multiplied through by K and solved for $A_{m,n+1}$, $E_{m,n+1}$, and $F_{m,n+1}$ they become

$$A_{m,n+1} = (1-2\lambda_A) A_{m,n} + \lambda_A (A_{m-1,n} + A_{m+1,n}) -$$

$$c_1 A_{m,n} + c_2 E_{m,n} F_{m,n} (F_{m,n} + C) \qquad (202)$$

$$E_{m,n+1} = (1-2\lambda_E) E_{m,n} + \lambda_E (E_{m-1,n} + E_{m+1,n}) +$$

$$c_1 A_{m,n} - c_2 E_{m,n} F_{m,n} (F_{m,n} + C) \qquad (203)$$

$$F_{m,n+1} = (1-2\lambda_F) F_{m,n} + \lambda_F (F_{m-1,n} + F_{m+1,n}) +$$

$$c_1 A_{m,n} = c_2 E_{m,n} F_{m,n} (F_{m,n} + C) \qquad (204)$$

where $\lambda_A = D_A K/h'^2$, $\lambda_E = D_E K/h'^2$, $\lambda_F = D_F K/h'^2$

$$c_1 = k_1 K \quad \text{and} \quad c_2 = k_2 K$$

It is seen from Equation (202) that $A_{m,n+1}$ can be generated from points located only in the n position in time. The same is true for $E_{m,n+1}$ and $F_{m,n+1}$. The values of $A_{m,o}$, $E_{m,o}$, and $F_{m,o}$ at zero time ($n=0$) are given for all space in the boundary conditions. From these values $A_{m,1}$, $E_{m,1}$, and $F_{m,1}$ can be generated by Equations (202), (203), and (204). $A_{m,2}$, $E_{m,2}$, and $F_{m,2}$ can then be obtained from the points at $n=1$. In this way the solution can be obtained for any given time period. The A grid is partially illustrated in Fig. 37.

n, time											
10	A_e	$A_{1,10}$	$A_{2,10}$	$A_{3,10}$	$A_{4,10}$	$A_{5,10}$	$A_{6,10}$	$A_{7,10}$	$A_{8,10}$	$A_{9,10}$	$A_{10,10}$
9	A_e	$A_{1,9}$	$A_{2,9}$	$A_{3,9}$	$A_{4,9}$	$A_{5,9}$	$A_{6,9}$	$A_{7,9}$	$A_{8,9}$	$A_{9,9}$	0
8	A_e	$A_{1,8}$	$A_{2,8}$	$A_{3,8}$	$A_{4,8}$	$A_{5,8}$	$A_{6,8}$	$A_{7,8}$	$A_{8,8}$	0	0
7	A_e	$A_{1,7}$	$A_{2,7}$	$A_{3,7}$	$A_{4,7}$	$A_{5,7}$	$A_{6,7}$	$A_{7,7}$	0	0	0
6	A_e	$A_{1,6}$	$A_{2,6}$	$A_{3,6}$	$A_{4,6}$	$A_{5,6}$	$A_{6,6}$	0	0	0	0
5	A_e	$A_{1,5}$	$A_{2,5}$	$A_{3,5}$	$A_{4,5}$	$A_{5,5}$	0	0	0	0	0
4	A_e	$A_{1,4}$	$A_{2,4}$	$A_{3,4}$	$A_{4,4}$	0	0	0	0	0	0
3	A_e	$A_{1,3}$	$A_{2,3}$	$A_{3,3}$	0	0	0	0	0	0	0
2	A_e	$A_{1,2}$	$A_{2,2}$	0	0	0	0	0	0	0	0
1	A_e	$A_{1,1}$	0	0	0	0	0	0	0	0	0
0	A_e	0	0	0	0	0	0	0	0	0	0
	0	1	2	3	4	5	6	7	8	9	10

m, space

Figure 37. A Grid

In the $\underline{E}$ and $\underline{F}$ grids the boundary conditions

$\partial\underline{E}/\partial\underline{x}_{\underline{x}=0} = 0$ and $\partial\underline{F}/\partial\underline{x}_{\underline{x}=0} = 0$ are satisfied by

making $\underline{E}_{1,\underline{n}}$ equal to $\underline{E}_{o,\underline{n}}$ and $\underline{F}_{1,\underline{n}}$ equal to $\underline{F}_{o,\underline{n}}$.

It is seen that a complete solution can be generated from Equations (202), (203), and (204) and the initial boundary conditions.

However, only $(\partial\underline{A}/\partial\underline{x})_{\underline{x}=0}$ is of interest here, i.e., $(\underline{A}_{\underline{e}}-\underline{A}_{1,\underline{n}}/\underline{h}')$. Thus, only a small part of the grid points have to be calculated.

To illustrate the number of grid points that need to be calculated, it is assumed that 9 points in time are desired. The appropriate $\underline{A}$ grid is illustrated in Fig. 38.

It is seen from Fig. 38 and Equations (202), (203), and (204) that only the points with a check mark need be calculated in order to obtain $\underline{A}_{\underline{e}}-\underline{A}_{1,\underline{n}}$ for 9 points in time.

A program was written for the IBM 650 computer in the Bell Interpretive Code which would calculate such a triangular distribution of points for $\underline{A}$, $\underline{E}$, and $\underline{F}$ from Equations (202), (203), and (204) and punch out the instantaneous absorption rate, $\underline{N}_{\underline{A}}$, after each interval in time and for as many intervals as desired.

In making such an integration one must be careful in choosing λ and $\underline{h}'$. λ cannot be greater than one-half; and if $\underline{h}'$ is too large, the solution does not become a good approximation of the actual solution. Blanch (71) discusses the choosing of λ and $\underline{h}'$ such that error and work

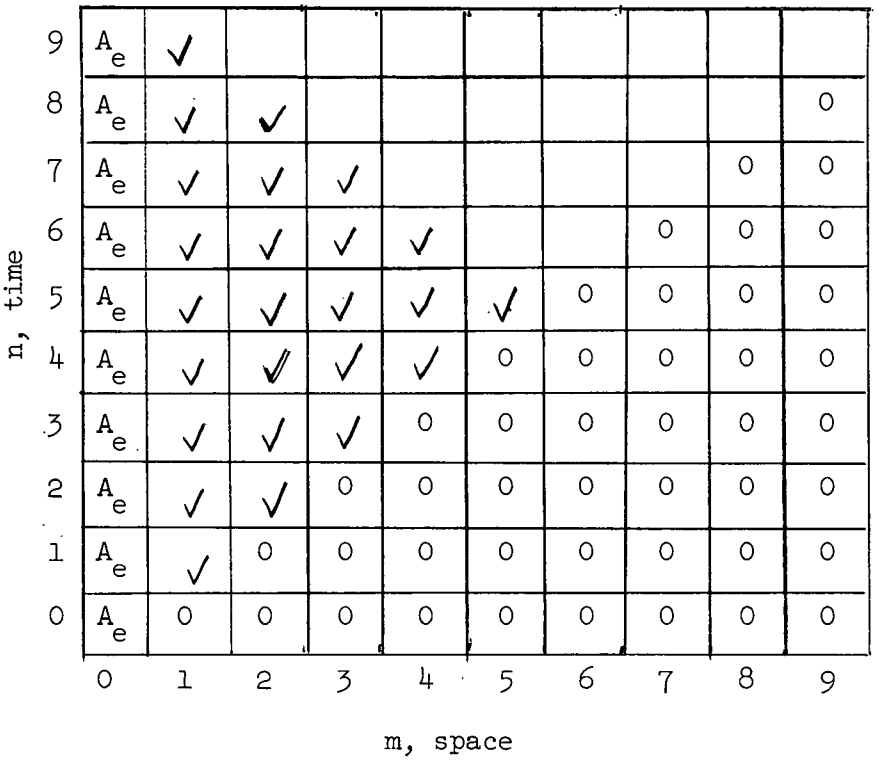

Figure 38. A Grid

are minimized. In this case, λ_F was chosen to be 0.5 because D_F is greater than D_E and D_A. h' was chosen to be .000127 cm. and K was .0003 second. This made λ_A equal to 0.278 and λ_E equal to 0.287.

To test the program and integration method the constant C was made to be 10 moles/liter so that the solution would be comparable to Equation (34) for physical absorption. The program was run, and the resulting instantaneous absorption rates were compared to Equation (34). The numerical solution was much lower than the analytical solution. It was felt that the numerical approximation to $(\partial A/\partial x)_{x=0}$ at very small times was not good because of the very large values of $(\partial A/\partial x)_{x=0}$ in this region. $\left((\partial A/\partial x)_{x=0} = \infty \text{ at } t = 0\right)$. In other words, the numerical solution did not get off to a good start.

The solutions to Equation (197) all lie between the case for physical absorption and the case for absorption with a first-order irreversible reaction. It was noticed that at very small times these two extreme solutions are very nearly the same; thus, any solution to Equation (197) would be the same. Because of this it was decided to calculate the grid points at small times in accordance with the analytical solution, Equation (115), and then let the numerical integration method take over when $\underline{A}_e - \underline{A}_{1,\underline{n}}/\underline{h}'$ became a good approximation of $(\partial \underline{A}/\partial \underline{x})_{\underline{x}=0}$ and while all the solutions were very close. Calculations showed that this point was after about 7 grid points in time.

The program was then run with the analytically calculated grid at $\underline{n}=0$ through $\underline{n}=7$ and the numerical solution generated. The resulting solution agreed very nicely with Equation (34) until at 0.02 second it began to become slightly less. At 0.03 second it was about 4% less. This was presumably due to the truncation of errors resulting from the numerical approximation. The average absorption rate, $\overline{\underline{N}}_{\underline{A}}$, at 0.03 second was only about 1% less, however. This is not felt to be a serious error in calculating $\bar{\Phi}$ because the ratio of average absorption rates is taken which would tend to cancel the errors.

The program was then run for various values of $\underline{C}$ which is governed by the initial pH of the solution. The results have been reported.

APPENDIX X

THE APPLICATION OF THE PENETRATION THEORY TO PACKED TOWERS

The hydrodynamic flow characteristics of a packed tower are extremely complicated and as yet cannot be subject to rigorous analysis. This situation prevents an accurate determination of the interfacial area and exposure time and thus limits the use of the penetration theory in packed towers. For the penetration theory to be applicable a liquid element would have to flow over an individual piece of packing without turbulence and then thoroughly mix before flowing over the next piece of packing. The proper exposure time would be the time that the liquid was exposed to the gas between mixings.

ESTIMATION OF INTERFACIAL AREA

If it is assumed that each piece of packing represents an individual wetted-wall column and that the flow over the packing is laminar, estimates can be made of the exposure time and interfacial area. The penetration theory gives the physical mass-transfer coefficient as

$$k_L^* = 2\sqrt{D/\pi t_e} \qquad (205)$$

provided that no concentration gradients exist before each exposure period.

The exposure time on a wetted-wall column with laminar flow is given by hydrodynamic considerations (34) as

$$t_e = h(9\, g\, \Gamma^2/8\mu\rho)^{-1/3} \qquad (206)$$

where Γ is the flow rate per unit of column perimeter, lb./hr. ft., and h is the column length.

The flow rate per unit of column perimeter can be estimated by considering a cubic foot of packing with an interfacial area, a sq. ft., and L lb./hr. of liquid flowing through it. If a cross section of this packing unit is taken and it is assumed that the wetted perimeter is the same in every cross section, it is seen that the wetted perimeter is a feet. Thus,

$$\Gamma = L/a \tag{207}$$

Substituting Equations (207) and (206) into (205) and multiplying through by a

$$k_L^* a = 2\sqrt{D/\pi h} \cdot (9\, g\, L^2 a^4/8\mu\rho)^{1/6} \tag{208}$$

If it is now assumed that the interfacial area can be represented by an exponential function,

$$a = bL^n \tag{209}$$

in the flow rate region encountered, Equation (208) becomes

$$k_L^* a = 2\sqrt{D/\pi h} \cdot (9\, g b^4 L^{4n+2}/8\mu\rho)^{1/6} = \text{constant} \times L^{4n+2/6} \tag{210}$$

The data of Craig (29) for the absorption of chlorine in 0.2N hydrochloric acid shows that for 1-inch Raschig rings

$$k_L a = 0.082\, L^{0.75} \ * \tag{211}$$

---

* $k_L a$ is in hours^{-1} and L is in lb./(hr.)(sq. ft.)

The exponent 0.75 is in exact agreement with the generalized Sherwood-Holloway correlation (76). Thus,

$$(4n + 2)/6 = 0.75$$

or

$$n = 0.625$$

and

$$b = (0.082/2)^{3/2} (D/\pi h)^{-3/4} (9\ g/8\mu\rho)^{-1/4} \qquad (212)$$

If it is assumed that the flow along a packing piece is always parallel to its axis, h can be taken as the leg length of the packing, i.e., 1 inch.

Thus, $b = 0.111$.

Therefore, $a = 0.111\ L^{0.625}$ (213)

with units of sq. ft./cu. ft. and lb. mass/(hr.)(sq. ft.)

Peaceman (31) made a similar calculation based on his data on a wetted-wall column rather than the penetration theory and obtained the equation

$$a = 0.184\ L^{0.58} \qquad (214)$$

Equation (213) gives an a which is 20% higher than Equation (214) at 1000 lb./hr. sq. ft. and 6% higher at 20,000 lb./hr. sq. ft.

According to Sherwood (78) the surface area of 1-inch Raschig rings is 58 sq. ft./cu. ft. Equation (23) states that L = 22,000 lb./(hr.)(sq. ft.) when a = 58 sq. ft./cu. ft. This value is very close to the point where Sherwood and Holloway (77) found that $k_L a$ for desorption of O_2 from water on 1-inch Raschig rings leveled off. At this leveling off point the packing was presumably completely wetted.

Grimely (79) measured the wetted area of 3/8-inch stoneware rings packing by an electrical resistance method. He found that the wetted area varied as $L^{0.63}$ for L values between 500 and 15,000 lb./(hr.)(sq. ft.). This is very close to the exponent calculated above. This agreement may be fortuitous because of the difference in packing; however, it is interesting to note.

ESTIMATION OF EXPOSURE TIME

The exposure time can now be calculated by substituting Equations (207) and (213) into Equation (206).

$$t_e = h\,(9\,g\,(9.02\,L^{0.375})^2/8\mu\rho)^{1/3}$$

or

$$t_e = 0.475/L^{0.25} \qquad (215)$$

where t_e is in seconds and L in lb./(hr.)(sq. ft.).

ESTIMATION OF THE HYDROLYSIS RATE CONSTANT

The data of Vivian and Whitney and of Craig can be used to estimate a value of the hydrolysis rate constant. The function, Φ, can be determined at various superficial flow rates, L, from Fig. 3 by dividing the absorption rates determined by Vivian and Whitney (absorption with chemical reaction) by the rates determined by Craig (29) (absorption without chemical reaction). In view of Equation (215) the function Φ can then be determined as a function of exposure time. This was done and the results are shown in Table XVI.

TABLE XVI

THE FUNCTION Φ FOR THE ABSORPTION OF CHLORINE WITH HYDROLYSIS VS. EXPOSURE TIME AS CALCULATED FROM THE PACKED TOWER DATA OF VIVIAN AND WHITNEY AND OF CRAIG

L, lb./hr. sq. ft.	t_e, sec.	Φ
1,500	0.0765	1.51
2,000	0.0711	1.45
3,000	0.0642	1.38
4,000	0.0598	1.31
5,000	0.0566	1.27
6,000	0.0539	1.23
8,000	0.0502	1.18
10,000	0.0475	1.16
15,000	0.0428	1.10

These values of t_e and Φ were substituted into Equation (146) and values of k_1 calculated. The resulting first-order reaction rate constants ranged from 7.0 to 20.0 sec.$^{-1}$ at 70°F. and were in direct correlation with Φ and t_e. The value determined from Fig. 15 at the same temperature is 13.0 sec.$^{-1}$.

It should be realized that the data of Vivian and Whitney and of Craig display considerable scatter. The Φ values calculated here were determined from the best lines that could be found through the data. That these lines are only crude approximations is indicated by examining Fig. 3. It is seen that the two lines would intersect at an L of about 25,000 lb./(hr.)(sq. ft.). It is known that this is impossible because

beyond this point the influence of chemical reaction would be to decrease the rate of absorption. Thus, the Φ values determined from these lines are also crude approximations, especially at the high flow rates or short exposure times. This then explains the range in the reaction rate constants calculated from the Φ values.

Nevertheless, the actual reaction rate constant lies well within the calculated range. This indicated that the assumptions made concerning the flow and mixing within the packed tower are fairly good first approximations to the actual situation.